INFORMATION TO USERS

This manuscript has been reproduced from the microfilm master. UMI films the text directly from the original or copy submitted. Thus, some thesis and dissertation copies are in typewriter face, while others may be from any type of computer printer.

The quality of this reproduction is dependent upon the quality of the copy submitted. Broken or indistinct print, colored or poor quality illustrations and photographs, print bleedthrough, substandard margins, and improper alignment can adversely affect reproduction.

In the unlikely event that the author did not send UMI a complete manuscript and there are missing pages, these will be noted. Also, if unauthorized copyright material had to be removed, a note will indicate the deletion.

Oversize materials (e.g., maps, drawings, charts) are reproduced by sectioning the original, beginning at the upper left-hand corner and continuing from left to right in equal sections with small overlaps.

ProQuest Information and Learning
300 North Zeeb Road, Ann Arbor, MI 48106-1346 USA
800-521-0600

THE STABILITY OF A D.C. SHUNT MOTOR

by

Ramesh C. Madhok

Submitted in partial fulfillment of the requirements
for the degree of
Master of Applied Science

Deparment of Electrical Engineering ,
Faculty of Pure and Applied Science ,
The University of Ottawa ,
Ottawa , Canada .

April , 1970 .

SUMMARY

Stability in various types of electrical machine is described and instability in a d.c. shunt motor is studied in detail . Commutation and the demagnetising effect of the armature reaction on the main flux are investigated in order to determine the exact cause of instability . Various methods of measuring the machine parameters are described . An equivalent model of the motor is developed and computer solutions of the speed/torque equations are compared to experimental observations of instability in the actual machine .

ACKNOWLEDGEMENTS

The auther wishes to express his gratitude to Prof. J. V. Marsh of the Electrical Engineering Department , University of Ottawa , who suggested the study of this problem , for his suggestions and guidance both in practical and theoretical works in the preparation of thesis . Thanks are also due to Mr. Rene LeHenaff , admimistration officer , for his practical assistance .

Financial assistance received from the National Research Council under Grant No. A4157 , is gratefully acknowledged .

TABLE OF CONTENTS

LIST OF SYMBOLS

B	=	Flux density
B_m	=	Maximum flux density
C	=	Transformation matrix
C_t	=	Transpose of C matrix
D	=	Rotational loss coefficient
ds	=	Stator direct axis
dr	=	Rotor direct axis
E_b	=	Voltage generated in motor i.e. back e.m.f.
F	=	Magnetomotive force
G	=	Torque matrix containing all the speed coefficients
I	=	Load current
J	=	Polar moment of inertia
k	=	Coefficient of coupling
L, M	=	Self and mutual inductances
L', M'	=	Speed coefficients , which differ from the unprimed inductances if the field form is not sinusoidal
N	=	Number of turns
p	=	Differential operator d /dt
qs	=	Stator qudrature axis
qr	=	Rotor quadrature axis
$\mathcal{R}$	=	Reluctance of the magnetic path
r_{qr}	=	Armature resistance
T	=	Torque
V	=	Supply voltage at the terminals
X	=	Transient reactance of the synchronous machine
Z	=	Transient impedance matrix for primitive machine
Z'	=	Transient impedance matrix for the actual machine
α	=	Angle of brush shift
β	=	Angle of commutation
δ	=	Torque angle in synchronous machine

θ = Shaft displacement angle

ϕ = Flux

ω = Angular velocity

CHAPTER I

INTRODUCTION

INTRODUCTION

It has always been the designer's objective to keep the operating range of a machine well below the limits of stability. However, in the past , the steady-state performance was of principal importance and to-day, especially, as components in control systems, machines are subjected to more stringent dynamic operating conditions, resulting in attention being focussed on transient stability as distinct from steady-state stability. An example of this could be a control-regulated feedback system such as in a rapid transit system where the train speed calculated according to a pre-fixed profile is compared with actual speed. Differences control the supply voltage to the d. c. series motor.

Whilst the phenomenon of instability has been understood in individual types of machines for many years, it is only comparatively recently that the generalised theory of electrical machines has been available to analyse the performances of any type of machine in terms of equations of a primitive machine that may be transformed to those of the particular machine under investigation. The primitive machine must contain all the essential elements of all actual machines so that the application of the primitive equations to a particular actual machine will consist of applying constraints to, or eliminating currents from , these equations.

This thesis considers the phenomenon of instability in a d. c. shunt machine and proposes an equivalent circuit in terms of a primitive machine that will enable the now well-established generalised theory to be applied in order to analyse the phenomenon. A method is presented here for deriving a linear transfer function of a d. c. shunt motor running at a particular operating point. Thus the transfer function represents the dynamic behaviour of the motor for small perturbations around the operating point. While the form of the trnsfer function does not vary with the different operating points , the coefficients do change.

In electro-mechanical energy conversion , one energy medium is electrical in nature and the other is mechanical. The stable operation of

such a system depends on the energy balance between the electrical and the mechanical media. Whenever the energy balance is disturbed, the system is potentially unstable. It is possible to show the unstable behaviour with the help of some mechanical models. A typical mechanical analogy for the case of a synchronous motor given by Kimbark[1] is described below :

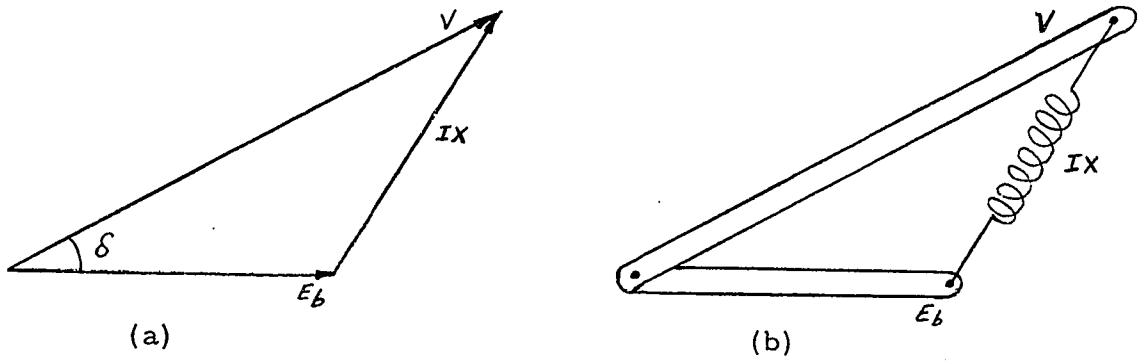

Fig. 1.1

The voltage diagram for this machine is shown in Fig. 1.1(a) and the mechanical analogy of the system is shown in Fig. 1.1(b). Two pivoted rigid arms representing V and E_b phasors, are joined at their extremeties by a spring representing the XI phasor. Lengths represent the voltages in the phasor diagram. The length of the spring XI is proportional to the tensile force (for simplicity an ideal spring is assumed which returns to zero length when the force is removed). Hence the tensile force can be considered to represent the current and the compliance of the spring (its elongation per unit force) to represent the reactance.

The torque exerted on the arm by the spring is equal to the product of the length of the arm , the tensile force of the spring and the sine of the angle between the arm and the spring. The torque multiplied by the speed of the rotation gives the mechanical power transmitted from one arm to the other. The mechanical model is regarded as being stationary , rather than rotating at synchronous speed, just as we regard the usual phasor diagram as stationary. The formula for torque (power) is

analogous to that for power in the phasor diagram , namely the product of the volt-amperes and the cosine of the phase angle. Since the XI phasor is 90 degrees ahead of the current phasor , the cosine of the angle between the voltage and the current is equal to the sine of the angle between the voltage and the XI phasor.

Loading of the machine could also be shown in the model described above by applying constant and equal torques to the two arms. This is done by attaching a drum to each arm and suspending a weight pan from a pulley hanging on a cord, one end of which is wound on each drum. As the weights are added to the pan in small increments , the two arms of the model gradually move apart till angle δ between them reaches 90 degrees at which position the torque is maximum. If further weights are added , the arms fly apart and continue to rotate in opposite directions until the cord is unwound from the drums. Thus the limit of stability is reached at δ = 90 degrees. Although from 90 to 180 degrees the spring force (current) continues to increase, the angle between the arm and the spring changes in such a way that torque decreases.

The above mechanical model may be extended to d. c. machines where angle δ is equal to zero and the voltage drop is purely resistive instead of reactive under steady-state operations. The point B in the Fig. (1. 2) for a d. c. machine can move up or down the slot in the arm representing E_b.

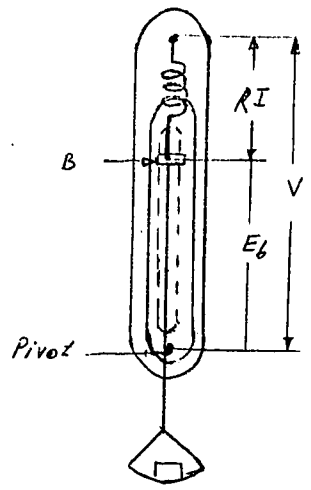

Fig. 1. 2

As more and more load is applied , the value of E_b decreases , thus increasing the length of the spring which represents the tensile force. Power output is the product of E_b and I.

Another equivalent model of the electrical machine is also possible starting from the torque equation. The torque of any electric machine is given by :

$$T = T_e + Jp^2\theta + Dp\theta$$

where T_e is the torque of electrical origin.

Taking the special case of a cylindrical rotor synchronous machine

$$T_e = (VE_b/X) \sin \delta$$
$$= K \sin \delta \qquad \text{if } VE_b/X = \text{constant} = K \qquad (1.1)$$

Taking the synchronous speed as the reference , the torque equation (1.1) then becomes

$$T = K \sin \delta + Jp^2\delta + Dp\delta \qquad (1.2)$$

Under steady-state conditions the torque due to the second and the third terms in eq. (1.2) becomes zero since δ is a constant. The eq. (1.2) is similar to the equation of motion for the mechanical system shown in Fig. (1.3).

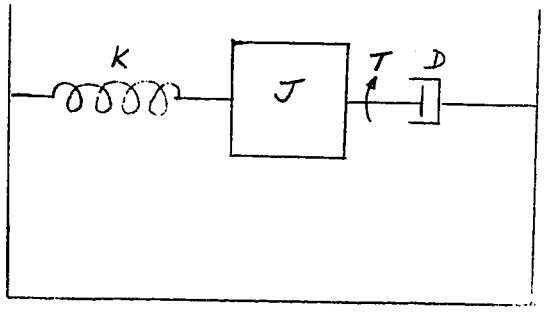

Fig. 1.3

The spring force is given by Ksin δ where δ is the torsional deflection of the spring at any time.

Since all rotating electrical machines have a stator , rotor and an air gap, it seems quite possible that mechanical models may be extended to explain or exhibit unstable behaviour in all machines. The study of these models in that case would throw some light on the behaviour of the

machines under various conditions of operation. The principal difference in behaviour between the mechanical models and the actual machines is that , due to the effects of magnetic saturation, configuration of coils and shape of the magnetic circuit (particularly the air gap) . The compliance of the spring is in fact dependent on several of the variables , so that non-linear differential equations formulate the voltage and torque. Examination of actual machine characteristics illustrates how far they deviate from the simple mechanical models and show why it is extremely difficult to develop a single unified treatment for instability analysis that would embrace all classes of electrical machines.

The electrical machine in operation develops a torque that is to be balanced by the retarding torque developed by the load. Once such an equilibrium is reached the machine is operating at a stable point. But now if, due to some reason, there is some increase in load , then the machine will have to slow down to develop more torque to balance the increased torque due to load. The machine characteristic in this case would be of the form shown in Fig. 1. 4 (a).

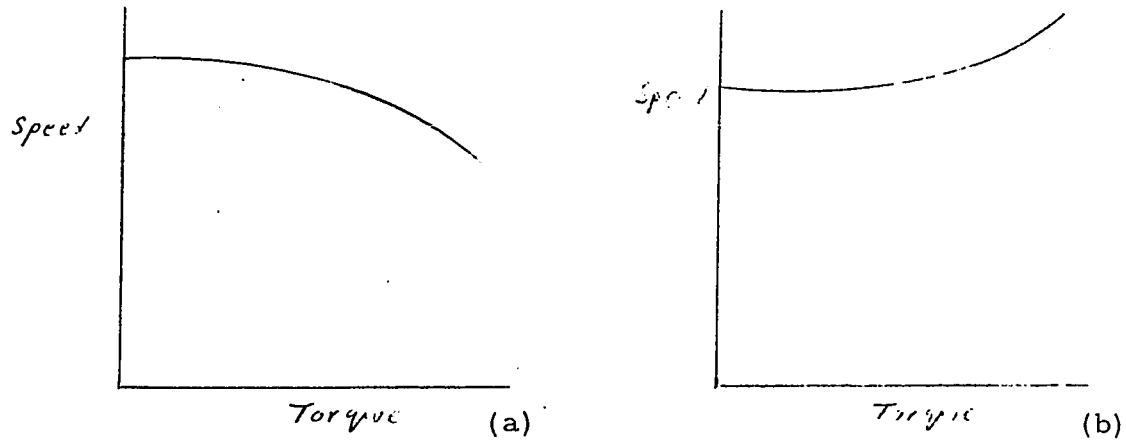

Fig. 1. 4

But on the other hand if the machine characteristic is as shown in Fig. 1. 4(b) , a reduction in the load will cause the net torque on the machine to be accelerating. Because of this type of characteristic an increase in speed results in an increase in torque of the machine, with the result that the

speed increases further until some part of the system fails electrically or mechanically; in other words the machine runs into instability.

If a machine has the characteristic as shown in Fig. (1.5), then it is

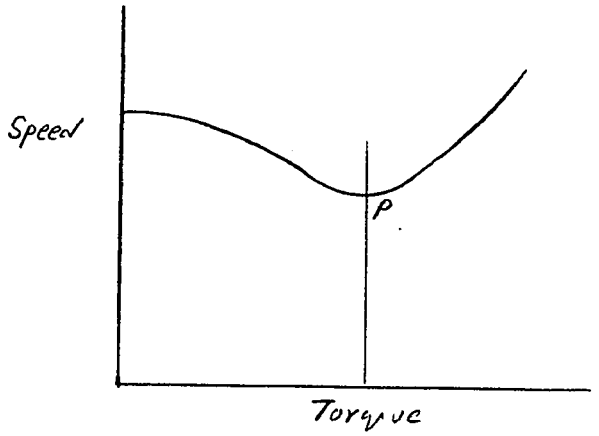

Fig. 1.5

evident that upto point P the machine operation will be quite stable, but after P the operation becomes unstable. In the case of a motor , the operation of the machine is stable so long the slope of the speed-torque characteristic is negative, but as soon as the slope becomes positive the machine runs into instability. The same thing is true in the case of a generator, which is stable so long the slope of the voltage-load current characteristic is negative, but runs into instability as soon as the slope becomes positive. An example of such a characteristic is shown in Fig. (1.6).

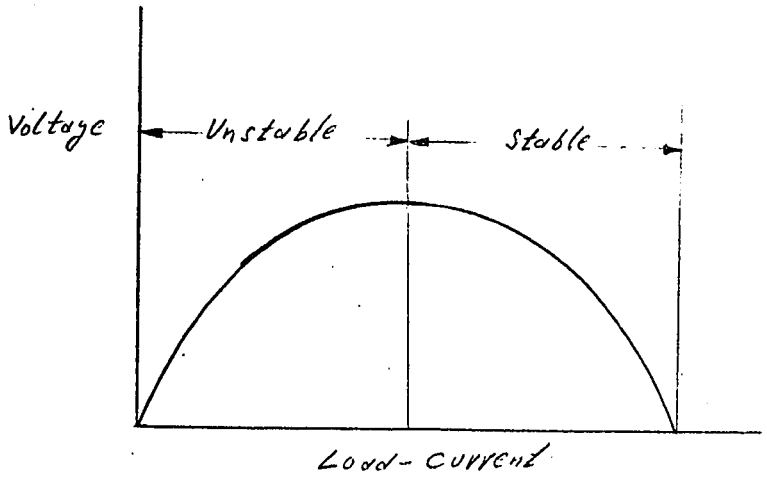

Fig. 1.6

CHAPTER II

INSTABILITY IN VARIOUS TYPES OF ELECTRIC MACHINES

INSTABILITY IN VARIOUS TYPES OF ELECTRICAL MACHINES

This chapter considers both a.c. and d.c. machines to show the type of instability they exhibit and under what conditions it takes place.

i) A.C. MACHINES

a) Synchronous Machines : Under steady-state conditions the synchronous machine rotates at a constant angular speed with a constant torque angle δ between the rotor pole axis and the axis of the rotating field caused by the three-phase currents in the stator. But if this relative position is disturbed for some reason, a synchronizing power flows in the machine to develop a synchronizing torque. The elastic nature of the magnetic link between stator and rotor gives rise to the oscillatory tendency.

A typical output-torque angle characteristic for a cylindrical rotor machine is shown in Fig. (2.1).

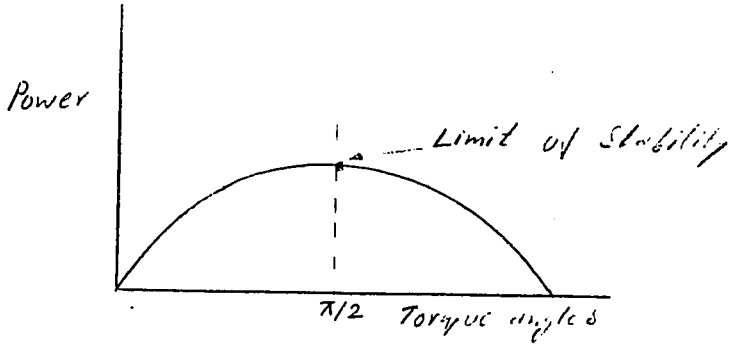

Fig. 2.1

Up to $\delta = 90$ degrees, the machine gives stable operation. This machine has two types of stability limits :

- Steady-state stability limit and
- Transient stability limit

The steady-state limit is the greatest possible power under given conditions of operation and excitation as the load is gradually increased.

The transient stability limit is the maximum power that the machine can carry and remain synchronized when subjected to a transient condition such as a sudden change in load, a fault or a switching operation.

The general stability of a synchronous machine thus concerns not only normal

operating equilibrium but also the ability to regain it after a disturbance.

b) Induction Machines : The normal full load torque in such machine is less than the maximum and may be less than one half. In accelerating from rest therefore, the motor runs through an unstable region in which a rising speed gives rising torque. This may not be important , except where the motor has to start against a considerable load torque. Fig. (2.2) gives a typical speed-torque curve and the normal load range is shown by a heavy line.

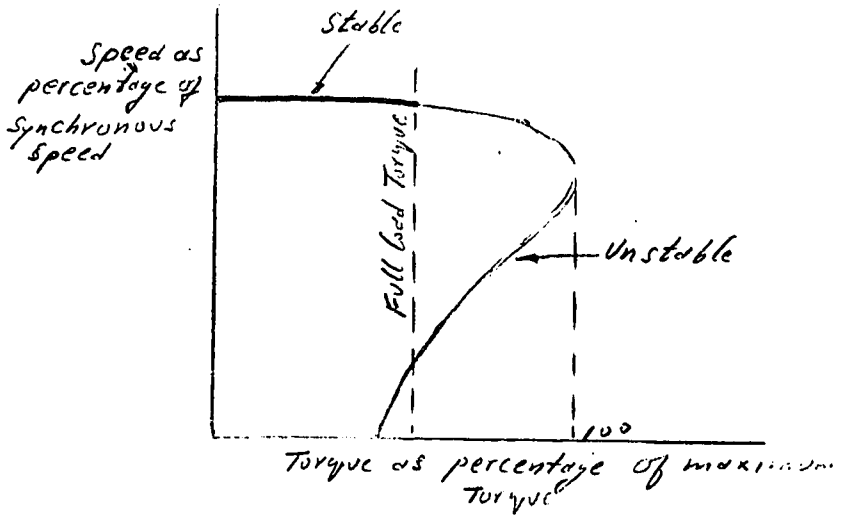

Fig. 2.2

The unstable region of the characteristic is not readily observable in practice, as the motor will not operate stably at any speed within the unstable range except where special loading devices are used. It is possible to obtain oscillations in this machine at no load if too much resistance is included in series with the supply circuit to the machine.

ii) D .C . MACHINES

a) Series Generator : This machine has the type of characteristic shown in Fig. (2. 3). The voltage depends entirely upon the value of the load current. The first part of the characteristic represents unstable conditions as an increase in current gives rise to an increase in voltage. Beyond the point of maximum voltage, however, the series generator is stable.

b) Series Motor : The m. m. f. due to the field coils increases in direct proportion to the load, the value of direct-axis flux will vary with the load current according to the magnetisation curve. Owing to the armature

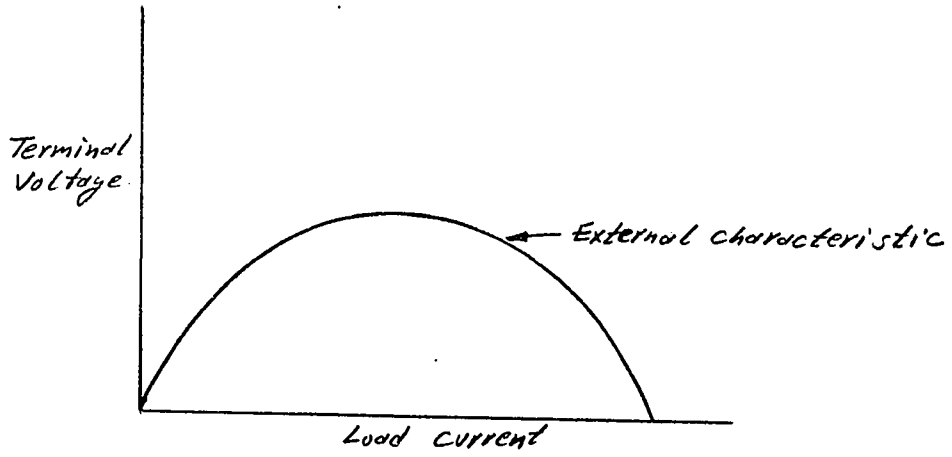

Fig. 2.3

reaction, even with the normal case of brushes in the geometric neutral position , the actual graph representing the total direct-axis flux is below the open-circuit magnetisation curve ; the fall being quite considerable at heavy values of current.

The initial portion of the speed -load current characteristic shown

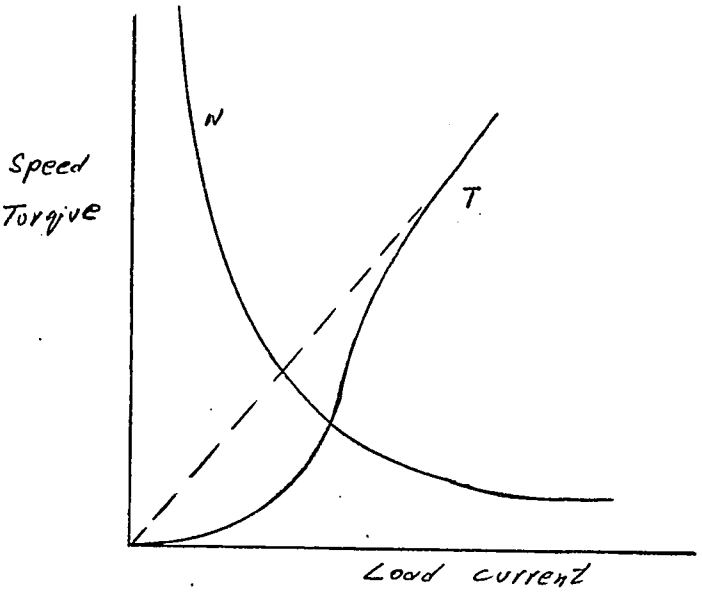

Fig. 2.4

in Fig. (2.4) is a rectangular hyperbola and if the effect of the q-axis m.m.f. on the d-axis flux is ignored, the final portion of the graph will merge into a straight line to give zero speed when $I = V/r_{qr}$ which is

very many times full-load value. The curve for the total torque will be first a parabola until the magnetisation curve ceases to be a straight line, but ultimately will merge into a straight line passing through the origin when the magnetic circuit is virtually saturated. The speed on no load will normally be many times the full-load speed, hence series motors are not used under conditions where there is any possibility of no-load working being encountered.

c) Shunt Generator : This machine has a voltage-load current characteristic shown in Fig. (2.5). After the load resistance is decreased to a certain value, any further decrease, instead of increasing the load current , ultimately results in the current decreasing. So the complete external

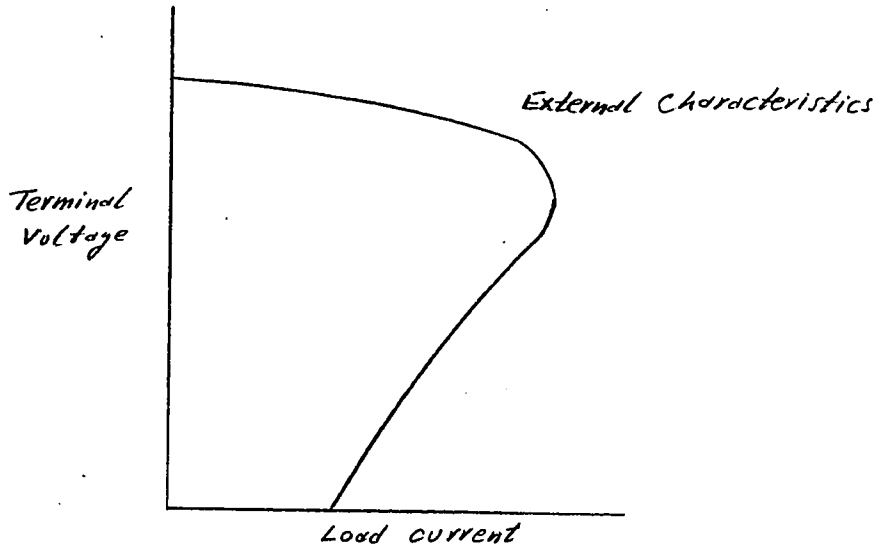

Fig. 2.5

characteristic of the generator may be divided into two parts :
Initially , as the load current increases , the terminal voltage decreases which represents stable conditions. For the later part of the curve, a decreased current corresponds to decreased terminal voltage , so the action is very unstable.

d) Shunt Motor : This machine would operate approximately at constant speed so long the shunt field remains unchanged. A typical characteristic of this machine is shown in Fig. (2.6). If the ratio field ampere turns/armature

reaction ampere turns is less than unity and with a fair degree of saturation

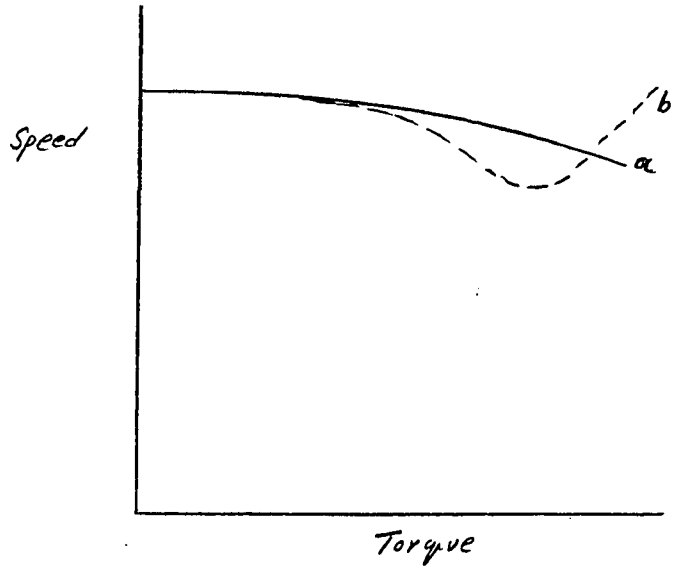

Fig. 2.6

in the armature teeth, the fall in flux with increasing armature current would be greater proportionally than the fall in back e. m. f. As a result the speed would increase with increasing load torque as shown in Fig. (2.6) by graph 'b' instead of falling continuously as shown by 'a' for a machine having a relatively strong field m. m. f.. Instability would thus result as the motor would tend to take a further increasing current and might actually accelerate. From the above discussion it is evident that a general approach to the study of instability applicable to all machines is likely to be too complicated to be of practical value. Consequently attention will now be confined to the machine under investigation i. e. the d. c. shunt motor.

CHAPTER III

CAUSES OF INSTABILITY IN THE D. C. SHUNT MOTOR

CAUSES OF INSTABILITY IN THE SHUNT MOTOR

Instability in the shunt motor, when operating with constant field current, results in an increase in both the speed of the motor and the armature current. The fact that the direct-axis field current is maintained constant indicates that there is some phenomenon that reduces the direct axis flux resulting in the rise in speed. Two possible reasons that may cause the reduction in the direct-axis flux are examined below :

a) Commutation as a factor contributing to instability : A negative voltage induced indirectly by the armature current in the ds-axis which reduces the effective m. m. f. of the field winding ; such a voltage might be attributable to commutation which occurs when the rotor coils are situated on the direct axis. This could be dismissed by the superficial argument that, apart from an alternating current due to the tooth ripple , it is well known that the field current maintains a constant value regardless of any increase in the armature current. Therefore, the ampere-turns produced by the field itself are independent of armature current. However, solid iron in the magnetic circuit, pole face windings and even laminated iron might well provide a path for direct-axis eddy currents resulting from induced voltages caused by mutual induction of unidirectional pulses of current in the rotor direct axis .

If such unidirectional currents could be shown to exist, Fig. (3. 1) shows how the m. m. f. associated with them could produce an increase in the leakage flux in the main field winding without decreasing the total flux associated with this winding.

It has been shown by Jones and Barton[3, 4, 5] that the process of commutation does in fact cause two components of voltage in the d-axis stator coil. One component is produced by the mutual coupling between the coils undergoing commutation and the other component is due to a speed voltage in the rotor coils during their travel over the non-commutating zone. Jones and Barton have shown that the two components are opposite in polarity and, although the duration of commutation is very short compared

with the time taken for a coil to travel one pole pitch, the average values of

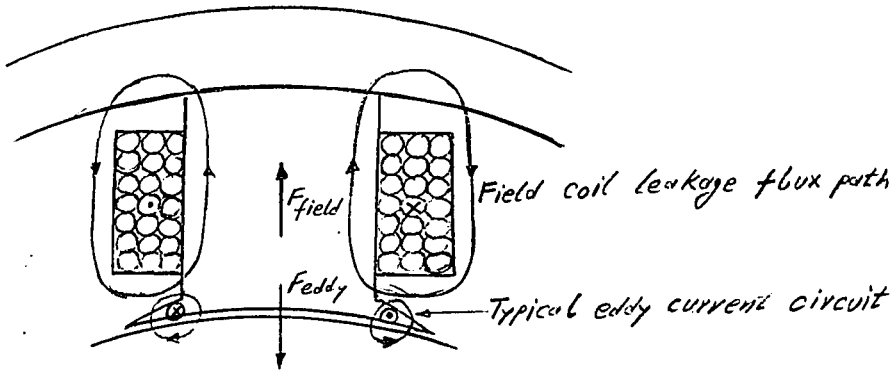

Fig. 3.1

the two components are assumed to be equal so that the net voltage produced in the field winding is zero. That the average value should be zero during normal operation of the machine is reasonable but the possibility of an unbalance occuring under abnormal cicumstances , such as poor commutation due to heavy load current, is worth investigating as a possible contributing factor in causing instability.

In the following analysis the ds-winding may be regarded as consisting of a closed eddy-current path, rather than the actual field coil, without affecting the validity of the argument because the crux of the argument is in the equality , or inequality , of the two voltage components caused by the current in an armature coil.

To investigate commutation as a possible cause, compare the transient impedance matrix of the commutator primitive machine given in eq. (3.1) with that derived from dynamic circuit theory.

$$Z = \begin{array}{|c|c|c|c|} \hline r_{ds} + L_{ds}p & M_d p & & \\ \hline M_d p & r_{dr} + L_{dr}p & L'_{qr}p & M'_q p\theta \\ \hline - M'_d p\theta & - L'_{dr}p\theta & r_{qr} + L_{qr}p & M_q p \\ \hline & & M_q p & r_{qs} + L_{qs}p \\ \hline \end{array} \qquad (3.1)$$

From dynamic circuit theory, the voltage equations are given by the matric eq. (3.2).

$$\begin{aligned} v &= ri + p(Li) \\ &= (r + Lp + (\partial L/\partial\theta)p\theta)i \end{aligned} \qquad (3.2)$$

This suggests that if measurements of resistance and inductance are made on a stationary machine , the elements of the inductance matrix $L(\theta)$ should enable the dynamic impedance to be determined. Plotting the various inductances , self and mutual,as functions of θ permits the coefficients of the speed voltages i.e. $\partial L/\partial\theta$ to be determined. Because the L matrix is symmetric, it follows that the $\partial L/\partial\theta$ matrix will also be symmetric.

The commutator primitive machine impedance matrix is clearly non-symmetric, there are no $\partial L/\partial\theta$ terms given in the stator coils and the terms associated with rotor speed voltages i.e. the primed inductances form a skew symmetric matrix. It is evident that the commutator machine impedance does not conform to the dynamic circuit theory eq. (3.1). The validity of the commutator machine impedance matrix may be readily verified by experiment. Open-circuit voltages may be measured when one coil at a time is excited with a known current while the rotor is being driven at a known speed. The results show that the primed inductances are in fact equal to their unprimed values.

However, it is noticed that M_d and L_{dr} when they are primed , appear in the qr row. This may be explained simply by recognizing that when, for example , the current in coil ds changes with time , a change in flux linkages occurs in coil dr. Hence an induced e.m.f. of mutual

induction (a transformer voltage) is produced in coil dr. No e.m.f. of mutual induction due to changing current in coil ds can appear in coil qr because the coil axis is perpendicular to the flux axis. If the rotor is moving , however, the direct-axis flux caused by the current in ds will cause a speed voltage in coil qr. If the rate of change of flux linkages in the coil dr is equal to the rate at which coil qr is "cutting" the flux, a condition that is fulfilled when coil ds is excited with alternating current and at the same time the rotor is driven at synchronous speed , then it is found that the transformer voltage across coil dr is equal to the speed voltage across coil qr. This proves that M_d is equal to M_d' . In this manner the commutator primitive machine impedance can readily be justified on an experimental basis.

The incompatability of these experimental measurements with the dynamic circuit theory eq. (3.2) remains unsolved. Measurements on a commutator machine appear to show conclusively that no speed voltage can exist in the stationary ds and qs coils.

In the case of a slip-ring primitive machine (see Appendix II), experiments show that the dynamic circuit theory eq. (3.2) is verified without any reservations. Speed voltages are present in the stator coils and the impedance matrix is symmetric for all coils. It is apparent that . if the dynamic circuit theory is universally true , then the description of the commutator primitive machine is incomplete in some respect. In both machines, measurements are made at the coil terminals. Currents entering the terminals of a slip-ring machine are one and the same as those in the actual rotor conductors. In the commutator machine, however, the currents entering the rotor are radically modified by commutator action. In terms of classical dynamics the slip-ring and the commutator machines comprise holonomic and quasi-holonomic systems respectively because the time integrals of the terminal currents give the actual conductor charges in the first case but not in the second because the position of a given conductor is unknown. The difficulties encountered in attempting to apply dynamic circuit theory to the commutator machine led Jones and Barton[3,4,5] to analyse the process of commutation in terms of dynamic circuit theory.

They showed that by considering the presence of an extra short-circuited coil to represent the coils undergoing commutation , it could be shown that there is in fact a speed voltage produced in the stator coils but also an additonal transformer voltage of opposite polarity. The existence of both these components of voltage was established experimentally but , although they showed their polarities to be in opposition, a proof was not given that they would exactly neutralize each other. They concluded that if the components were not equal in magnitude , then the flux produced by the field coil of a d. c. machine would either grow or decay indefinitely due to the unbalance in the transformer and speed voltages set up by a rapid succession of coils undergoing commutation. Because such a growth or decay cannot be observed in normal operation of the machine, the conclusion was that the magnitude of the components must be equal. In studying stability of a commutator machine , the possibility of there being a direct connection between field weakening as a consequence of unbalance of the two components was considered to be worth exploring. Should such a connection be established then it would have added to the known causes of instability in d. c. machines.

i) A summary of Jones'[4] work : Consider a d. c. shunt machine shown in Fig. (3. 2) with only two coils for the purposes of analysis. The same explanation could be extended to any commutator machine.

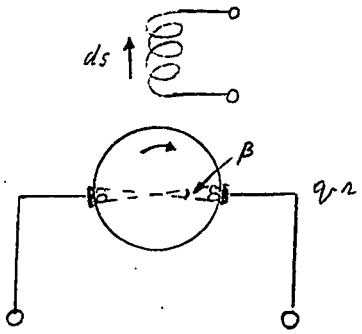

Fig. 3. 2

Consider the coils undergoing commutation when the brushes are making contact with fixed points on the rotor coils. The current in these coils changes

from + I/2 to - I/2 during commutation and is not a constant value as is the case with the rest of the armature turns not undergoing commutation. So it is seen that the short-circuited turns carry different current during the commutation period. These turns lie in the d-axis which is 90 degrees to the axis of main armature m. m. f.

Hence the above commutator machine can be analysed by considering a slip-ring machine which has one winding made of short-circuited turns and the other of rest of the turns. This machine is shown in Fig. (3. 3).

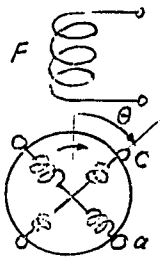

Fig. 3. 3

The inductance matrix of this machine will be of the form as in eq. (3. 3)

$$L = \begin{array}{c} \\ f \\ a \\ c \end{array} \begin{array}{c} \begin{array}{ccc} f & a & c \end{array} \\ \begin{bmatrix} L_f & M_{af} & M_{cf} \\ M_{af} & L_{aa} & M_{ac} \\ M_{cf} & M_{ac} & L_{cc} \end{bmatrix} \end{array} \qquad (3.3)$$

The plot of variations of the above inductances with the angular displacement is shown in Fig. (3. 4). Explanation of these curves is given below :

L_f = This is constant since a smooth rotor is assumed.

L_{aa} = This varies because of the saliency of poles and is a minimum at $\theta = 0$ i. e. when the coil is lying along the q-axis

L_{cc} = At $\theta = 0$ the coil is lying along the d-axis and the flux path is through teeth , rotor , two air gaps , pole shoes and the yoke and this remains fairly constant until the coil comes underneath

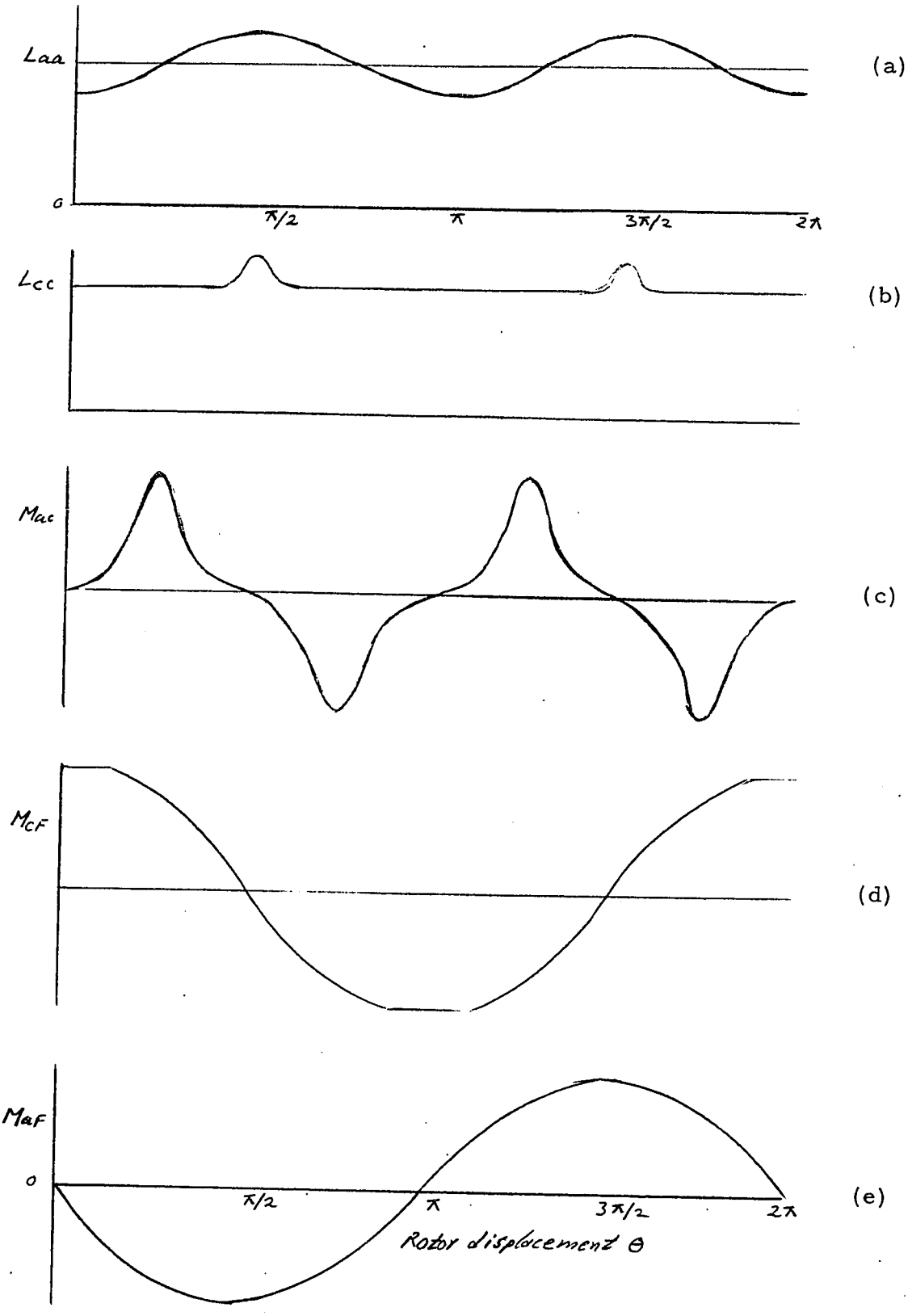

Variation of various inductances with rotor displacement

Fig. 3.4

the pole shoes. As the coil comes under the pole shoes, the length of the flux path starts reducing since the flux surrounding the coil sides now travels through the teeth, the small length in pole shoes and the two air gaps. Hence the value of L_{cc} starts rising up since the inductance goes up as the reluctance of the magnetic path goes down. So the peak of L_{cc} occurs at $\theta = 90$ degrees.

M_{ac} = This is a function of the second harmonic of a sine wave.

M_{cf} = This remains constant when the coil 'c' is lying in the d-axis which explains the trapezoidal shape.

M_{af} = This is a sine wave.

Considering the voltage equation for the field circuit only, since this is the one that needs investigation :

$$V_f = r_f i_f + L_f p i_f + M_{cf} p i_c - (\partial M_{af}/\partial\theta) i_a p\theta \qquad (3.4)$$

Since it is a two-pole machine and assuming that the brush width is such that it short circuits two segments, then during the commutation it is evident that two coils will be short circuited. So for evaluating V_f, consider $\theta = \pm \beta/2$ and one specific pair of coils. The mutual inductance of this pair of coils with field i.e. M_{cf} is shown in Graph 1(a) which is essentially the same as Fig. 3.4(d). For normal direct current operation, the current in the coils i_c as a function of rotor position θ is shown in Graph 2(a) which is constant except during commutation when the variation is approximately linear. The term M_{af} in the equation for the field voltage as given in eq. (3.4) will be replaced by M_{cf} since only one specific pair of coils is being considered during a travel of π radians.

The last two terms of the field voltage equation are of interest here. The value of M_{cf}, β=10 degrees and the angle which the poles subtend = 45 degrees have been taken from the work of Jones in order to plot the form of transformer and speed voltages in the field winding as shown in Graph 1(b) and 2(b). The positive pulses are seen to occur over the region where M_{cf} is constant and therefore represents $M_{cf} i_c p\theta$ i.e. a transformer voltage. The negative parts of the curve occur when i_c is constant and

therefore represent a speed voltage $(\partial M_{cf}/\partial\theta)i_c p\theta$. Each pair of coils therefore produces a transformer voltage during commutation and a speed voltage during the remainder of its rotation . The mean value over each half cycle of the total induced voltages from both sources is found to be zero. This mean value of V_f in Graph 1(b) and 2(b) is found by integration . Graph 3 gives the voltage produced bv one pair of coils over a complete revolution . The reaction on the field of a completely uniformly wound armature may be found as follows :

Consider the instant at which the pair of coils concerned is in the centre of the commutation zone.. Their instantaneous induced voltage is given by the positive peak in Graph 2(b) . The voltage induced by each of the remaining coils is given by erecting ordinates in the same Graph 2(b) at uniformly displaced angles equal to one commutator segment pitch . The voltage of all the remaining coils will be in the negative region of speed voltage . Added together they give the total voltage produced in the field circuit due to the rotor currents . The net voltage from all the coils is the sum of the individual voltages , both speed and transformer . If the mean value over each segment pitch is zero then the instantaneous value can differ from zero only by a small quantity at commutator ripple frequency . Neglecting this ripple the effect of commutation on the field coil would be zero and it could be said that the commutation itself does not contribute to instability in d. c. machines.

ii) Further extension of Jones' work : It is possible to calculate mathematically the areas under the transformer and speed voltage curves by forming proper equations . For the salient-pole machine considered by Jones , the two areas are calculated below and then the same calculations are extended to our machine which is a smooth air gap machine to see if the two areas are still the same .

Transformer voltage V_{tr} : This is given by the relation given below :

$$V_{tr} = M_{cf} pi_c \text{ volts}$$

but $pi_c = i_c 2\omega/\beta$ if linear perfect commutation is assumed .

Hence $$V_{tr} = M_{cf} i_c 2\omega/\beta \text{ volts}$$

CHAPTER IV

EQUIVALENT MODEL OF D. C. SHUNT MOTOR AND ITS DYNAMIC BEHAVIOUR

The area under the rectangle for a rotation of $\beta/2$ will then be equal to

$$\text{Area (transformer voltage)} = M_{cf} i_c \omega \quad \text{volts. rad.}$$

Note that this area is independent of β .

Speed voltage V_s : This is given by the following relation

$$V_s = \omega i_c \partial M_{cf} / \partial \theta \text{ volts}$$

Let the angle subtended by the pole arc be α and also assume that the shape of curve for M_{cf} follows a cosine wave in between the flat portions . This is a fair assumption from a practical view of machines . The peak value of the trapezoidal wave is M_{cf} . Let the cosine wave being followed by rest of the curve be defined by $A\cos\theta$.

Then $$M_{cf} = A\cos\alpha$$

$$\text{and } A = M_{cf}/\cos\alpha$$

Hence speed voltage $$V_s = \omega i_c A \sin\theta \text{ volts}$$

The area under the speed voltage curve from 0 to 90 degrees will be given by

$$\text{Area (speed voltage)} = \omega i_c \int_{\alpha}^{90} A \sin\theta d\theta$$

$$= - A\omega i_c \cos\alpha$$

Substituting the value of A ,

$$\text{Area (speed voltage)} = - M_{cf} i_c \omega \quad \text{volts. rad.}$$

Thus it is seen that both the areas are equal and have a value of $M_{cf} i_c \omega$ volts. rad.

Case of a smooth air gap machine : Because of the smooth air gap the shape of the curve for M_{cf} will not be trapezoidal but a cosine wave since the reluctance of the magnetic circuit is same for any value of θ . The peak of this cosine wave will have a value equal to M_{cf} instead of A for the salient pole machine . The plot of M_{cf} for the two cases is shown in Fig. (3.5) . The transformer voltage and the speed voltage for the smooth air gap machine will be of the form shown in Fig. (3.6) . The area of the transformer voltage will remain the same as calculated above in the case of the salient - pole machine.

Area of the speed voltage curve will be given by

$$\text{Area (speed voltage)} = \int_0^{90} (\partial M_{cf}/\partial\theta) \cos\theta \omega i_c \, d\theta$$

$$= - \omega i_c M_{cf} \quad \text{volts . rad.}$$

Hence it is seen that the net voltage in ds-axis winding iszero in the case of a

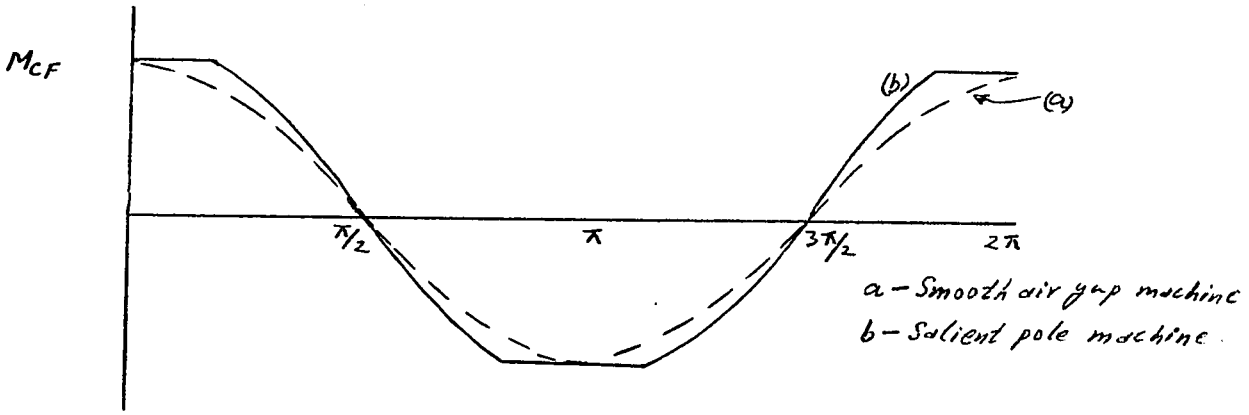

Fig. 3.5

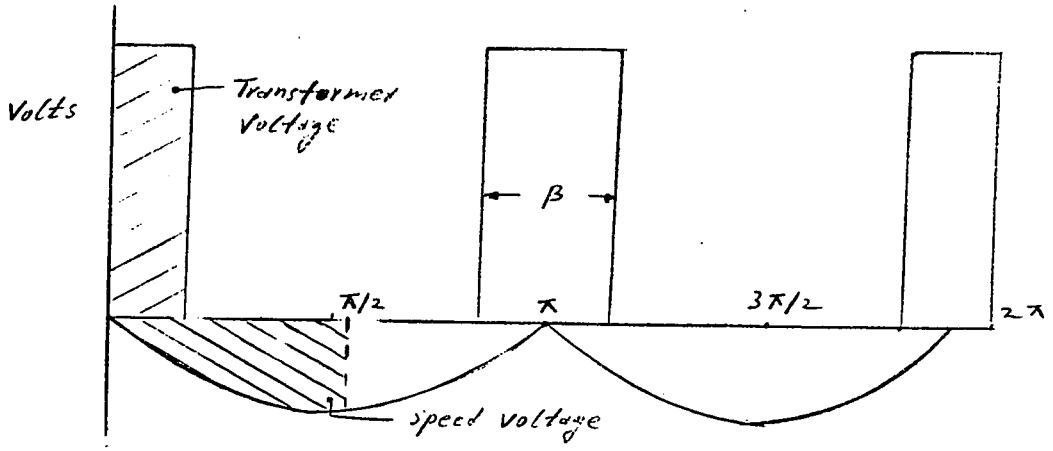

Fig. 3.6

smooth-rotor machine also . But in the case of a smooth-rotor machine there will be a speed voltage during the period of commutation also , which is not the case in a salient-pole machi ne .

We can , then, confidently rule out commutation as being the cause of producing a reduction in the ds-axis flux which in turn gives rise to instability .

iii) To establish the direction of transformer and speed voltages in terms of positive d-axis flux : Although it has been shown above that both the transformer and speed voltages being produced in the ds winding exactly neutralize each other , it would be of interest to know the polarity of these voltages with respect to the d-axis flux .

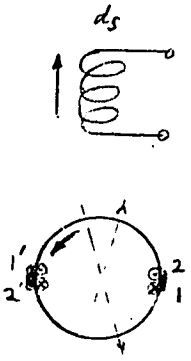

Fig. 3.7

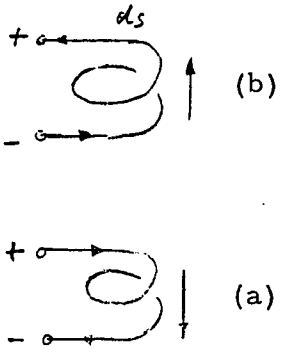

Fig. 3.8

In Fig . (3.7) the direction of the voltage and hence the current in the conductors of the pair of short - circuited coils during the period of commutation is determined by using the left hand rule . With the direction of rotation shown , the coil 1-1' is about to undergo commutation whereas the coil 2-2' has just passed through commutation . So just before the commutation the polarity of the e. m. f. is such as to produce a positive m. m. f. on the d axis and just after the commutation the e. m. f. has a polarity that produces a negative m. m. f. Hence the effect of the coil pair undergoing commutation is to convert the magnetising effect into de-magnetising effect . Thus it is possible to fix the direction of current in the short-circuited coil in Fig. 3.8(a) such that it produces a demagnetising effect on the d axis . The direction of the transformer voltage induced in the d s-winding and hence the direction of m. m. f. due to this voltage can be easily fixed as shown in Fig. 3.8(b).

So it is evident that the transformer voltage induced in the d s-winding is magnetising which makes the speed voltage demagnetising since the two

have been proved to have opposite polarities.

b) Demagnetising effect of armature reaction :

This is investigated below first for a salient-pole machine and then for the case of a smooth rotor machine .

Considering a salient-pole machine , the effect of the armature current on the flux distribution is studied for the following two cases :

i) when magnetic saturation is entirely absent and

ii) when magnetic saturation is present .

i) In the absence of magnetic saturation , the value of the flux density at a point in the air gap may be taken to be proportional to the ampere-turns acting along the magnetic path passing through that point . It is then permissible to determine separately the flux distribution curves due to the main field coils and the armature . The corresponding ordinates of these curves may then be added to obtain the total flux distribution curve , due to the joint action of both the main d_s-winding and the armature winding .

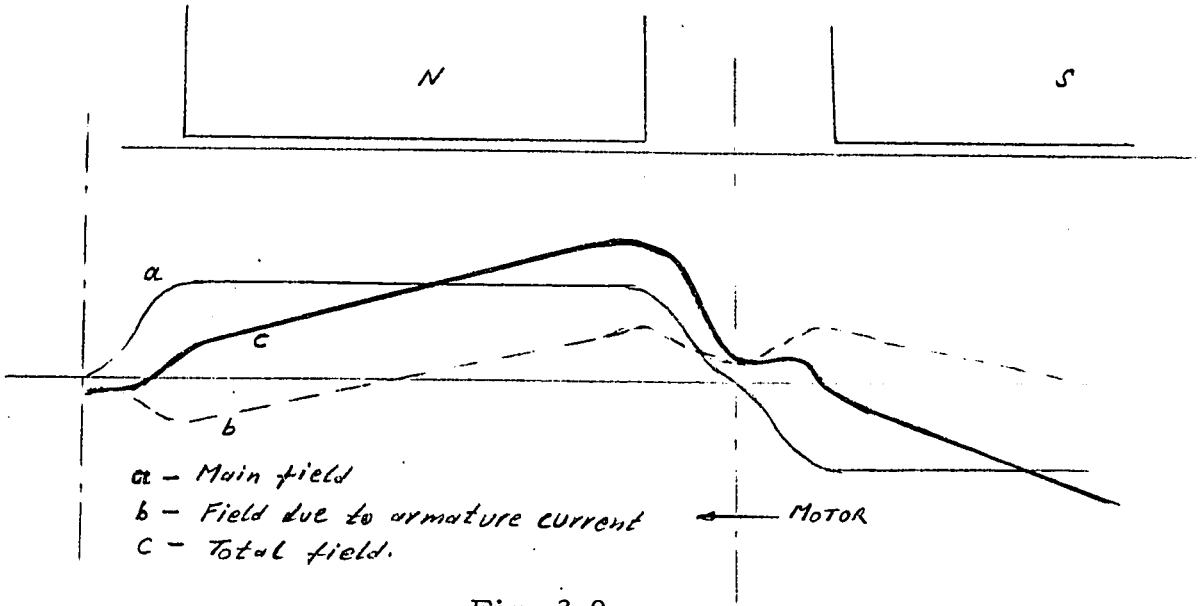

Fig. 3.9

The field form as shown in Fig. (3.9) is thus severely distorted and is no longer a symmetrical curve about the direct axis centered on the pole shoe. For this case, assuming negligible reluctance of the iron parts of the magnetic circuit and the brushes in the geometric neutral position , it can be shown

that the value of the useful flux per pole is unaltered from its value on no load because the decrease in flux on one side is compensated for by an increase on the other side . So the only effect is that the distributibution of the flux is altered .

ii) Effect of magnetic saturation : The value of e. m. f. generated in each conductor of the armature is determined at any instant by the flux density in the air gap at the point through which the conductor is passing. If the flux density in the air gap is increased much above the no-load value , the maximum value of voltage existing between adjacent segments of the commutator may become excessive .

By normally working the armature teeth at a higher degree of saturation , the effect of the armature reaction upon the flux density under one pole tip is very much reduced , although at the same time the actual value of the total flux is reduced thereby . This is illustrated in the Fig. (3. 10) which has been

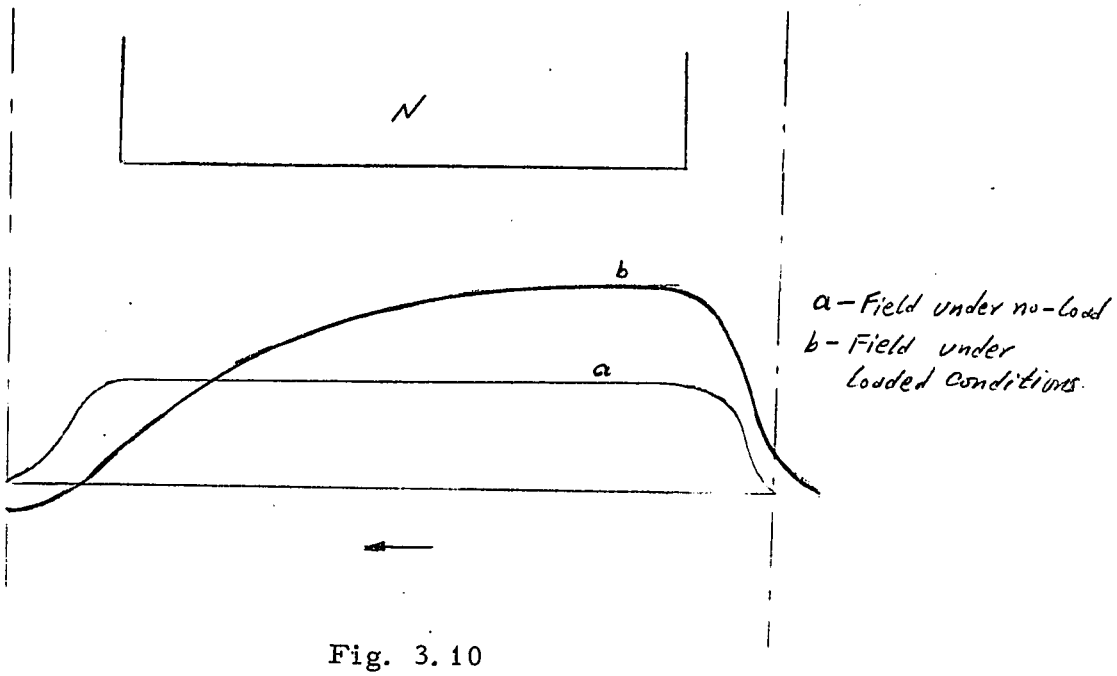

Fig. 3. 10

constructed for a uniform gap under the pole-shoe and brushes in the geometric neutral axis . Since the value of the resulting m. m. f. due to the combined effect of armature reaction and the main field winding varies uniformly over the pole arc i. e. according to a linear law , the field form under the pole-

shoe will be simply a reproduction of the portion of the magnetisation characteristic for the teeth and air gap portions of the magnetic circuit . This is shown in Fig. (3. 11) .

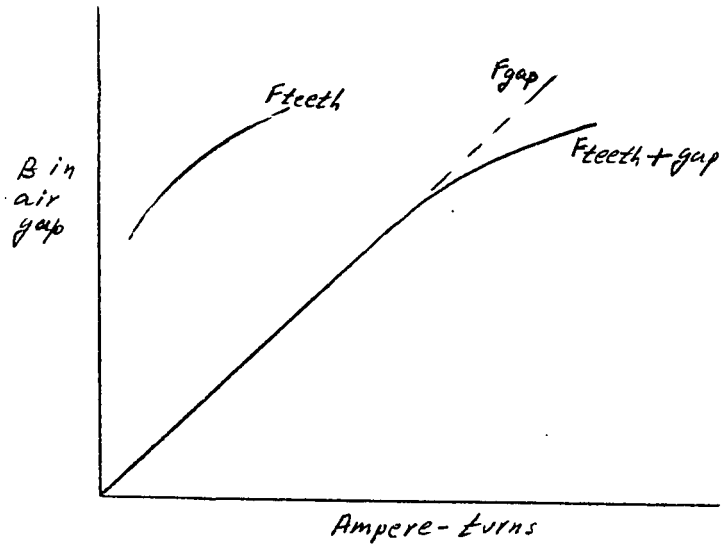

Fig. 3. 11

The actual field form for the loaded machine can then be constructed as shown in Fig. (3. 10) . For the interpolar parts of the field form , an accurate enough approximation is can be made from the shape of the open-circuit field form .

So it can be concluded that in a machine with an air gap of constant length over the whole of the pole arc , it is evident that with teeth worked at a higher degree of saturation , extreme saturation will be obtained in the teeth at the leading tip and , as a result , the total flux per pole is seriously reduced when the machine is heavily loaded .

For the case of a smooth air gap machine which is the actual machine under study , graphs similar to Fig. (3. 10) have been drawn for the resultant field form to find out the percentage reduction in the d-axis flux . The area under the flux wave form between the brushes, which are assumed to be on the geometric neutral axis , has been evaluated for three different values of the armature current and then these are compared with the area when the armature current is zero . The difference in the areas for these two conditions represent

the change in d-axis flux . Table (3. 1) shows the results of this study and the corresponding field forms are shown in Graphs (5) to (7) .

Table (3. 1)

I_{ds}	Percentage reduction in d-axis flux			
	I_{qr}	2A	4A	8A
1. 0A		2. 3	6. 0	18

A simple test on the machine can illustrate the effect of q-axis m. m. f. on the d-axis flux or vice versa . The open-circuit voltage V_r is measured across the brushes by rocking the brushes from 0 to 2π and V_r is then plotted against the brush shift . Figures (3. 12) to (3. 14) show typical results that will be obtained .

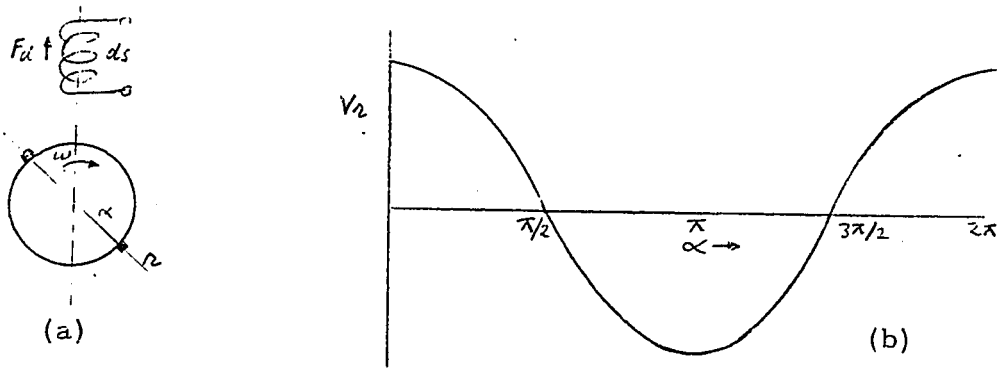

Only ds-axis excitation present

Fig. 3. 12

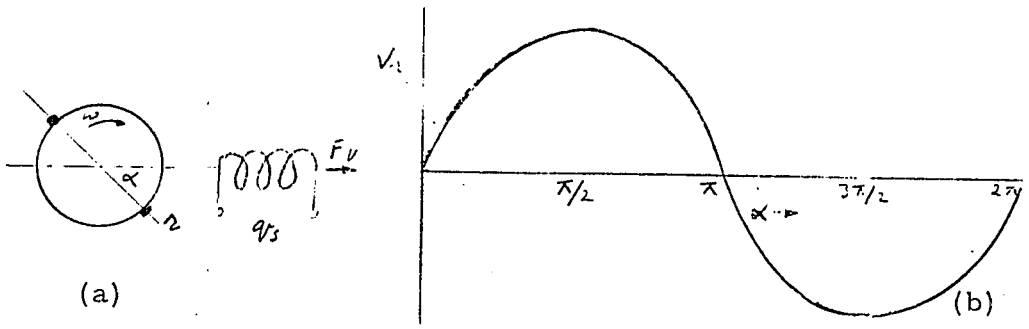

Only qs-axis excitation present

Fig. 3. 13

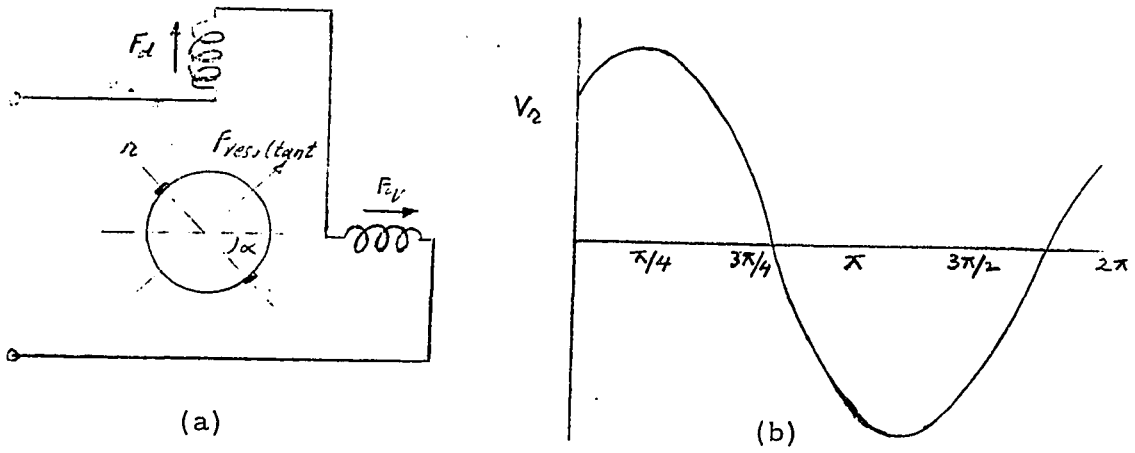

Bothds and qs-axes excitation present

Fig. 3.14

If the resultant is still below the saturation value , then

V_r in Fig. (3.14) = $\sqrt{2}$ of V_r at $\alpha=0$ in Fig. (3.12)
or at $\alpha=\pi/2$ in Fig. (3.13)

If the resultant exceeds the linear range of the magnetisation curve , then the above result is no longer true..

Another simple test to show the weakening effect of the armature m.m.f. on the direct axis flux is to drive any d.c. generator with the field separately excited from a regulated power supply . If the generator is loaded to give a heavy armature current when the field excitation is weak , opening and closing of the switch to apply and remove the load produces no perceptible effect on the field current . However , if the test is repeated for the same value of the armature current but a higher field current so that the magnetic circuit is partially saturated , a transient is oberved in the field current as shown in Fig. (3.15) .

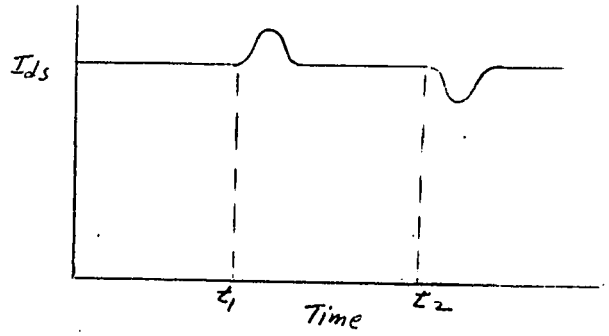

t_1 = moment of closing load switch
t_2 = moment of opening load switch

Fig. 3.15

The reduction in flux can also be explained in a different way . Since the ds-axis m. m. f. is being kept constant by the shunt field current , the flux is reduced because the reluctance of the ds axis increases .

Since Flux = m. m. f. /reluctance

= Ni/R

And also Inductance = $Nd\phi/di$

= N^2/R

So if the value of reluctance R has increased , then the value of the incremental inductance should fall since N is constant . So for a constant value of m. m. f. , the only way that the value of inductance can fall is by altering the open-circuit characteristic as shown in Fig. (3. 16).

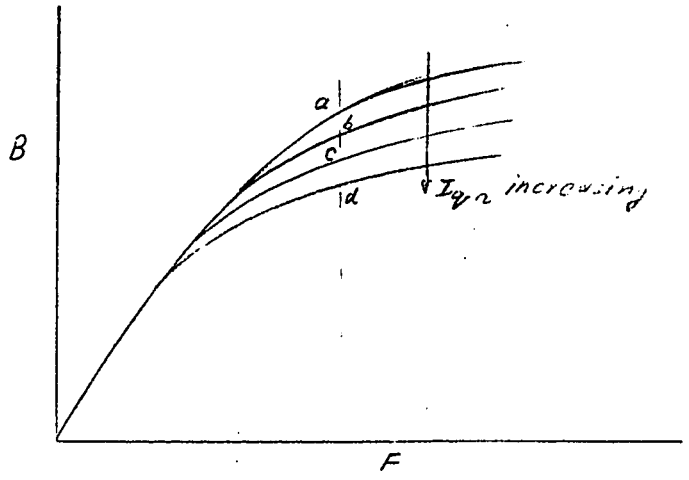

Fig. 3. 16

Reduction in the slope of the curve at points a, b, c and d indicates a fall in the value of L .

Tests I, II and III in chapter VI further confirm experimentally that the armature current does cause a demagnetising effect on the d-axis flux .

EQUIVALENT MODEL OF A D. C. SHUNT MOTOR AND ITS DYNAMIC BEHAVIOUR

a) Equivalent model : The effect of a reduction of d-axis flux which increases with increasing armature current can be simulated by assuming a fictitious winding on the ds axis producing an m. m. f. in opposition to the main field winding on the ds axis . This equivalent machine is shown in Fig. (4. 1) .

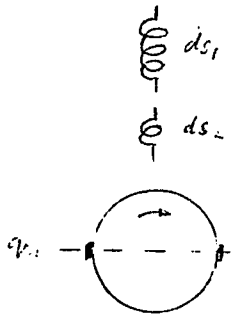

ds_1 - main field winding
ds_2 - fictitious winding simulating demagnetising effect of armature current.

Fig. 4. 1

Using the primitive commutator machine and the principles of electro-mechanical energy conversion , it is possible to predict the dynamic behaviour of this modified equivalent machine at various operating points . The impedance matrix of the primitive machine shown in Fig. (4. 1) is given by eq. (4. 1) . (see Appendix I)

$$Z = \begin{array}{c|ccc} & ds1 & ds2 & qr \\ \hline ds1 & r_{ds1} + L_{ds1}p & M_{12}p & \\ ds2 & M_{12}p & L_{ds2}p + r_{ds2} & \\ qr & -M_1'p\theta & -M_2'p\theta & r_{qr} + L_{qr}p \end{array} \qquad (4.1)$$

The actual machine is connected as shown in Fig. (4. 2) ; the connection matrix 'C' is given in eq. (4. 2) .

$$C = \begin{array}{c|cc} & i_{ds} & i'_{qr} \\ \hline i_{ds1} & 1 & \\ i_{ds2} & & -1 \\ i_{qr} & & 1 \end{array} \qquad (4.2)$$

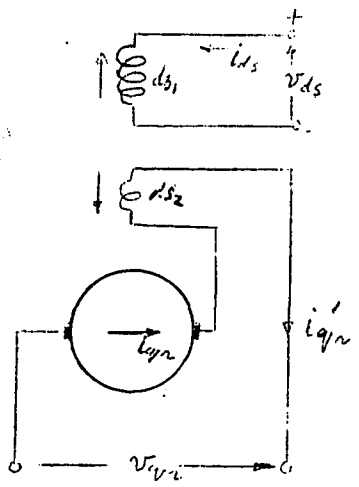

Fig. 4.2

The impedance matrix Z' of the actual machine is given by

$$Z' = C_t Z C \tag{4.3}$$

Substituting the values in eq. (4.3) gives

$$Z' = \begin{array}{c|c|c} & ds & qr \\ \hline ds & r_{ds1} + L_{ds1}p & -M_{12}p \\ \hline qr & -M_{12}p - M_1'p\theta & L_{ds2}p + M_2'p\theta + r_{qr} + L_{qr}p \\ \hline \end{array} \tag{4.4}$$

Note : r_{ds2} is considered and included in r_{qr} .

The torque equation is given by

$$T = Jp^2\theta + Dp\theta - iGi \quad \text{.... for motor}$$

$$Gi = -M_1'i_{ds} + M_2'i'_{qr}$$

$$iGi = (-M_1'i_{ds} + M_2'i'_{qr})i'_{qr}$$

$$-iGi = M_1'i_{ds}i'_{qr} - M_2'i'^2_{qr}$$

$$T = Jp^2\theta + Dp\theta + M_1'i_{ds}i'_{qr} - M_2'i'^2_{qr}$$

Hence three equations for equilibrium for the machine are given below :

$$v_{ds} = (r_{ds1} + L_{ds1}p)i_{ds} - M_{12}pi'_{qr} \tag{4.5}$$

$$v_{qr} = (-M_1'p\theta - M_{12}p)i_{ds} + (L_{ds2}p + L_{qr}p + r_{qr} + M_2'p\theta)i'_{qr} \tag{4.6}$$

$$T^r = (Jp + D)p\theta + M_1'i_{ds}i'_{qr} - M_2'i'^2_{qr} \tag{4.7}$$

Taking $p\theta$ as analogous to voltage and T^r analogous to current[7], inertia will then be represented by a capacitor of value J in mks units and the damping coefficient D by a conductance , it is then possible to make an electrical analogue for the above three equations i.e. eq.(4.5) to (4.7) using the three port circuit shown in Fig. (4.3). (see Appendix III).

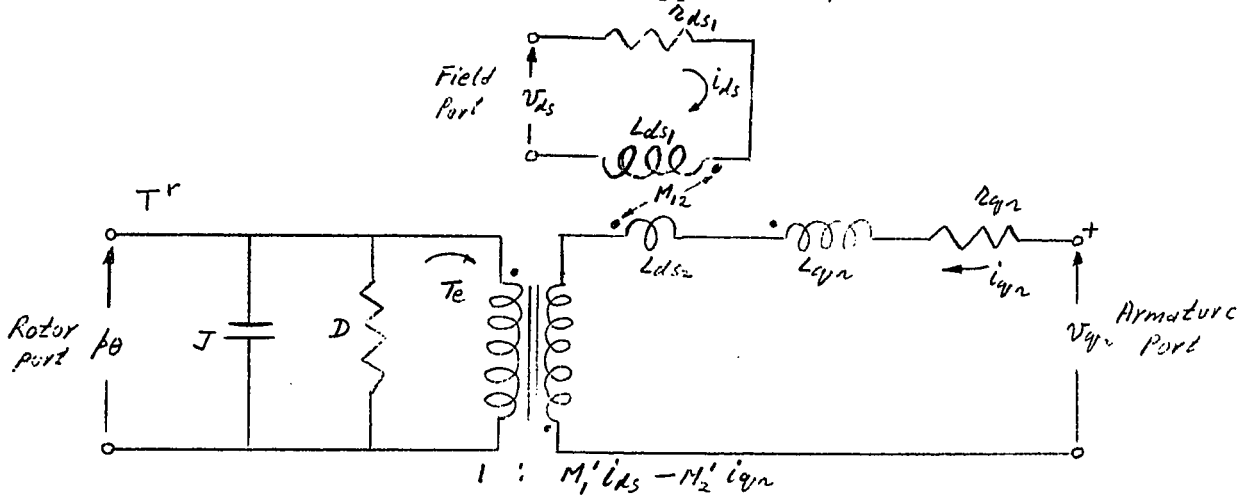

Fig. 4.3

This electrical equivalent represents the transient model and can be reduced to give a steady-state model by making all terms involving p equal to zero . The steady-state model is shown in Fig. (4.4) .

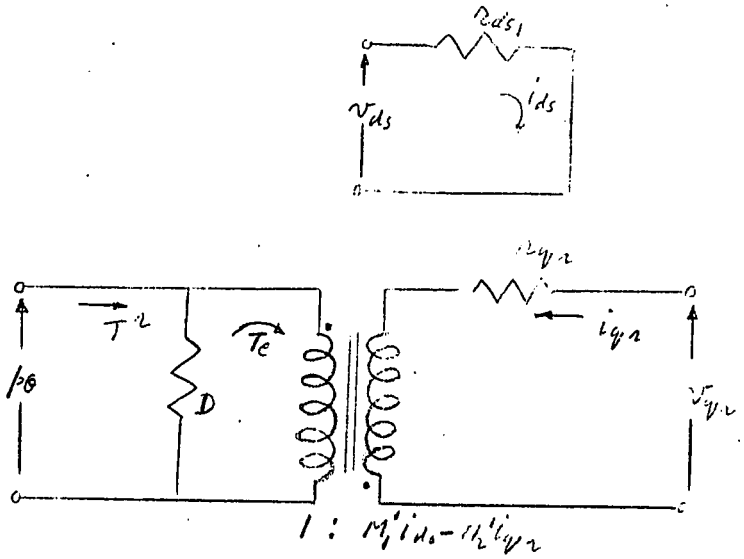

Fig. 4.4

b) Dynamic behaviour of the machine : The basic assumption in the forthcoming analysis is that all the machine parameters are constant over a certain region of operation . As long as the machine is operating in a small region about some steady-state point , the parameters can most reasonably be assumed constant and linear analysis can then be performed .

Incremental technique is extended by introducing a piecewise-linear model . Such a model assumes the machine parameters to be constant only over a certain range of operation and when the operation proceeds to another region , these parameters take new values . A linear set of differential equations describes such model in each region of operation . In order to obtain linear equations of the motor at a given operating point , each of the dependent variables will consist of two terms :

- the steady-state value of the variable that permits the motor to operate at the operating point in question , designated by subscript 0 .

- a small perturbation of the variable around the operating point designated by subscript 1 . This will represent the time-varying portion of the variable .

$$v_{ds} = v_{d0} + v_{d1} \quad , \quad v_{qr} = v_{q0} + v_{q1}$$

$$i_{ds} = i_{d0} + i_{d1} \quad , \quad i_{qr} = i_{q0} + i_{q1}$$

$$T^r = T_0 + T_1 \quad , \quad \omega = \omega_0 + \omega_1$$

Substituting these variables in the three equations of equilibrium i.e. eq. (4.5) to (4.7), the following equations are obtained :

$$v_{d0} + v_{d1} = (r_{ds1} + L_{ds1}p)(i_{d0} + i_{d1}) - M_{12}p(i_{q0} + i_{q1})$$

$$v_{q0} + v_{q1} = \{-M_1'(\omega_0 + \omega_1) - M_{12}p\}(i_{d0} + i_{d1}) + \{L_{ds2}p + L_{qr}p + r_{qr} + M_2'(\omega_0 + \omega 1)\}(i_{q0} + i_{q1})$$

$$T_0 + T_1 = (Jp + D)(\omega_0 + \omega_1) + M_1'(i_{d0} + i_{d1})(i_{q0} + i_{q1}) - M_2'(i_{q0} + i_{q1})^2$$

On expanding the above equations , we get

$$v_{d0} + v_{d1} = (r_{ds1} + L_{ds1}p)i_{d0} + (r_{ds1} + L_{ds1}p)i_{d1} - M_{12}pi_{d0}$$

$$v_{q0} + v_{q1} = -M_1'\omega_0 i_{d0} + (L_{ds2}p + L_{qr}p + r_{qr} + M_2'\omega_0)i_{q0} - M_{12}pi_{d0} -$$

$$M_1'\omega_0 i_{d1} - M_1'\omega_1 i_{d0} - M_1'\omega_1 i_{d1} - M_{12}pi_{d0} + (L_{ds2}p + L_{qr}p +$$

$$r_{qr})i_{q1} + M_2'\omega_1 i_{q0} + M_2'\omega_1 i_{q1} + M_2'\omega_0 i_{q1}$$

$$T_0 + T_1^r = (Jp + D)\omega_0 + M_1'i_{d0}i_{q0} - M_2'i_{q0}^2 + (Jp + D)\omega_1 + M_1'i_{d1}i_{q1} +$$

$$M_1'i_{d1}i_{q0} - M_2'i_{q1}^2 - 2M_2'i_{q0}i_{q1}$$

The values of higher order terms involving the product of incrementals are negligible . Substituting the steady-state values from the above equations , we are left with only the time-varying portions of the above equations which are given below :

$$v_{d1} = (r_{ds1} + L_{ds1}p)i_{d1} - M_{12}pi_{q1}$$

$$v_{q1} = (-M_1'\omega_0 - M_{12}p)i_{d1} + (L_{ds2}p + L_{qr}p + r_{qr} + M_2'\omega_0)i_{q1} +$$

$$(M_2'i_{q0} - M_1'i_{d0})\omega_1$$

$$T_1^r = (Jp + D)\omega_1 + M_1'i_{q0}i_{d1} + (M_1'i_{d0} - 2M_2'i_{q0})i_{q1}$$

Let the Laplace transforms of the above time-varying quantities be represented by capital letters and that of $\omega(t)$ by Ω_1 . Also assuming that the initial values of these quantities are zero for all time-varying variables and taking the Laplace trnasforms , we have the following equations :

$$V_{d1}(s) = (r_{ds1} + L_{ds1}s)I_{d1} - M_{12}sI_{q1} \tag{4.8}$$

$$V_{q1}(s) = (-M_1'\omega_0 - M_{12}s)I_{d1} + (L_{ds2}s + L_{qr}s + r_{qr} + M_2'\omega_0)I_{q1} - (M_1'i_{d0} - M_2'i_{q0})\Omega_1 \tag{4.9}$$

$$T_1^r(s) = (Js + D)\Omega_1 + M_1'i_{q0}I_{d1} + (M_1'i_{d0} - 2M_2'i_{q0})I_{q1} \tag{4.10}$$

Then the incremental equivalent circuit for the motor is given below in Fig. (4.5) :

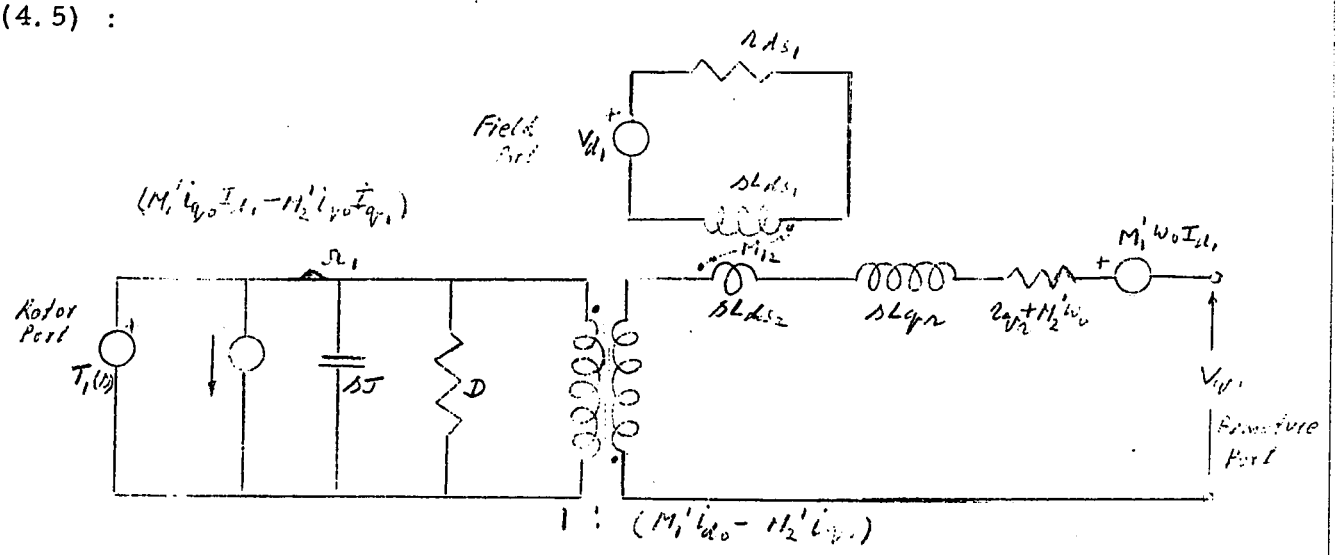

Fig. 4.5

On drawing the block diagram for the above circuit , we have

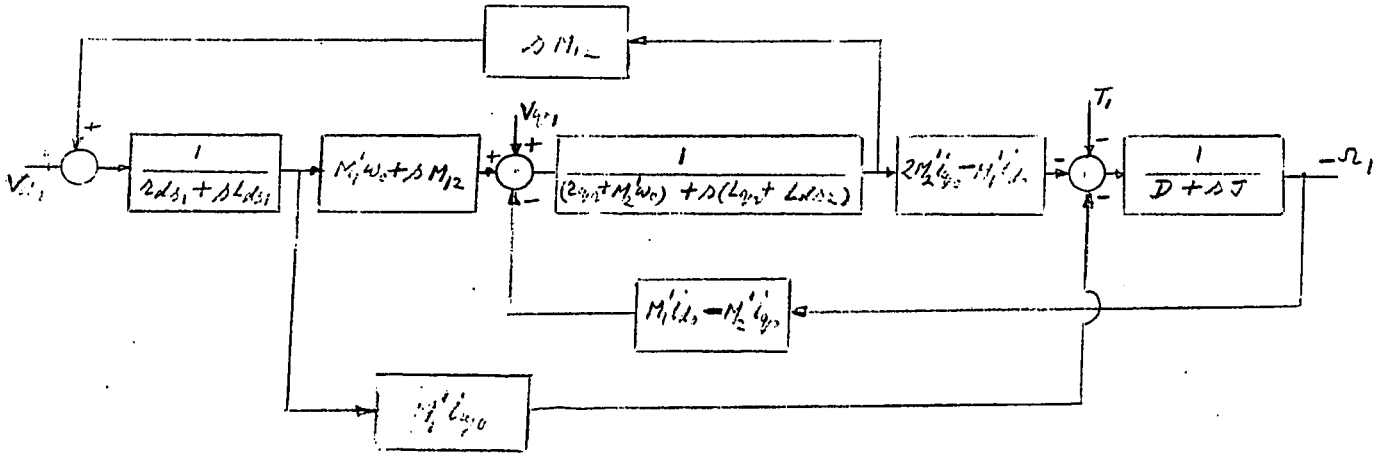

Fig. 4.6

Using the block diagram in Fig. (4.6) , it is now possible to simulate this on an analogue computer for further detailed study of the motor.

But as we are interested in the variation in speed , or rather the response Ω_1 , with a torque input which may be a step input . So $v_{d1} = v_{q1} = 0$ and the block diagram of Fig. (4.6) reduces to the one shown in Fig. (4.7).

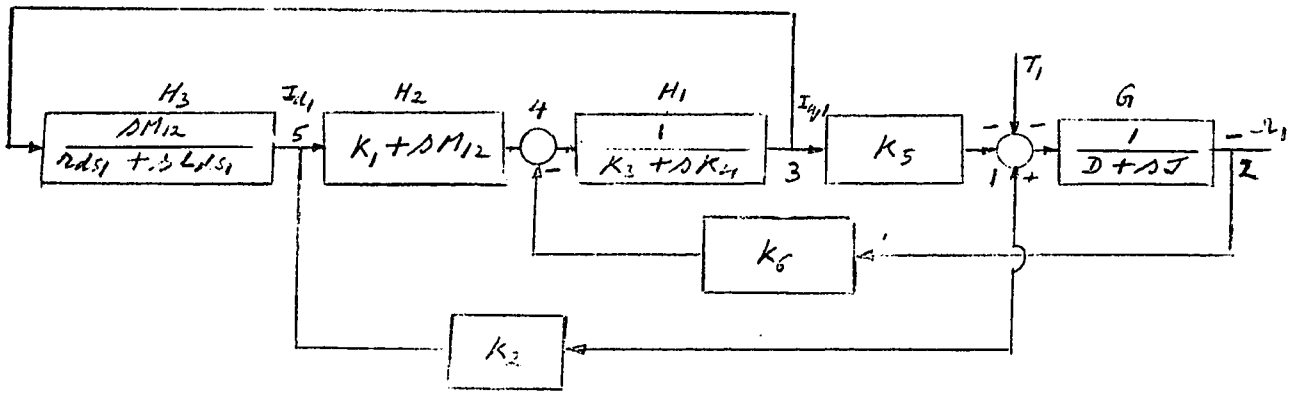

Fig. 4.7

To find the transfer function Ω_1 / T_1 , signal flow technique is used [8] and the signal flow diagram is shown in Fig. (4.8) .

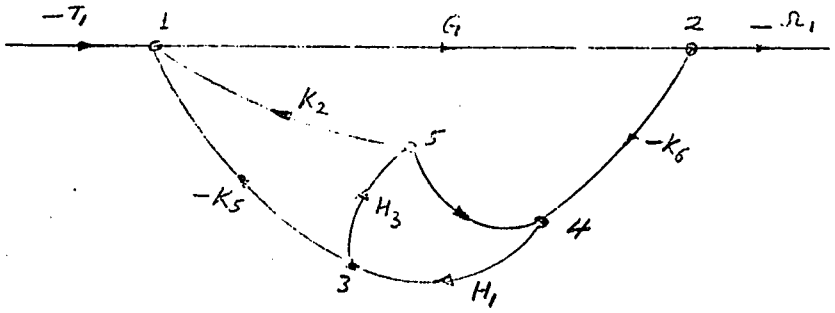

Fig. 4.8

$$\Delta = 1 - GK_5K_6H_1 - H_1H_2H_3 + GK_6K_2H_1H_3$$

$$\frac{\Omega_1}{T_1} = \frac{G(1 - H_1H_2H_3)}{1 - K_5K_6GH_1 - H_1H_2H_3 + K_2K_6GH_1H_3}$$

$$\frac{\Omega_1}{T_1} = \frac{\beta_2 s^2 + \beta_1 s + \beta_0}{s^3 + a_2 s^2 + a_1 s + a_0} \qquad (4.11)$$

where $\beta_2 = 1/J$

$$\beta_1 = \frac{(L_{qr} + L_{ds2})r_{ds1} + (r_{qr} + M_2'\omega_0)L_{ds1} - M_{12}M_1'\omega_0}{J\{(L_{qr} + L_{ds2})L_{ds1} - M_{12}^2\}}$$

$$\beta_0 = \frac{(r_{qr} + M_2'\omega_0)r_{ds1}}{J\{(L_{qr} + L_{ds2})L_{ds1} - M_{12}^2\}}$$

$$\alpha_2 = \frac{J(L_{qr} + L_{ds2})r_{ds1} + L_{ds1}\{J(r_{qr} + M_2'\omega_0) + D(L_{qr} + L_{ds2})\} - M_{12}(DM_{12} + M_1'\omega_0 J)}{J\{(L_{qr} + L_{ds2})L_{ds1} - M_{12}^2\}}$$

$$\alpha_1 = \frac{\begin{array}{l} DL_{ds1}(r_{qr} + M_2'\omega_0) + r_{ds1}\{J(r_{qr} + M_2'\omega_0) + D(L_{qr} + L_{ds2})\} \\ -M_{12}DM_1'\omega_0 - L_{ds1}(2M_2'i_{q0} - M_1'i_{d0})(M_1'i_{d0} - M_2'i_{q0}) \\ + M_{12}M_1'i_{q0}(M_1'i_{d0} - M_2'i_{q0}) \end{array}}{J\{(L_{qr} + L_{ds2})L_{ds1} - M_{12}^2\}}$$

$$\alpha_0 = \frac{r_{ds1}D(r_{qr} + M_2'\omega_0) - (2M_2'i_{q0} - M_1'i_{d0})(M_1'i_{d0} - M_2'i_{q0})r_{ds1}}{J\{(L_{qr} + L_{ds2})L_{ds1} - M_{12}^2\}}$$

c) Results obtained from the equivalent model : It will give support to the equivalent model developed above if it can be demonstrated that instability results from the substitution of numerical values in the equations that are known to produce instability in the actual machine . Also , it should be possible to show that an increase increase in I_{ds} will restore stability , such an increase corresponding to a compensating effect for the d-axis flux weakening that initiated the instability .

Experimentally it was observed that motor was unstable at the operating point defined below :

i_{qo} = 3.1A , i_{do} = 0.8A , ω_o = -2650 r.p.m. = -278 rad./sec.

Open circuit voltage at 1800 r.p.m. = 28 volts

M_1' = o.c. voltage/$\omega_o i_{do}$ = 28/0.8 x 0.188

= 0.186 H/rad.

$T_e = M_1' i_{do} i_{qo}$ = 0.186 x 0.8 x 3.1 = 0.462 N.m.

Since the machine was on no load , we have

$Dp\theta = T_e$ Hence D = 0.462/278 = 0.0017 N.m./rad./sec.

To determine the demagnetising effect of i_{qr} , the equivalent i_{qs} is first calculated and then the corresponding value of the drop is read from Graph(11)

$$i_{qs} = 140 \times 3.1/324 = 1.34A$$

Voltage drop from Graph(11) = 1.5 volts

Hence $M_2' = 1.5/188 \times 3.1 = 0.00255$ H/rad.

Now if a sinusoidal distribution of the flux is assumed , then M_2' will have the same value as the mutual inductance between the qr and ds2 windings as it would if ds2 were on the q-axis .

Hence $M_2' = k\sqrt{L_{qr} L_{ds2}}$

$$L_{ds2} = M_2'^2/k^2 L_{qr}$$

$$= 0.00255 \times 0.00255/0.8^2 \times 0.05$$

$$= 0.0002 \text{ H}$$

The value of k=0.8 was found experimentally by exciting the qs winding with alternating current and measuring the voltage induced in the qr winding .Knowing the turn ratio it is possible to calculate the value of k . Using this value of

L_{ds2} , it is now possible to calculate the value of the mutual inductance M_{12} between the ds1 and ds2 windings. Since both of these windings have been assumed to be on the ds axis , the value of k can be assumed to be unity .

Hence $M_{12} = k\sqrt{L_{ds1} L_{ds2}}$

$= \sqrt{0.4 \times 0.0002} = \sqrt{0.00008} = 0.009$ H

Using the above values and $r_{qr} = 0.5\Omega$, the transfer function is given by eq. (4.12) .

$$\frac{\Omega_1}{T_1} = \frac{42.2s^2 + 1090s - 1240}{s^3 + 26s^2 - 10.5s + 108} \qquad (4.12)$$

To find the step response of the transfer function of eq. (4.12) , a digital computer was used to solve the following three first-order differential equations obtained from the transfer function using state space techniques[9]. (see Appendix IV)

$$\dot{x}_1 = -26x_1 + x_2 + 42.2$$

$$\dot{x}_2 = 10.5x_1 + x_3 + 1090$$

$$\dot{x}_3 = -108x_1 - 1240$$

$$\Omega_1 = x_1$$

Now for the same fixed torque , which is the no-load torque and hence assumed to be constant , the above calculations were repeated for the following operating point :

$i_{do} = 3.5$A , $i_{qo} = 0.91$A , $\omega_o = 1100$ r.p.m.

The results are shown in Graph (9) . This shows that the system which was unstable at $i_{do} = 0.8$A has now become stable at $i_{do} = 3.5$A . Also this system at $i_{do} = 0.8$A becomes stable when M_{12} is put equal to zero i.e. when there is no fictitious winding d_{s2} . This is exactly what is expected from the motor , thus supporting the validity of the above equivalent model .

The value of r_{qr} substituted in the above equations requires some comment because several computer runs showed that instability did not occur until r_{qr} was reduced to a value of 0.5Ω which is well below the

practical value measured in the laboratory . (see Graph (13))

The equations were derived for incremental disturbances about a steady-state operating point . Observations in the laboratory , especially when oscillations in the motor speed occurred , showed that the speed and armature current i_{qr} were always in excess of the steady-state values immediately preceding the onset of instability . Consequently it was decided to choose a new set of values to represent the mean operating point about which the oscillations were occurring . (see Test V)

The step response of the motor was now calculated at a new operating point defined below :

i_{qo} = 15A , i_{do} = 0.8A , ω_o = 3000 r.p.m. and r_{qr} = various values ranging from 1Ω to 2Ω . Graph (14) shows the variation of the amplitude of the oscillation in speed with different values of r_{qr} within the practical range . The system is found to be unstable for all values of r_{qr} within the range of the practical values . Graph (14) has been drawn for amplitude at a time of 1 second after the application of the step function .

d) Discussion of results : From the various calculations using the above model , it was found that the value of r_{qr} = 0.5 ohm gave results corresponding to instability . Substitution of the more realistic value r_{qr} = 1.8 ohms damped out any oscillations unless the other parameters were changed to represent the average values following the application of the step function .

Since the equivalent model is based on small increments about an average value , it was decided that for more accurate results , the values of operating point as described in c(i) above should have been higher . From experimental observations , a value of i_{qo} = 15A and ω_o = 3000 r.p.m. were selected and step response of the model was determined for various values of r_{qr} between the practical range of 1Ω to 2Ω . This system was found to be unstable .

Graph (14) shows the variation of amplitude with various values of r_{qr} and it can be seen that system is stable when r_{qr} is made much larger than 2Ω .

By reducing the value of i_{qo} , say to a value of 10A or 7.5A , it might be possible to obtain oscillations with the value of r_{qr} between 1Ω and 2Ω . It is evidentally very difficult to fix the operating point about which the oscillations should be assumed which would agree with the practical results .

Another variable factor is the proper value of r_{qr} . Since as the value of i_{qr} goes up the value of r_{qr} falls down which thus creats a cumulative effect in making the system more unstable . So what exact value of r_{qr} should be taken is again a matter which makes the analysis more of an approximation .

To get results which would agree exactly with the experimental values, the assumption of small increments cannot be valid since the oscillations have quite a large amplitude as observed during the experiments . For such a complete solution the initial values of parameters should be those corresponding to conditions immediately preceding instability . Then , for successive instants in time following instability , the parameter values require repeated revision for each instant . Since this way the analysis would be very laborious and time-consuming , an incremental model analysis would be more straightforward , although less accurate , if the operating point is to be taken as the average value about which oscillations take place .

The equivalent model is thus more useful in determining whether the steady-state conditions are close to the limit of stability rather than in analysing the conditions during oscillatory instability .

CHAPTER V

MACHINE PARAMETERS - DISCUSSION OF

MACHINE PARAMETRES

When the motor is to become a component in an actual system , it is essential to know the exact value of the various parameters of the machine in order to predict its dynamic behaviour . The methods used for their measurement will be governed by the actual conditions under which the motor is going to operate . For example if the value of the inductance is to be measured then , depending upon the actual conditions of operation , we will have to use the value of apparent inductance , transient inductance or incremental inductance . For steady-state operation of a. c. machines the apparent inductance is to be used ; for a sudden change of operating conditions the transient inductance is to be used and if it is an oscillatory system with small oscillations then incremental inductance value will have to be used . So now depnding upon which value of inductance is to be used , the method of its measurement will have to be selected .

This chapter describes , briefly , the different types of parameters and the various methods available for their measurement so that given the actual working conditions of the machine , the appropriate method can be used . A table at the end of the chapter gives the values of the parameters and method of measurement used for the purposes of analysis of the shunt motor .

Referring to eq. 4. 4 , the impedance matrix $\mathbf{Z}'$ of the actual machine , the various parameters are r_{ds1} , r_{qr} , L_{ds1} , L_{ds2} , L_{qr} , M_1' , M_2' and M_{12} . Also there are mechanical constants J and D , which appear in the torque equation .

a) Machine resistances : The resistance r_{ds1} could be measured by means of the voltmeter-ammeter , Wheatstone , or Kelvin bridge methods . The resistance of the armature consists of that of conductors , carbon brushes and the brush contact resistance . Since the carbon has a non - linear resistance , its value varies with current and also the contact resistance varies with speed . Thus the total armature resistance cannot be assumed to be constant . Three methods for the measurement of r_{qr}

are outlined below :

i) A simple method of measuring r_{qr} will be to run the machine at a constant speed and find out the values of resistance for the various values of armature current using the voltmeter-ammeter method . The armature is supplied with a variable voltage d. c. supply . This test can be repeated for various speeds .

There will be an error in this method due to the speed voltage generated by the residual magnetism which may add to , or subtract from , the external voltage applied to the armature depending upon the direction of residual flux . One way to overcome this error is to repeat the tests with the direction of rotation reversed . The mean of these two curves will give the correct results provided that the brushes are mounted so that they bear radially on the commutator surface .

ii) Another method for the measurement of r_{qr} has been suggested by Saunders[10] . In this method short-circuit current and open- circuit voltage characteristics of the machine , as functions of the field current , are obtained when the machine is being run as a generator for two different speeds ω_1 and ω_2 . This test is confined to the lower portion of the saturation curve where cross magnetisation due to the armature current does not introduce a net demagnetisation of the poles .

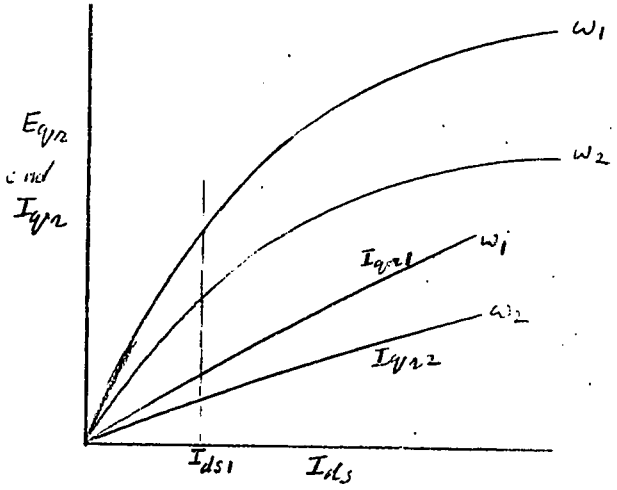

Fig. 5.1

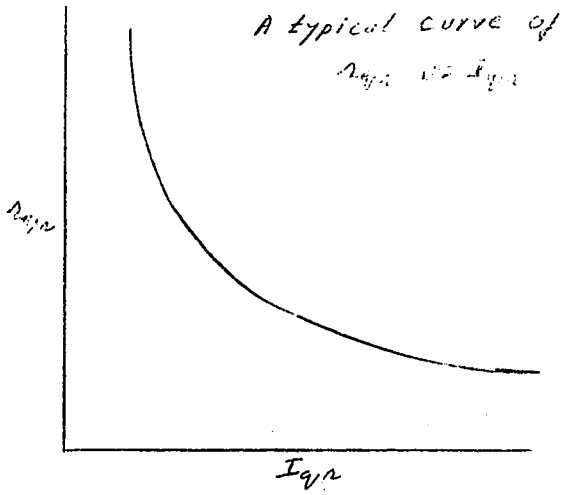

Fig. 5.2

Then if K_a is the speed voltage constant for voltage measured at the brushes because of the armature current , we have ,

$$E_{qr1}/I_{qr1} = r_{qr} - K_a\omega_1$$

Also $$E_{qr2}/I_{qr2} = r_{qr} - K_a\omega_2$$

From these two equations , we have

$$r_{qr} = \frac{1}{\omega_2 - \omega_1}\,\omega_2\{(E_{qr1}/I_{qr1}) - (\omega_1 E_{qr2}/I_{qr2})\}$$

The assumption made in this method is that r_{qr} is constant at all speeds which is not strictly true . But the error may not be significant since the effective resistance is more a function of armature current than of speed[12] .

To plot the variation of r_{qr} with speed , it is necessary to maintain the field current and the short-circuit current constant throughout the speed range. This is because r_{qr} has been shown to vary with different field currents when the speed is maintained constant . The adjustment of the short-circuit armature current at each speed will be made by a variable resistance put across the armature terminals . Instead of E_{qr} , the above equation for r_{qr} will have $E_{qr} - V_t$ where V_t is the voltage across the variable resistance .

iii) The third method , believed to be original , is applicable only in cases where the qr-axis m. m. f. can be simulated by a qs-axis m. m. f. The machine is run as a generator and a voltage vs. armature current characteristic is plotted , field current and speed being maintained constant . The voltage drop because of the loading consist of two parts : a drop $I_{qr}r_{qr}$ and the drop due to the demagnetising effect of I_{qr} . Now since it is possible to produce the effect of I_{qr} on the flux by using the qs winding , another graph of voltage vs. equivalent I_{qr} can be plotted . The drop in this case will be exclusively due to the demagnetising effect of I_{qr}. From Fig. (5. 3) the armature resistance will be

$$r_{qr} = bc / I_{qr}$$

The range of values of r_{qr} was taken from the results obtained by using method (i) above . These results are plotted in Graph (13) .

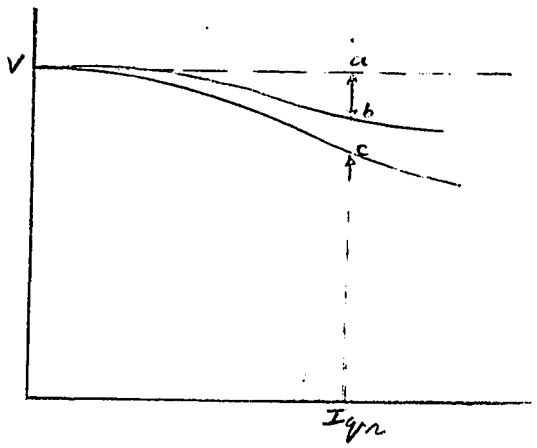

Fig. 5.3

b) Machine inductances : The value of inductance may vary depending upon the actual working conditions and hence it is necessary to befamiliar with different types of inductances before going into their measurements . Inductance is defined as the change of flux-linkages with exciting current . For practical purposes , an assumption is often made that flux is proportional to the current . However , due to the presence of saturation , inductance is a variable quantity . Hence in all inductance measurements effects oi saturation and hysteresis should be considered .

Mutual inductance is said to exist when a current flowing in one circuit sets up a flux that links with second circuit . Then mutual inductance M_{12} is given by :

$$M_{12} = N_1 \phi_1 / I_2$$

There are three different types of inductances :

i) Steady-state or apparent inductance

ii) Transient inductance

iii) Incremental inductance

i) Steady-state or apparent inductance : It should be considered when there is a. c. excitation giving symmetrical working on the B - H loop . This can be measured by the conventional voltmeter-ammeter method .

ii) Transient inductance : If a load is suddenly applied or if a short circuit occurs or if the input voltage changes by a step , the sudden change

introduces eddy currents in any solid iron parts of the machine resulting in transient magnetomotive forces that change the air gap flux . The appropriate inductance cannot be explained in terms of the B-H loop because the eddy current magnetomotive forces distort the hysteresis loop during the transient period . The general effect is to reduce the value of inductance below the steady-state value due to high frequency components of current causing eddy-current magnetomotive forces which oppose the original m. m. f. and drive the flux into leakage paths . During the transient period , the inductance increases from the initial value to the final steady-state value .

iii) Incremental inductance : If a d. c. machine is driving a load with a fluctuating torque e. g. a d. c. motor driving a reciprocating compressor , the torque fluctuations produce corresponding current pulsations in the armature circuit at a frequency proportional to the rotor speed and an alternating current is thereby superimposed on the direct current . The inductance offered to this small component of alternating current is called the incremental inductance .

Thus the incremental inductance depends upon the magnitude of both a. c. and d. c. magnetisation and upon the magnetic history of the core . The effect is the presence of a minor hysteresis loop on the usual hysteresis loop as shown in Fig. (5. 4) .

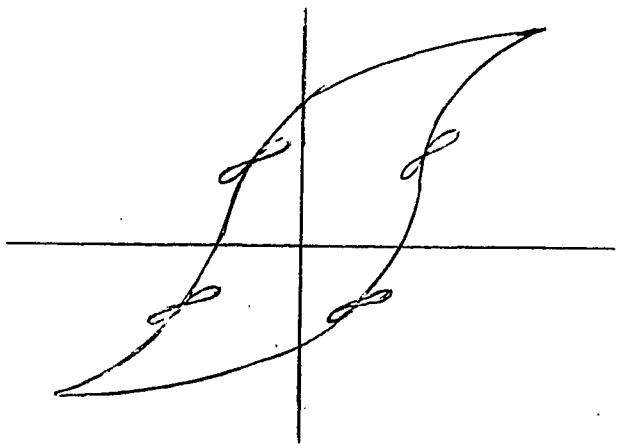

Fig. 5. 4

In general , in dealing with the incremental inductance , one must distinguish between the consequence of superimposing an incremental d. c.

magnetisation and an incremental a. c. magnetisation . In the former case it is also necessary to distinguish between the effects of positive polarity increment and a negative polarity increment ; each increment gives a loop but one loop slopes upward and the other downwards as in Fig. (5.4) . The butterfly shape of the loop comes from the fact that both positive and negative increments of magnetisation are illustrated . The incremental permeability and hence the incremental inductance is proportional to the slope of the line joining the tips of this loop .

c) Measurement of transient inductance : Two methods are outlined below :

i) A transient method suggested by Bowers and quoted by Saunders[12] :

This method calls for the measurement of the time constants by means of oscillograms when step values of voltage are applied to the various circuit elements . Fig. (5.5) shows the circuit necessary to obtain L_{ds1} and M_{1qr} .

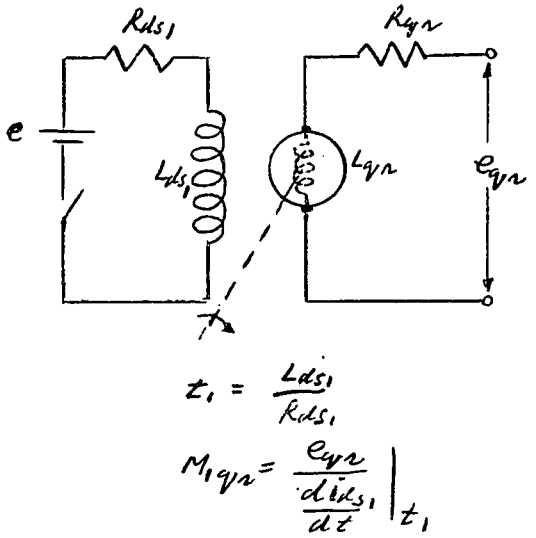

Fig. 5.5

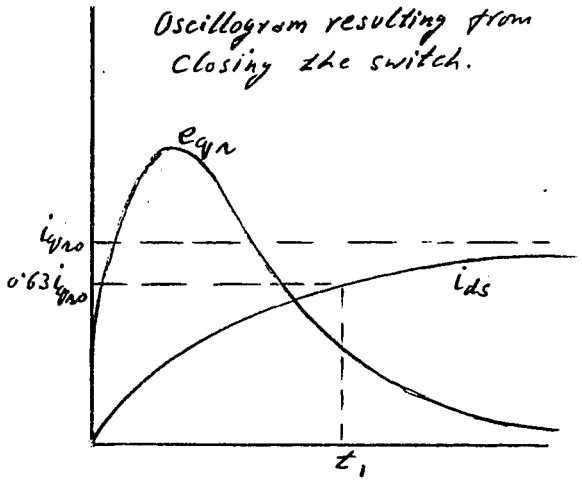

Fig. 5.6

Even though the armature rotation may introduce some erroneous results , it is considered better to have it rotating slowly , say at ten percent speed . This will take into account some effects of commutation . If there is a coupling linkage between armature and the field , this test should be performed at standstill i. e. $\omega = 0$.

This method is laborious in that interpolation of the oscillograms

consumes a considerable time . Also it is difficult to associate the value of inductance found by this method with the degree of saturation because the flux during this period is produced not only by the actual coil m. m. f. , but by the resultant of this and the eddy current m. m. f..

ii) D. C. Methods : Jones[3] , Prescott and El-Kharashi[16] and Barton[5] have used these methods employing direct current . Fundamentally all these d. c. methods are similar : they differ in the device employed to measure the flux linkages . The principle involved will be clear from the following :

For the two circuits (1) and (2) the e. m. f. induced in circuit (1) by a change in current i_2 in circuit (2) is given by :

$$e_1 = d(M_{12}i_2)/dt$$

During a period from t_1 to t_2

$$\int_{t_1}^{t_2} e_1 dt = (M_{12}i_2'') - (M_{12}i_2')$$

Where the current changes from i_2' to i_2'' during the period in question . If the current reverses from I_2 to $-I_2$, then

$$\int e_1 dt = 2M_{12}I_2$$

$$M_{12} = \int e_1 dt \,/\, 2I_2$$

The integration can be carried out by a flux meter , a ballistic galvanometer or an electronic integrator . The circuit diagram for this method used by Prescott and El-kharashi[16] is given in Fig. (5.7) .

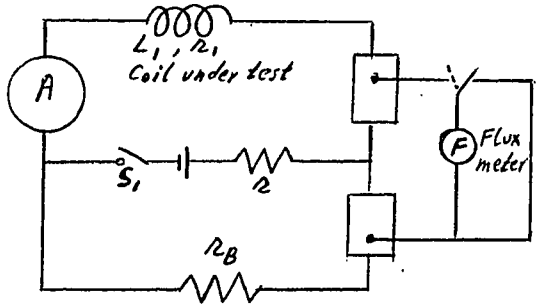

$$L_1 = \frac{\Delta\phi}{\Delta I} = \frac{\phi_0 - \phi_1}{I_0 - I_1}$$

ϕ_0 = Initial flux in coil A
ϕ_1 = Final flux in coil A
I_0 = Initial current in coil A
I_1 = Current flowing in the coil A at time t_1 after opening S_1

Fig. 5.7

The circuit used by C. V. Jones[3] is given in Fig. (5.8) .

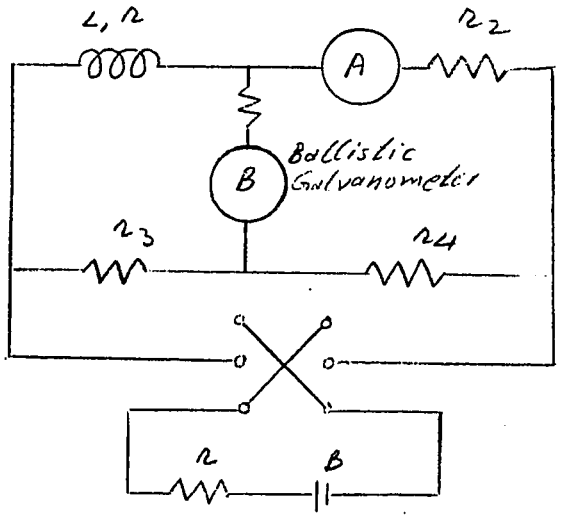

$L = \frac{1}{2}\frac{\lambda}{I}\frac{r_3 + r_4}{r_4}$

λ = flux linkages.

Fig. 5.8

d) Measurement of incremental inductance :

i) A. C. Method suggested by Saunders[12] :

This method involves the use of alternating current of either low or power frequency in place of the direct current employed by Bowers . Figs. (5.9) and (5.10) show the development of the equivalent circuit . The circuit in Fig. 5.9(a) permits the superposition of direct current upon alternating current employed for the measurement of inductance , while the circuit in Fig. 5.9(b) finds the inductance of an essentially unsaturated machine .

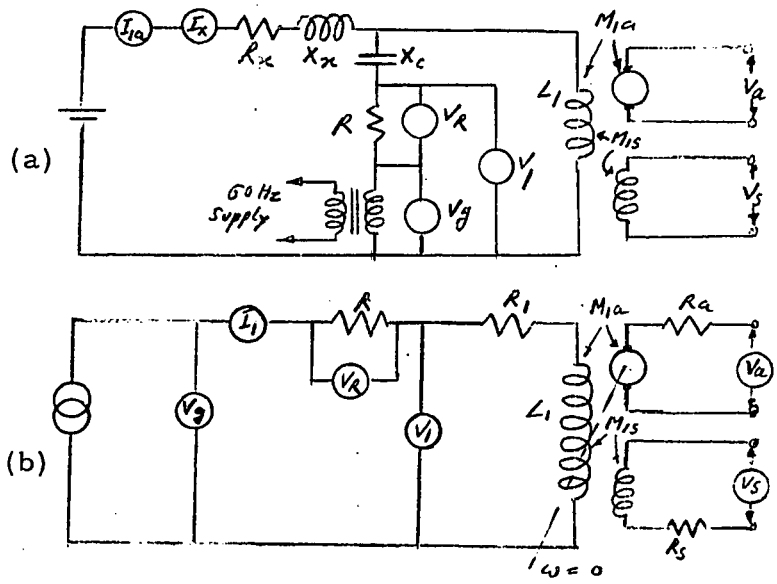

Fig. 5.9 (contd.)

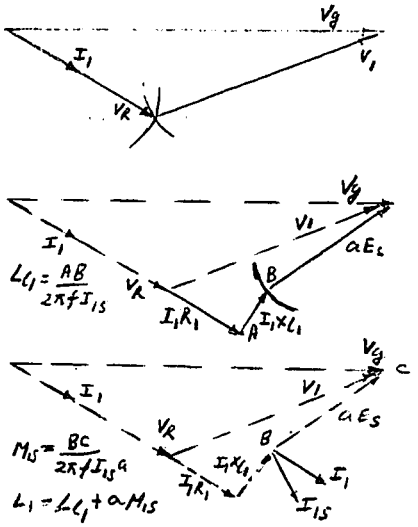

Fig. 5.10

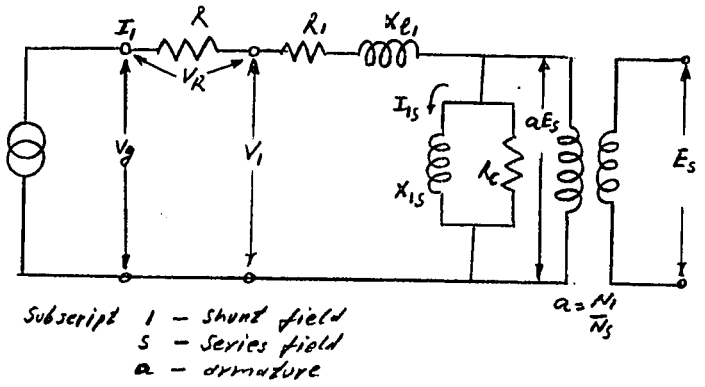

Fig. 5.10

Fig. 5.9(a) For measuring machine parameters by a.c. test in which effects of superimposed d.c. fields can be included.

5.9(b) Same as (a) but when no d.c. is to be superimposed or when battery circuit a.c. impedence is high compared to the d.c. machine.

5.9(c) Equivalent circuit of the d.c. machine while undergoing a.c. tests.

Fig. 5.10. Evolution of circuit diagram of the circuit in Fig. 5.9(c) by triangulation methods. The dotted lines indicate the vectors found in the preceding figure.

ii) A. C. Bridge method : Bridges can be used to measure the resistance , inductance or capacitance . Most of the bridges can be set up in the laboratory using 60 Hz. Hay's and Maxwell's bridges are especially useful for this purpose. With direct current superimposed , the incremental inductance is measured .

The values of inductances to be used in investigating the dynamic behaviour of the equivalent model should be the incremental inductances since this model is based on small perturbations being assumed about the operating point . For this , the A. C. method suggested by Saunders or the A. C. bridge method are suitable .

Over the linear range of operation , the values of incremental and apparent inductances are the same . For the calculations using the model in chapter IV (c) , the values of apparent inductances were used since a ds-field current of 0. 8A does not cause magnetic saturation in the d-axis and similarly a current of 3. 1A in the qr axis does not cause saturation in the q axis . The values of apparent inductances L_{ds1} and L_{qr} were obtained using the voltmeter-ammeter method with excitation of 1A at 60Hz .

The values of rotational inductances were calculated from the open-circuit voltage characteristic given in Graph (4) at the appropriate point of operation .

The equivalent machine also contains a fictitious winding representing the demagnetising effect of the armature m. m. f. on the d axis . An indirect method is used to find out the self inductance L_{ds2} and the mutual inductance

with the ds1 winding, denoted by M_{12} . The voltage drop due to the demagnetising effect of armature current was found from Graph (11) . Since this drop in voltage is due to a negative speed voltage , it is possible to calculate the value of the speed coefficient M_2' between the armature and the fictitious winding .

If a sinusoidal field form and a uniformly distributed winding are assumed , then it can be shown that the speed coefficient is the same as the mutual inductance between these two windings i.e. the fictitious winding and the armature winding .

Hence $$M_2' = k_1 \sqrt{L_{ds2} L_{qr}}$$

and M_{12} is given by

$$M_{12} = k_2 \sqrt{L_{ds2} L_{ds1}}$$

where k_1 = Coupling factor between the fictitious winding and the armature winding which can be assumed to be same as between the ds1 winding and the armature winding .

k_2 = Coupling factor between ds1 and ds2 windings which may be assumed to be unity .

e) Mechanical Constants :

i) Measurement of Moment of Inertia J : There are various methods for the measurement of J , but only one method , considered to be the most accurate will be described here . Under this test a small peg is attached to the shaft of the rotor . Over this peg a loop at the end of a length of a string , to which a weight is attached , is hooked . The weight is dropped through a known height and the number of revolutions that this flywheel makes before it comes to rest . The initial angular velocity is also measured . This is the velocity at the instant the string leaves the peg .

$$mgh = 1/2\, mv^2 + 1/2\, \omega^2 (1 + n_1/n_2)$$

Where

m = Mass of the weight

h = Height through which the weight is dropped

ω = Initial angular velocity

n_1 = Number of turns required to wind up the weight to the

starting point

n_2 = Number of revolutions made after the string leaves the peg .

The value of moment of inertia for the machine under study could not be determined experimentally because of some practical problems of connecting the drum . The generalised machine is used with the work-load machine permanently coupled to the shaft and a torquemeter in the coupling makes it difficult to fit a drum for the purposes of measuring J . Hence the value of J was taken from the manufacurer's data .

ii) Measurement of the Rotational Loss constant D : If the motor is running at no load the only damping torque on the motor is due to the mechanical and iron losses which is $Dp\theta$. Also the torque of the motor is given by $M_d' i_{ds} i_{qr}$ which can be calculated from readings during the test . The value of M_d' will depend upon the operating point on the magnetisation curve . Hence D would be given by

$$D = M_d' i_{ds} i_{qr} / p\theta$$

f) Effect of various parameters on the stability of the motor : From the study of the transfer function for the motor any increase in r_{qr} , J and D will make the motor more stable . But any increase in the value of M_{12} makes the motor more unstable . This means that if the motor also has speed control through armature resistance being varied with the help of a series resistance of the armature , it may not run into instability for a case in which the motor would otherwise be unstable . Also the use of a compensating winding would neutralise the armature m.m.f. to some extent and hence will reduce the value of M_{12} , thereby making the motor more stable .

Table (5.1) shows the values and the methods used to determine them for the various parameters for the purposes of analysis of the dynamic behaviour of the motor .

Table 5.1

Parameter	Method used	Value
L_{ds1}	Voltmeter-ammeter	0.4 H
L_{qr}	Voltmeter-ammeter	0.05 H
r_{qr}	Method a(i) page (43)	1.2 to 1.8 Ω Graph(13)
M_1'	from o.c. characteristic	0.186 H/rad. Graph(4)
M_2'	from o.c. characteristic	0.00255 H/rad. Graph(4)
M_{12}	as on page 50 -51	0.009 H
L_{ds2}	as on page 50 -51	0.0002 H
J	Manufacturer's data	0.0237 kg.-$m.^2$
D	Method e(ii) page (52)	0.0017 N.m./rad./sec.

CHAPTER VI

LABORATORY TESTS

LABORATORY TESTS

TEST 1 : To compare the field forms produced by qr-axis and qs-axis m. m. f.

The purpose of this test was to establish whether the effect of the armature current on the field form could be simulated by an equivalent m. m. f. produced by the qs winding . If it can be shown that such an equivalence is valid , then an accurate measure of the reduction in the d-axis flux due to q-axis m. m. f. can be undertaken . The justification for this is given under Test 2 for which Test 1 is a prerequisite .

The two qs windings were connected in series such that the m. m. f.'s in them add to each other . The number of turns on the qs coil is 324 and there are 140 turns on qr coil . Hence the value of equivalent I_{qs} that will produce the same m. m. f. as I_{qr} is given in eq. (6. 1). (see Appendix V)

$$324\, I_{qs} = 140\, I_{qr} \qquad (6.1)$$

Before starting the experiment , qs, qr and the ds-axis windings were completely demagnetised by applying a decreasing alternating voltage at 60 Hz through an auto-transformer . The machine was then driven as a shunt generator at a speed of 450 r. p. m. . To obtain the field form , the voltage produced in a search coil , due to rotation in the field caused by a qr-coil m. m. f. was plotted by a pen recorder . The relatively low speed was chosen to suit the recorder chart paper speed that would give the most satisfactory scales . Pen recordings on charts (1) to (3) were obtained for armature current values of 1A, 2A and 3A , the equivalent current I_{qs} in the qs winding being 0. 43A , 0. 86A and 1. 29A . Plots of the field forms are found to be similar for the two sources of magnetomotive forces and hence the qs coil can be used to produce the same effect as the armature current, on the direct-axis flux .

TEST 2 : To show the demagnetising effect of the q-axis m. m. f. on the d-axis flux .

The aim of this test was to prove experimentally that there is a reduction in the d-axis flux caused by the q-axis m. m. f. . For this test the result of Test 1 (that a qr-coil m. m. f. can be replaced by an equivalent qs-coil m. m. f.) was used . The windings were demagnetised by an alternating voltage applied to the windings as in Test 1 . The machine was run as a generator at 1800 r. p. m. . The voltage generated in the qr coil which is a speed voltage , is proportional to the d-axis flux . Hence if the field current in the ds winding and the speed of the machine are maintained constant , the voltage across the brushes , which are in the neutral axis , should be a measure of the d-axis flux . So any reduction in the voltage across the brushes would mean a reduction in the d-axis flux , if the speed and the ds coil current are maintained constant . This is the principal used in this test .

To observe the demagnetising effect of the q-axis m. m. f. on the d-axis flux , either of the two windings i. e. qr or qs could be used to produce the q-axis m. m. f. . But it is much better and more accurate to use the qs winding to observe the effect directly . This is because it is not possible to measure accurately the carbon brush and contact resistances which vary with armature current and speed respectively . This variation makes it difficult to determine the reduction in generated voltage at various values of armature current . So the qs winding was used to produce the equivalent m. m. f. to simulate the effect of armature current . The machine was run at a constant speed of 1800 r. p. m. . For various fixed values of ds-axis winding current I_{ds} , the qs-axis m. m. f. was varied and the corresponding values of open-circuit voltage across the brushes were plotted against qs - winding current I_{qs} .

Graph (11) shows these curves which were

obtained during the test and it is evident that there is a fall in the open-circuit voltage which is an indication that there is a reduction in the d-axis flux . This proves that the q-axis m. m. f. does have a demagnetising effect on the d-axis flux .
It is extremely important for this test that the brushes are placed exactly in the neutral axis which is at 90^{o} to the d axis since a small shift of the brushes from this axis will also produce a demagnetising effect. Hence a separate test as described below was performed to determine the neutral axis most accurately .

The graph of open-circuit voltage vs. qs-axis m. m. f. as described above , when plotted for both positive and negative qs-axis m. m. f. should give a symmetrical curve about the vertical axis of the graph . This is the principle used for the determination of the neutral axis . The experiment was repeated for various fixed values of shift of the brush axis about the marked neutral axis on the machine . The graph was found to be symmetrical at 357.5^{o} on the scale fixed on the machine . These graphs are shown in Graph (10) .

TEST 3 : Effect of q-axis m. m. f. on the d-axis flux .

This is another test that confirms that q-axis m. m. f. produces a reduction in the d-axis flux . The principle used in this test is that the voltage induced in the search coil in the machine when the machine is rotating , is proporional to the rate of change of flux-linkages . Since the number of turns in the search coil is constant , the voltage induced will be proportional to the rate of change of flux . Hence the area under the voltage wave form gives the flux in the air gap . Before starting the experiment all the three windings i. e. qr . qs and ds were demagnetised as in Test 1 . The machine was run at a constant speed of 450 r. p. m. and for a fixed value of I_{ds} , I_{qs} was varied from 0 to 8A . At $I_{qr} = 0$, the neutral axis is exactly at 90^{o} to the d-axis and can be

identified on the pen recordings at points where the voltage is zero . As the value of I_{qr} increases , there is a shift in the voltage wave depending upon the resultant of the d and q-axes magnetomotive forces .

In order to be able to recognize the neutral axis points of the pen recording $I_{qr} = 0$ on other recordings when $I_{qr} \neq 0$, it is necessary to have some reference on the pen recordings . For this purpose , the position of a fixed point on the rotor was marked on the pen recordings with the help of a relay which operated the "event marker" on the pen recorder whenever that fixed point on the rotor touched the relay contacts .

To find out the reduction in the d-axis flux , pen recordings for $I_{ds} = 1.5A$ are given in Chart (4) to (11) for the purpose of explanation of the method . The points 'a' and 'b' on Chart (4) represent the brush position on the neutral axis when it is exactly at 90^{o} to the d-axis . The area of the curve between these points is measured . The position of these two points , which represent the original position of the neutral axis with respect to the shifted neutral axis on recordings for $I_{qr} \neq 0$, can be identified by superimposing the recording of Chart (4) on the other recordings and making the event markings of the two to coincide with each other . The position of points 'a' and 'b' of the original axis could be then marked directly on the pen recording placed below . The area of the other recordings between these points will be the value of the flux in the d-axis .

A table below shows the percentage reduction in the in the d-axis flux for $I_{ds} = 1.5A$ and various values of I_{qr} .

Table 6.1

I_{qr}(A)	2	3	4	5	6	7	8
Percentage reduction in flux	0	0	0	7.7	15.4	28.2	43.5

TEST 4 : Effect of compensation of the armature m. m. f. on stability .

The machine was driven as a shunt motor with a supply voltage of 50 volts for the armature . The choice of this low supply voltage for the armature was necessary since under the weak field and a supply voltage of 110 volts , the speed of motor goes out of the safe limit fixed by the mechanical strength of the machine . The motor was run on no load which also included the rotor of the drive motor . For the armature current being taken by the motor under the no-load conditions , the qs winding was excited first to produce a m. m. f. in the same direction as that of the armature current . The rise in the speed was noted for various values of I_{qs} until the machine finally ran into instability . The direction of the q_s-winding m. m. f. was then reversed so that now it is in opposition to that produced by the armature current so that there is a compensating effect . The variation of speed was again plotted against different values of I_{qs} . No external resistance was included in the armature circuit , otherwise the machine would have been more stable . Graph (12) shows the plot of these curves for various fixed values of I_{ds} . It is is evident that the motor becomes very stable when there is compensation of the armature reaction by the qs winding .

TEST 5 : Sustained oscillations of the motor

The shunt motor is loaded by the d. c. generator coupled to it which supplies a resistance load . There are two ways to obtain sustained oscillations in the motor .

The first is by keeping the generator load current constant but decreasing the motor field current very slowly and in small steps . As the field current is decreased , the speed of the motor goes up . After making the adjustment to the field , a delay of a few seconds was allowed so that the motor settled down at the new operating point . At a particular value of field current the speed of the motor will increase and then will immediately slow

down to the steady-state value of the speed . This process is repeated at this operating point and we get oscillations at the rate of about 10 cycles per minute . If the field is now decreased further , the speed of the motor will keep on rising until the armature circuit breaker opens because of excessive armature current . On the other hand if the field current is increased slightly , the motor runs stably . The oscillations will also die out if the armature resistance is increased slightly .

The second method of obtaining the above oscillations is by keeping the motor field current constant at a low value but increasing the generator load current which in turn increases the motor armature current . As the load is increased slowly and in small increments , there is no significant rise in the speed of the motor until at a particular operating point the motor speed suddenly increases but then again slows down to the steady-state value . This is repeated giving oscillations at a frequency of about 10 cycles per minute . As in the first method the oscillations could be made to die out either by decreasing the load current or by increasing the motor field current or by increasing the armature resistance .

Other Tests : In addition to the above tests , the following tests were also performed in order to obtain the machine characteristics :

i) Open-circuit voltage characteristic as a shunt generator (Graph 4)

ii) Speed characteristic as a separately excited shunt motor (Graph 8)

CONCLUSIONS

Although all electrical rotating machines have many common features , a single analytical approach to instability applied to a primitive machine is not feasible . Each class of machine has its distinctive characteristics and whereas a high-resistance armature in a d. c. machine will have a damping effect it will , in the case of synchronous and induction machines , stimulate oscillations in speed . Therefore , in studying instability , each class of machine has to be treated individually .

It has been shown conclusively that commutation , whether good or poor , does not contribute in any way to instability in the d. c. shunt motor (if the brushes are on the geometrical neutral axis) . The demagnetising effect of quadrature m. m. f. on the direct -axis flux has been well established as the principal cause of instability . Further , the reduction of the armature circuit resistance with current resulting from the non-linear resistance of the brush material , reduces the damping , thereby making the motor even more prone to instability when the quadrature m. m. f. increases .

The equivalent model of the motor can be used to test whether or not the motor will be stable at the particular operating point under consideration , but may not prove to be very accurate if it is desired to study oscillations during instability . If the motor is found to be unstable at an operating point , then any one of the follwing three operations will restore stability : compensating for the effects of armature reaction , increasing the armature resistance , or increasing the direct-axis field current . An advantage of using the equivalent model is that the fictitious direct -axis coil provides a demagnetising magnetomotive force assiciated with the armature current and leaves the value of the principal speed coefficient as a function of only field excitation .

Many methods are available for measuring the machine parameters under appropriate conditions of excitation . The method used for determining the reduction of direct-axis flux by exciting the quadrature-axis stator coil gave , with very little trouble , a clear idea of the reduction of total flux per pole in the machine for various field currents . It also enabled the value of the

speed coefficient appropriate to the fictitious direct-axis stator coil to be determined with little difficulty . The value of armature resistance presented the greatest problem due to its non-linearity . It has a critical effect on stability and is difficult to estimate under actual working conditions . The disparity between the theoretical results and those from actual tests could be attributed chiefly to the values taken for this parameter .

APPENDIX I

KRON'S COMMUTATOR PRIMITIVE MACHINE

The first primitive machine is assumed to consist of a cylindrical rotor and a salient-pole stator . There are two sets of brushes at right angles in space that serve as reference axes . Two pairs of coils ds and qs are on the stator and dr and qr on the rotor . The convention adopted here is that rotation is positive clockwise and direction of magnetisation is upward along the direct axis and from left to right along the quadrature axis q . Fig. (I. 1) shows the machine described above .

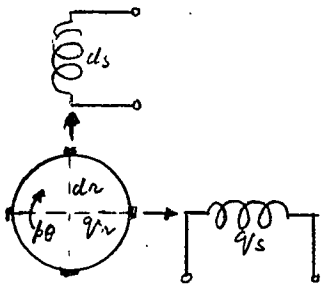

Fig. I. 1

If the coils are considered one at a time and the equation of voltage is written in the form :

Applied voltage = Sum of voltage drops

The resulting equations can then be arranged in matrix form as shown in eq. (1. 1)

$$\begin{vmatrix} e_{ds} \\ e_{dr} \\ e_{qr} \\ e_{qs} \end{vmatrix} = \begin{array}{c} \\ ds \\ dr \\ qr \\ qs \end{array} \begin{vmatrix} r_{ds}+L_{ds}p & M_d p & 0 & 0 \\ M_d p & r_{dr}+L_{dr}p & L_{qr}'p\theta & M_q'p\theta \\ -M_d'p\theta & -L_{dr}p\theta & r_{qr}+L_{qr}p & M_q p \\ 0 & 0 & M_q p & r_{qs}+L_{qs}p \end{vmatrix} \cdot \begin{vmatrix} i_{ds} \\ i_{dr} \\ i_{qr} \\ i_{qs} \end{vmatrix} \qquad \text{(I. 1)}$$

ds dr qr qs

If first, the rotor is considered stationary and only ds coil is excited, there will be :

- A voltage drop due to the resistance of the coil r_{ds} and this is $r_{ds} i_{ds}$
- An induced voltage in coil ds which is $L_{ds} p i_{ds}$
- An induced voltage in coil dr which is $M_d p i_{ds}$

If now the rotor is made to rotate in the assumed positive direction there will, in addition, be a voltage drop between the quadrature brushes $-M_d' p\theta i_{ds}$ and M_d' may be called a mutual inductance between the coils d_s and q_r existing only as a result of rotation because these coils are mutually non-inductive. The right hand rule gives the sign.

Three components of the impedance matrix can be abstracted as shown below from eq. (I. 1) :

i) The resistance R, elements of which appear along the diagonal.

$$R = \begin{array}{c|cccc} & ds & dr & qr & qs \\ \hline ds & r_{ds} & & & \\ dr & & r_{dr} & & \\ qr & & & r_{qr} & \\ qs & & & & r_{qs} \end{array} \qquad \text{(I. 2)}$$

ii) The inductance matrix. The inductances can always be abstracted from the complete impedance matrix by selecting terms with p. It is symmetrical and is given in eq. (I. 3).

$$L = \begin{array}{c|cccc} & ds & dr & qr & qs \\ \hline ds & L_{ds} & M_d & & \\ dr & M_d & L_{dr} & & \\ qr & & & L_{qr} & M_q \\ qs & & & M_q & L_{qs} \end{array} \qquad \text{(I. 3)}$$

The self inductances appear along the diagonal and the mutual inductances in the other spaces . They give rise to the induced voltages which , by their similarity with the voltages induced in the transformer , are often called 'transformer voltages' .

iii) By abstraction from the impedance matrix the terms with $p\theta$ there results a matrix G which is not symmetrical and is given in eq. (I. 4) .

$$G = \begin{array}{c|cccc} & ds & dr & qr & qs \\ \hline ds & & & & \\ dr & & & L_{qr}' & M_q' \\ qr & -M_d' & -L_{dr}' & & \\ qs & & & & \end{array} \qquad (I.4)$$

Since $p\theta$ is the speed of the rotor and the components of G are the coefficients of $p\theta$, these are referred to as speed coefficients . They give rise to the voltage drops that are called 'speed' or 'generated' voltages and a machine with four coils arranged as in Fig. (I. 1) will have four speed coefficients and four generated voltages terms . The principal torque in a machine is produced by rotor current i_{qr} interacting with the stator-produced flux $M_d' i_{ds}$. The principal generated e. m. f. is produced by the flux $M_d' i_{ds}$ being cut by the rotor conductors on coil qr .

APPENDIX II

SLIP - RING PRIMITIVE MACHINE

This machine is shown in Fig. (II. 1) .

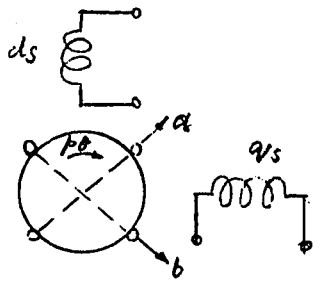

Fig. II. 1

Coils 'a' and 'b' are windings at 90 degrees to each other and connected to slip rings . A salient-pole machine is considered for the purposes of generality . When the rotor is in motion , the values of mutual inductances and rotor self inductances are not constant but are functions of the rotor angle θ . The impedance matrix of this machine can be derived from two approaches :

i) The dynamic circuit theory approach

ii) By transformation from the commutator primitive machine

According to the dynamic circuit theory , in a stationary circuit neglecting saturation

$$e = Zi = ri + Lpi$$

But when the coils are in motion , the Lpi term is no longer applicable , since in a salient-pole machine , the inductance changes with θ . So the above voltage equation has to be re-written as

$$e = Zi = ri + p(Li)$$
$$= ri + Lpi + ip\theta\, \partial L/\partial\theta \qquad \text{(II. 1)}$$

The inductance matrix L , for the slip-ring machine will be of the form shown in eq. (II. 2)

$$L_{dz} =$$

	ds	a	b	qs
ds	L_{ds}	$M_{ad}\cos\theta$	$-M_{bd}\sin\theta$	0
a	$M_{ad}\cos\theta$	L_{aa}	$-L_{AB}\sin 2\theta$	$M_{aq}\sin\theta$
b	$-M_{bd}\sin\theta$	$-L_{AB}\sin 2\theta$	L_{bb}	$M_{bq}\cos\theta$
qs	0	$M_{aq}\sin\theta$	$M_{bq}\cos\theta$	L_{qs}

(II. 2)

where

$$L_{aa} = \frac{L_{ad} + L_{aq}}{2} + \frac{L_{ad} - L_{aq}}{2}\cos 2\theta = L_S + L_D\cos 2\theta$$

$$L_{bb} = \frac{L_{bd} + L_{bq}}{2} - \frac{L_{bd} - L_{bq}}{2}\cos 2\theta = L_S - L_D\cos 2\theta$$

$$\frac{\partial L}{\partial \theta} =$$

	ds	a	b	qs
ds	0	$-M_{ad}\sin\theta$	$-M_{bd}\cos\theta$	0
a	$-M_{ad}\sin\theta$	$-2L_D\sin 2\theta$	$-2L_{AB}\cos 2\theta$	$M_{aq}\cos\theta$
b	$-M_{bd}\cos\theta$	$-2L_{AB}\cos 2\theta$	$2L_D\sin 2\theta$	$-M_{bq}\sin\theta$
qs	0	$M_{aq}\cos\theta$	$-M_{bq}\sin\theta$	0

(II. 3)

substituting $M_{ad} = M_{bd} = M_d$

$M_{aq} = M_{bq} = M_q$

It is now possible to write the impedance matrix for the machine by collecting all the terms as given in eq. (II. 1) to give eq. (II. 4) .

$Z =$

	ds	a	b	qs
ds	$r_{ds} + L_{ds}p$	$M_d p\cos\theta$	$-M_d p\sin\theta$	0
a	$M_d p\cos\theta$	$r_a + p(L_S - L_D\cos 2\theta)$	$-L_{AB}p\sin 2\theta$	$M_q p\sin\theta$
b	$-M_d p\sin\theta$	$-L_{AB}p\sin 2\theta$	$r_b + p(L_S + L_D\cos 2\theta)$	$M_q p\cos\theta$
qs	0	$M_q p\sin\theta$	$M_q p\cos\theta$	$r_{qs} + pL_{qs}$

(II. 4)

This is the impedance matrix for the slip-ring primitive machine and note that it has 14 elements and is symmetric .

ii) By transformation from the commutator primitive machine :

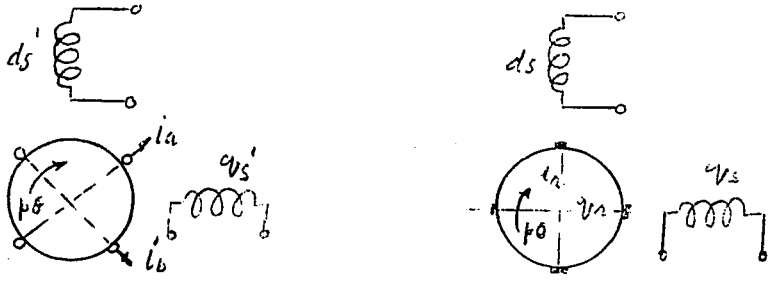

(a) (b)

Fig. II. 2

On writing the currents in the slip-ring machine in terms of i_{dr} and i_{qr} using Fig. II. 2(a) and (b) , we get

$$i_{dr} = i_a\cos\theta - i_b\sin\theta \qquad \text{(II. 5)}$$

$$i_{qr} = i_a\sin\theta + i_b\cos\theta \qquad \text{(II. 6)}$$

Hence the transformation matrix or connection matrix 'C' can now be written as given in eq. (II. 7) .

$$C = \begin{array}{c|cccc} & ds & a & b & qs \\ \hline ds & 1 & 0 & 0 & 0 \\ a & 0 & \cos\theta & -\sin\theta & 0 \\ b & 0 & \sin\theta & \cos\theta & 0 \\ qs & 0 & 0 & 0 & 1 \end{array} \qquad \text{(II. 7)}$$

The impedance matrix Z' of the slip-ring machine can now be derived as below:

$$\begin{aligned} e &= Zi \\ &= ZCi' \\ &= (r + Lp + Gp\theta)Ci' + Lp\theta i'\partial L/\partial\theta \end{aligned}$$

The condition of invariance of power gives

$$\begin{aligned} e &= C_t e \\ &= C_t(r + Lp + Gp\theta)Ci + C_t Li' p\theta \partial C/\partial\theta \\ Z' &= C_t ZC + C_t Lp\theta\, \partial C/\partial\theta \end{aligned} \qquad \text{(II. 8)}$$

When the equation for Z' is solved , the impedance matrix of the slip-ring machine is found to be given in eq. (II. 4) . It is evident , then , that due to the constraints imposed by postulating invariance of power when transforming from the commutator to the slip ring primitive machine , the transformation eq. (II. 7) gives a truly equivalent machine . However , the commutator machine impedance matrix eq. (I. 1) contains only 12 elements and for that reason it is more frequently used for analysis purposes due to voltage equations having fewer terms . Even when the actual machine has slip rings , such as a wound rotor induction motor , analysis in terms of an equivalent commutator primitive machine is quite valid and simpler than analysis in terms of the slip ring primitive . In cases where slip rings are connected to another stationary circuit or machine , the analysis has to be started in actual i. e. slip-ring reference frame in order to be able to write the equations of current constraints . Subsequently an equivalent commutator machine may may be used . On the other hand , when the actual machine has a commutator

and an analysis of commutation is required , the only valid starting point for the analysis is the slip-ring primitive. This is due to the fact that the process of commutation itself is ignored in the commutator machine equations .

APPENDIX III

EQUIVALENT MODEL OF THE COMMUTATOR PRIMITIVE MACHINE

The method of establishing the equivalent model of a machine could be best explained by considering the commutator primitive machine shown in Fig. (III. 1) .

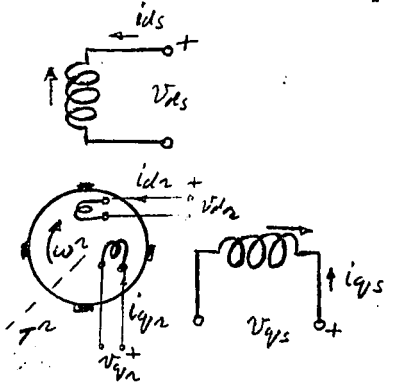

Fig. III. 1

The terminals of the four electrical windings and the mechanical shaft of the machine represent the places where energy can flow in or out of the primitive machine . The assumed positive sense for all winding terminal voltages is so chosen that the energy is flowing into the winding or the port if positive power is assumed . Thus if the winding current is actually flowing in the assumed direction, then a positive terminal voltage indicates an instantaneous flow of energy into the winding . For an electric motor which converts electrical energy into mechanical energy, we would expect that the average port power would actually be positive at the electrical ports of the device . But with a generator , converting mechanical energy into electrical energy , average power will be negative in certain ports .

For the single mechanical port , physically the shaft of the machine , the assumed positive direction for the angular velocity ω^r is taken to be clockwise . In order to again have a positive mechanical port power , corresponding to energy flow into the mechanical port, the assumed direction of the externally applied torque T^r is also taken to be clockwise . If the energy,in reality , is flowing out of the mechanical port , then either ω^r or T^r will turn out to be negative or opposite to the assumed positive direction

and the mechanical port power will be a negative quantity .

a) Electrical equilibrium equations : As given in Appendix I , the electrical equilibrium equations of machine shown in Fig. (III. 1) are given in eq. (III. 1) .

$$\begin{bmatrix} v_{ds} \\ v_{dr} \\ v_{qr} \\ v_{qs} \end{bmatrix} = \begin{bmatrix} r_{ds} + L_{ds}p & M_d p & 0 & 0 \\ M_d p & r_{dr} + L_{dr}p & L_{qr}'p\theta & M_q'p\theta \\ -M_d'p\theta & -L_{dr}'p\theta & r_{qr} + L_{qr}p & M_q p \\ 0 & 0 & M_q p & r_{qs} + L_{qs}p \end{bmatrix} \begin{bmatrix} i_{ds} \\ i_{dr} \\ i_{qr} \\ i_{qs} \end{bmatrix} \qquad \text{(III. 1)}$$

b) Mechanical equilibrium equations : There is only one mechanical port and the equilibrium equation for this port is formulated in the same fashion as as for the electrical equilibrium equations . The torque externally applied to the shaft must be opposed by certain generated torques . These generator torques include inertia effects , a viscous or windage torque and a compliance torque due to the twisting of shaft and lastly a torque exerted on the rotor from electrical origin . This mechanical torque of electrical origin is actually the interaction between the electrical and the mechanical ports and makes the energy conversion process possible .

In any practical machine the twist of the shaft is small enough to be considered negligible . Therefore the compliance torque is neglected in all torque equations . Now the torque equation for the machine in Fig. (III. 1) can be written as given below :

$$T^r = Jp\omega^r + D\omega^r + T_e \qquad \text{(III. 2)}$$

where T^r = externally applied torque

and T_e = torque of electrical origin

Positive T^r means that an external torque is applied in the direction of positive angular velocity ω^r . All the remaining torques oppose the applied torque and are taken as being positive when opposite to the direction of positive angular velocity . The energy conversion could be represented in

in the block form as shown in Fig. (III. 2) .

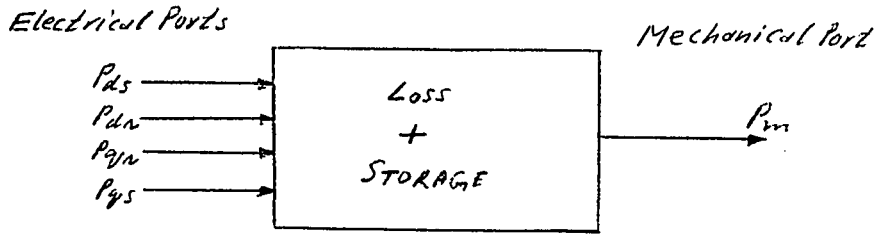

Fig. III. 2

To formulate T_e , we define the quantity P_e as that portion of the total power supplied at the electrical ports , not going into either loss or storage , then

$$T_e = - P_e/\omega^r \qquad \text{(III. 3)}$$

If the quantity P_e is instantaneously positive , then T_e according to eq. (III. 3) must be negative . A negative T_e means that the torque of electric origin is in the direction of the positive angular velocity . This means that the electric currents are generating a torque which is trying to turn the rotor in the direction of the positive speed . If the rotor actually turns in the direction of T_e , we have motoring operation or the conversion of electrical power to mechanical power . P_e is the electric power supplied to the electric ports converted to mechanical power .

c) Ideal transformer : Before going into the electro-mechanical model , it is necessary to introduce , a rather unusual , idealised circuit element . The usual ideal transformer in Fig. (III. 3) is this element . The port currents are defined positive when taken into the dotted side of each winding . In addition the port voltages are taken positive in such fashion that energy flow is into the port for positive current and voltage . The ratio of turns is marked as $1 : N_2$ indicating that winding 2 has N_2 times the number of turns as shown in

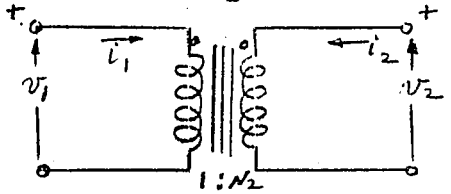

Fig. III. 3

winding 1 . By definition , the ideal transformer imposes the port constraints

$$v_2 = N_2 v_1$$

$$i_2 = -i_1 1/N_2$$

Multiplying the above equation by i_2 gives

$$v_2 i_2 = -v_1 i_1$$

Receiving a power $P_1 = v_1 i_1$ at a port 1 , the device transfers the energy without any loss and delivers an equal power $P_2 = -v_2 i_2$ at winding 2 . The minus sign indicates flow out of port 2 , provided this flow is into port 1 .

d) Primitive machine equivalent circuit : The complete set of equilibrium equations for the primitive machine is obtained from eq. (III. 1) and (III. 2) . These five equilibrium equations , one for each of the five ports are given below :

$$v_{ds} = (r_{ds} + L_{ds}p) i_{ds} + M_d p i_{dr}$$

$$v_{dr} = M_d p i_{ds} + (r_{dr} + L_{dr}p) i_{dr} + L_{qr}' p\theta i_{qr} + M_q' p\theta i_{qs}$$

$$v_{qr} = -M_d' p\theta i_{ds} - L_{dr}' p\theta i_{dr} + (r_{qr} + L_{qr}p) i_{qr} + M_q p i_{qs}$$

$$v_{qs} = M_q p i_{qr} + (r_{qs} + L_{qs}p) i_{qs}$$

$$T^r = Jp\omega^r + D\omega^r + T_e$$

Now it is possible to draw a complete equivalent circuit of the five-port primitive machine and it is shown in Fig. (III. 4) .

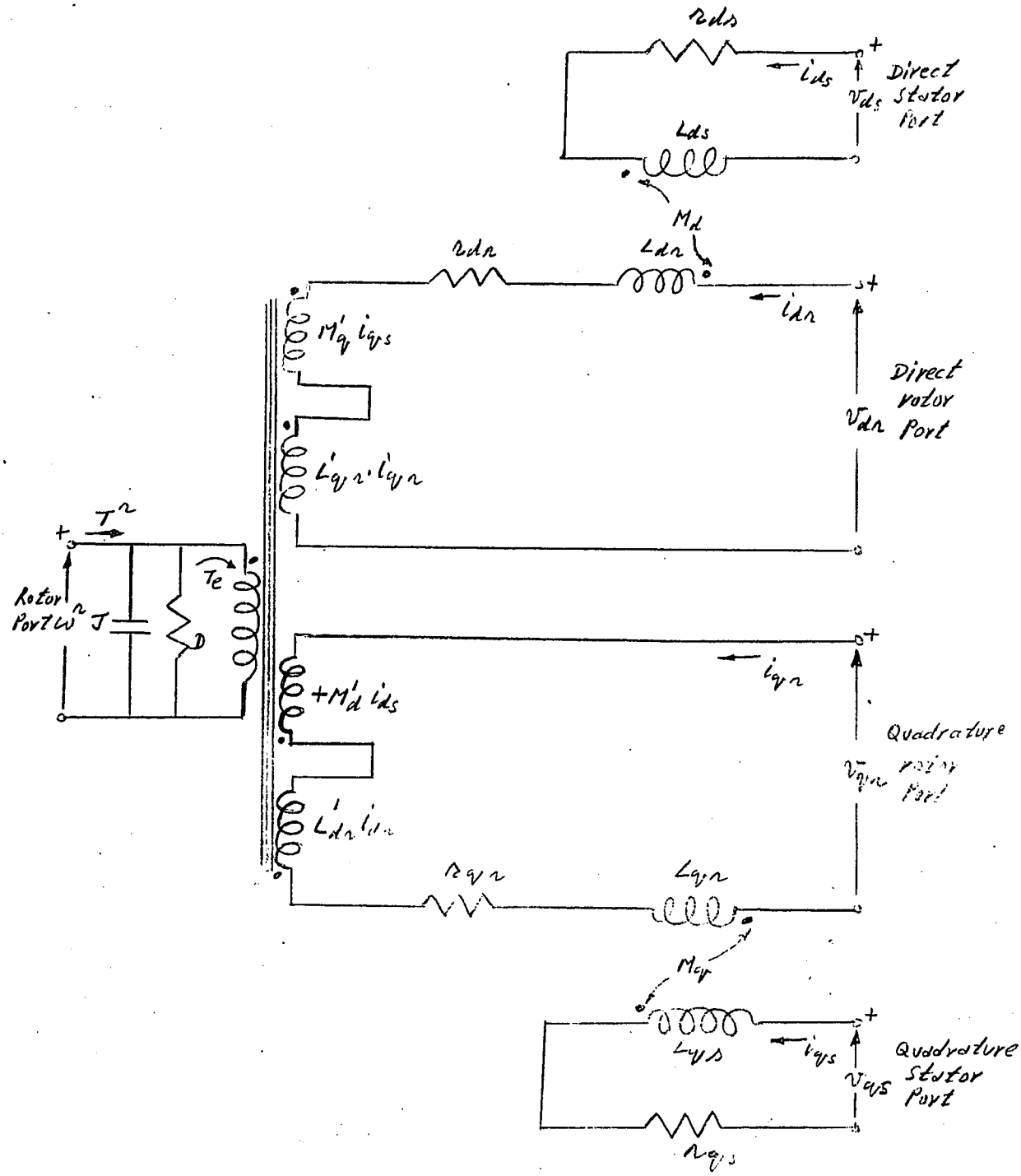
r_{ds}
i_{ds}
Direct Stator Port
v_{ds}
L_{ds}
M_d
r_{dr}
L_{dr}
i_{dr}
$M'_q i_{qs}$
Direct rotor Port
v_{dr}
$L'_{qr} i_{qr}$
T_e
Rotor Port ω_r J
D
i_{qr}
$+M'_d i_{ds}$
Quadrature rotor Port
v_{qr}
$L'_{dr} i_{dr}$
r_{qr}
L_{qr}
M_q
L_{qs}
i_{qs}
Quadrature Stator Port
v_{qs}
r_{qs}

Fig. III. 4

APPENDIX IV

STATE SPACE FORMULATION OF TRANSFER FUNCTION

The most general form of the transfer function is given by eq. (IV. 1)

$$\frac{Y(s)}{V(s)} = \frac{\beta_n s^n + \beta_{n-1} s^{n-1} + \ldots\ldots\ldots + \beta_1 s + \beta_0}{s^n + a_{n-1} s^{n-1} + \ldots\ldots\ldots + a_1 s + a_0} \qquad \text{(IV. 1)}$$

It is desired to obtain the state-space formulation for a case when $\beta_n = 0$, and the transfer function then reduces to as in eq. (IV. 2) .

$$\frac{Y(s)}{V(s)} = \frac{\beta_{n-1} s^{n-1} + \beta_{n-2} s^{n-2} + \ldots\ldots + \beta_1 s + \beta_o}{s^n + a_{n-1} s^{n-1} + \ldots\ldots\ldots + a_1 s + a_0} \qquad \text{(IV. 2)}$$

This formulation is shown in Fig (IV. 1) .

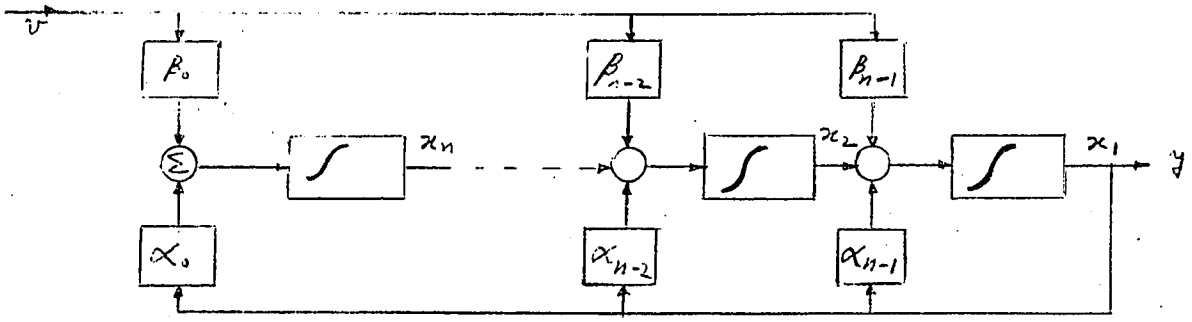

Fig. IV. 1

Defining the output of each integrator as elements of a state vector x , the corresponding state equations are given below :

$$\begin{bmatrix} \dot{x}_1 \\ \dot{x}_2 \\ \\ \\ \\ \dot{x}_{n-1} \\ \dot{x}_n \end{bmatrix} = \begin{bmatrix} -a_{n-1} & 1 & 0 & \ldots\ldots & 0 \\ -a_{n-2} & 0 & 1 & \ldots\ldots & 0 \\ \vdots & & & & \\ -a_1 & 0 & 0 & \ldots\ldots & 1 \\ -a_0 & 0 & 0 & \ldots\ldots & 0 \end{bmatrix} \begin{bmatrix} x_1 \\ x_2 \\ \\ \\ \\ x_{n-1} \\ x_n \end{bmatrix} + \begin{bmatrix} \beta_{n-1} \\ \beta_{n-2} \\ \vdots \\ \beta_1 \\ \beta_0 \end{bmatrix} v$$

$$y = x_1$$

APPENDIX V

DETAILS OF GENERALISED MACHINE SET

Various experiments were performed on the Westinghouse generalised machine set working as a shunt machine . Details of the machine are given below :

ROTOR :

i) Mechanical specifications

Moment of inertia of rotor	0. 26 lb-ft^2
Roror core length	3. 00 in. net
Number of rotor slots	28
Slot skew	1 slot pitch
Commutator O. D.	3 . 0 in.
Number of commutator bars	56

ii) Rotor punchings

Material : Electrical sheet steel	
Silicon content	1 -1. 3%
Thickness	0. 025 in.
Area	11. 9 in.^{2}
Weight	3. 4 lb per inch length

iii) Electrical specifications

Number of rotor conductors	560
Number of parallel paths	2
Number of turns per coil	5

Winding : 2- pole continous , full pitch coils , four coil sides per slot .

Bar connections : Bar No. 1 through one coil to bar No.. 2 , Bar No. 2 through another coil sharing the same slots , to Bar No. 3 etc .

Wire sizes : Coils are wound with two number 20 AWG (No. 21 SWG) , wires of 0. 032 in. dia.

Rotor resistance (at $25^{\circ}C$) 0.46 ohms.

Inductances :

L^r = rotor self-inductance 0.05 H (for excitation current of 1 A RMS at 60 Hz

STATOR :

i) Mechanical specifications

Stator bore	4.631 in.
Stator outside diameter	7.50 in.
Length of stator iron	3.00 in net
No. of stator slots	36

ii) Stator punchings

Material : Electrical sheet steel

Area	19.5 in^2
Weight	6 lb. per in. length

iii) Electrical specifications

Winding : 4 groups , 9 coils per group , 18 turns per coil, coil span : 11 slot pitches

Wire sizes : Coils are wound with one number 19 AWG(No. 20 SWG) , wire of 0.036 in. diameter

Stator resistance (at $25^{\circ}C$) 1.4 ohms per winding

Inductances :

L^s (series) = stator self-inductance from β_1^s to β_2^s, stator connected $\beta_1^s - \beta_1^{1s}$ to $\beta_2^s - \beta_2^{1s}$

= 0.40 H

L^s (parallel) = stator self-inductance from $\beta_1^s - \beta_1^{1s}$, stator connected β_1^s to $\beta_2^s - \beta_2^{1s}$ to β_1^{1s}

= 0.10 H

Note : Values of inductances are for excitation of 1 A RMS current at 60 Hz

Moment of inertia of the Rotor Drive Motor (armature and shaft) = 0.30 lb-$ft.^2$

The stator coils are connected into four groups of which two are symmetrically on the direct axis and the other two are on the quadrature axis . Terminals are brought out from each of the groups so that the pairs of coils on each axis may be connected either in series or in parallel . The winding data gives the current sheet representation as shown in Fig. (V. 1). Due to some slots being shared by coils of ds and qs windings , some ampere-turns are cancelled and a trapezoidal force distribution around the air gap is produced .

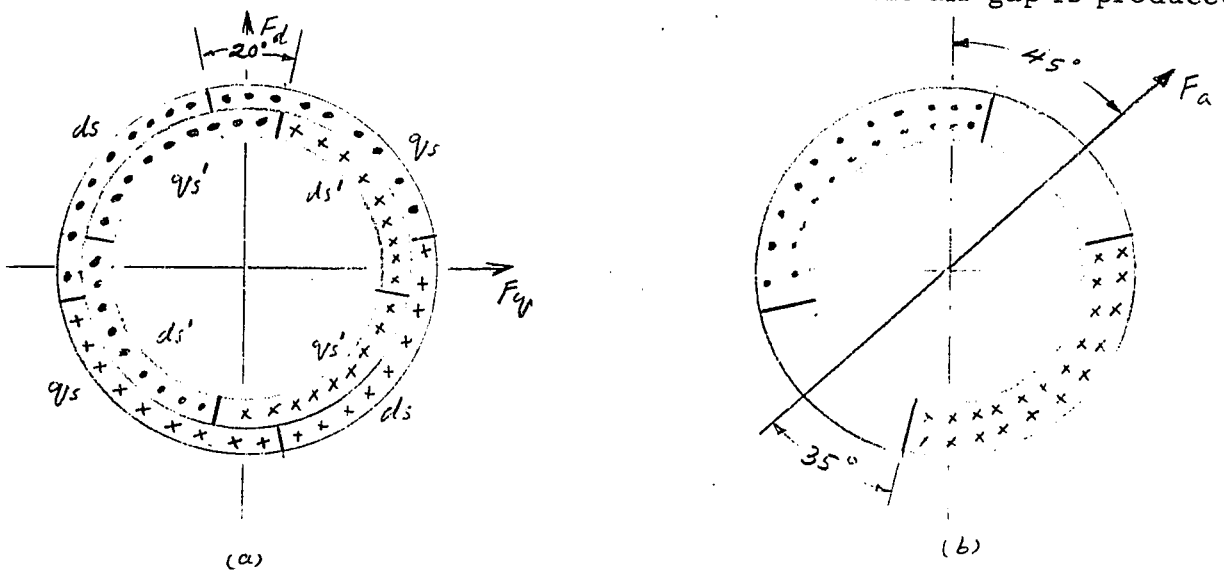

Fig. V. 1

The number of turns on both direct and quadrature stator windings are 324 .

In the case of the rotor winding , the machine has 56 full pitched coils in 28 slots and each having 5 turns . There are two parallel paths each carrying a current of $I_{qr}/2$ giving an overall m. m. f. of $140I_{qr}$ ampere-turns, if the coils undergoing commutation are ignored . The armature m. m. f. distribution, therefore, around the air gap is triangular in shape .

When the qs winding is connected for armature reaction compensation the two groups of qs coils are connected in parallel so that each coil carries a current of $I_{qr}/2$ or $162\ I_{qr}$ acting in the conventional negative direction .

REFERENCES

(1) Kimbark, E. W. : 'Power system stability' volume I ,(John Wiley and and Sons, Inc., New York, 1967) .

(2) Clayton , A. E. : 'The performance and design of direct current machines' . (Pitman) .

(3) Jones , C. V. : 'An analysis of commutation for the unified machine theory' . Proceedings I. E. E. Monograph No. 302 , September, 1958 (105C , pp 476-88) .

(4) Jones , C. V. : 'The unified theory of electrical machines'. (London, Butterworths , 1967 .

(5) Jones , C. V.
Barton , T. H. : ' A practical commutator primitive for generalised machine theory'. Transactios A. I. E. E. , Power apparatus and systems, June 1960, No. 48 Vol. 3 pp. 277-81

(6) Kron , G. : 'Tensors for circuits' . (Dover)

(7) Meisel , J. : 'Principles of electromechanical energy conversion'. (Mc Graw-Hill Book Company, New York, 1966)

(8) Benjamin , C. Kuo : 'Automatic control systems'. (Prentice Hall)

(9) Derusso , P. M.
Roy , R. J.
Close , C. M. : 'State variables for engineers '.(Wiley, 1965)

(10) 'Generalised Machine Laboratory Manual'. MB-1902 C-59(Westinghouse Electric Corporation)

(11) Marsh , J. V. : 'Measurement of machine parameters and steady-state performance of a d. c. synchronous tie'. Technical report No. 66-1(January, 66), University of Ottawa .

(12) Saunders, R. M. : 'Measurement of d. c. machine parameters'. Transaction A. I. E. E. 1951 vol. 70 pp. 700-706.

(13) O'Connor , J.
Cybulsky , J. : Discussion of paper under reference (12).

(14) Rutta , A.R. : 'Difference between inductances and speed coefficients in a practical machine '. B.A.Sc. thesis , April 1967 , University of Ottawa .

(15) Sharma, K.J. : 'The inductances of a d.c. machine under transient conditions'. M.A.Sc. thesis, 1964 , University of Ottawa .

(16) Prescott, J.C.
El-Kharashi, A.K. : 'A method of measuring self inductance applicable to large electrical machines'. Proc. I.E.E. , April 1959 , Paper No. 2871M .

GRAPH 1

DERIVATION OF SPEED VOLTAGE CURVE

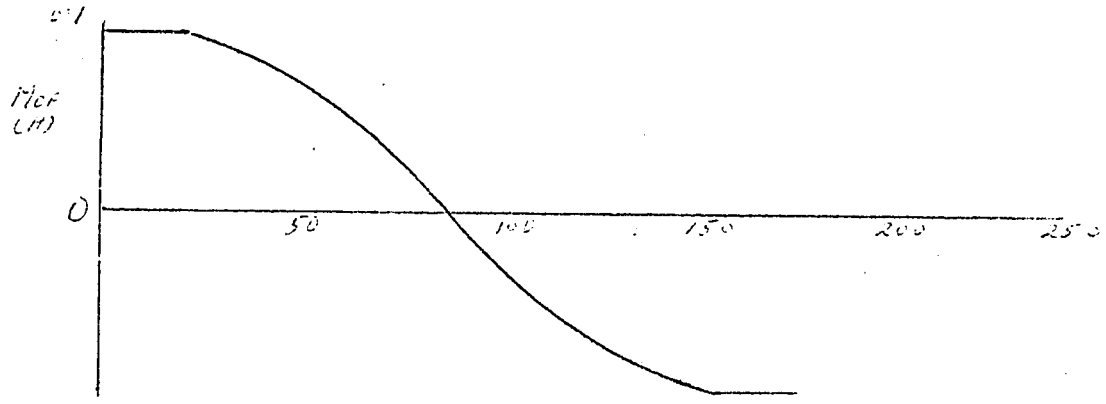

(a)

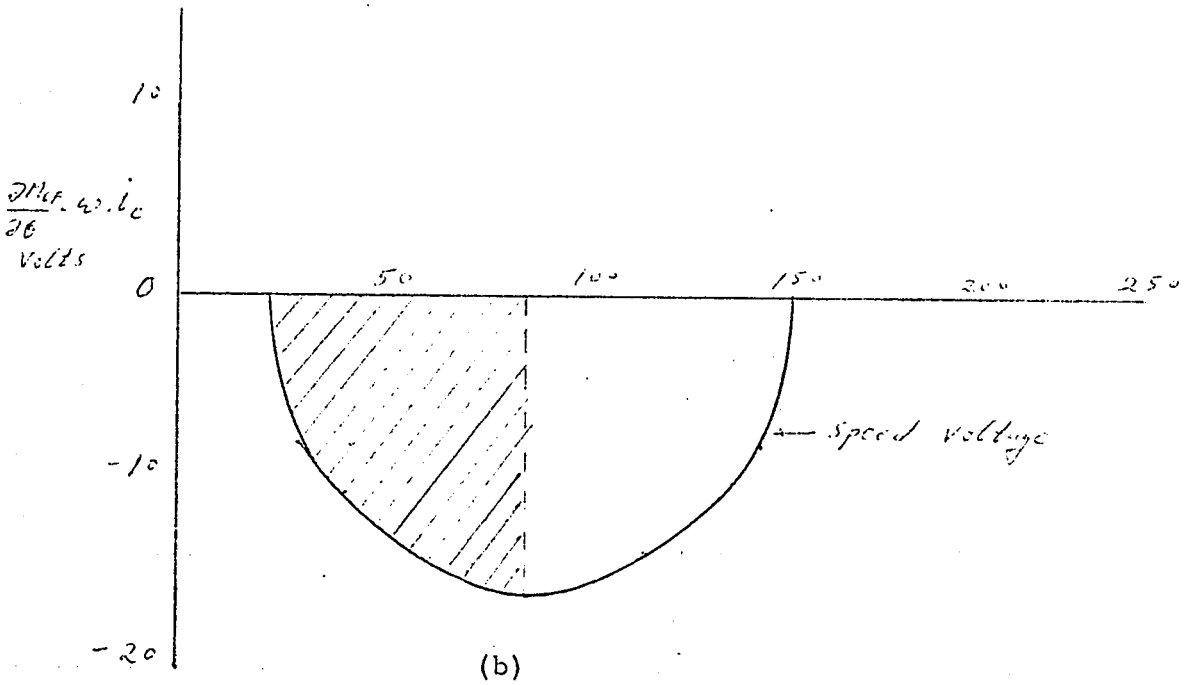

(b)

Shaded Area = 825 Volt degree

GRAPH 2

DERIVATION OF TRANSFORMER VOLTAGE CURVE

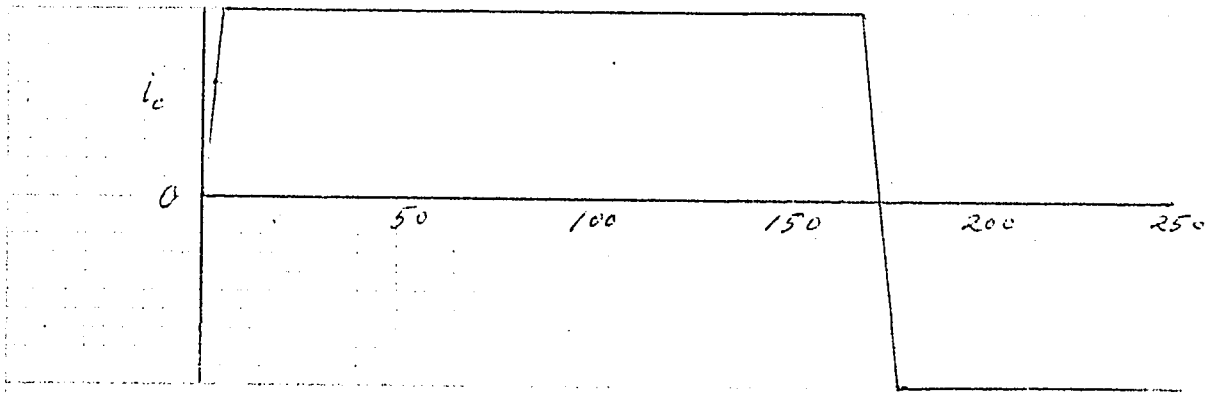

(a)

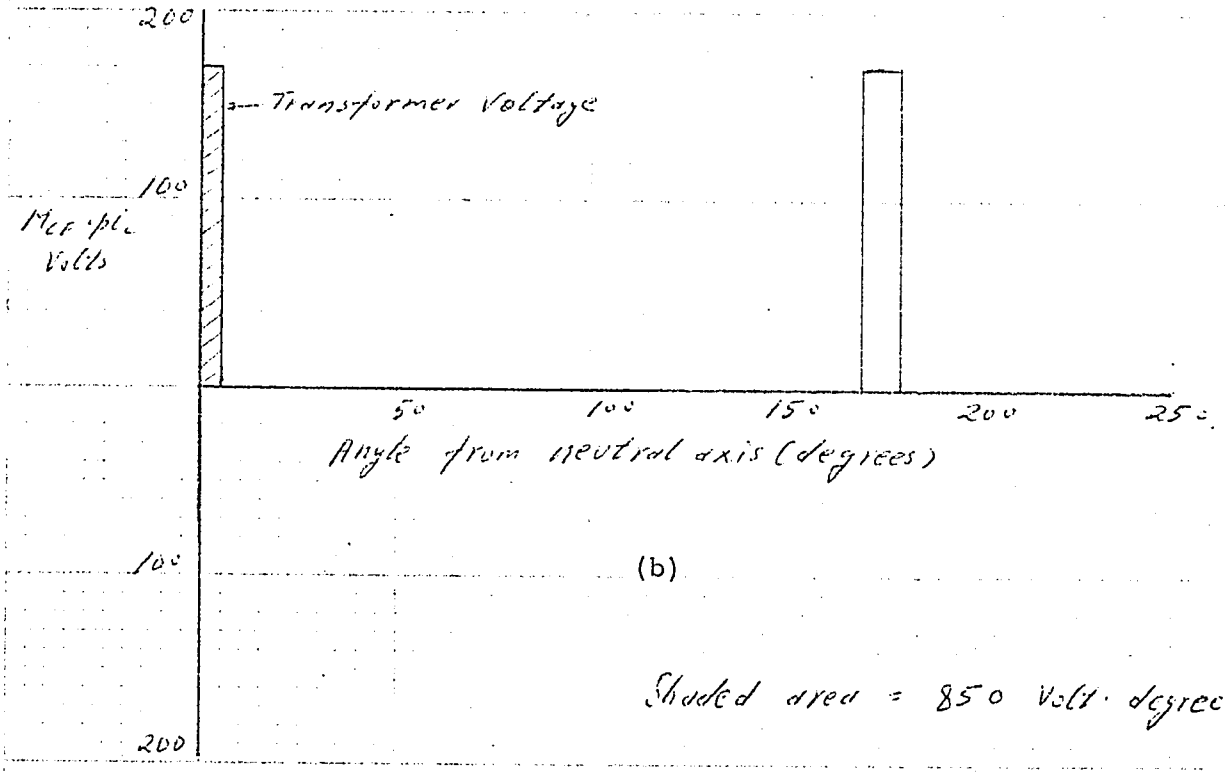

(b)

Shaded area = 850 Volt · degree

GRAPH 3

TOTAL VOLTAGE IN ds WINDING CAUSED BY COMMUTATION

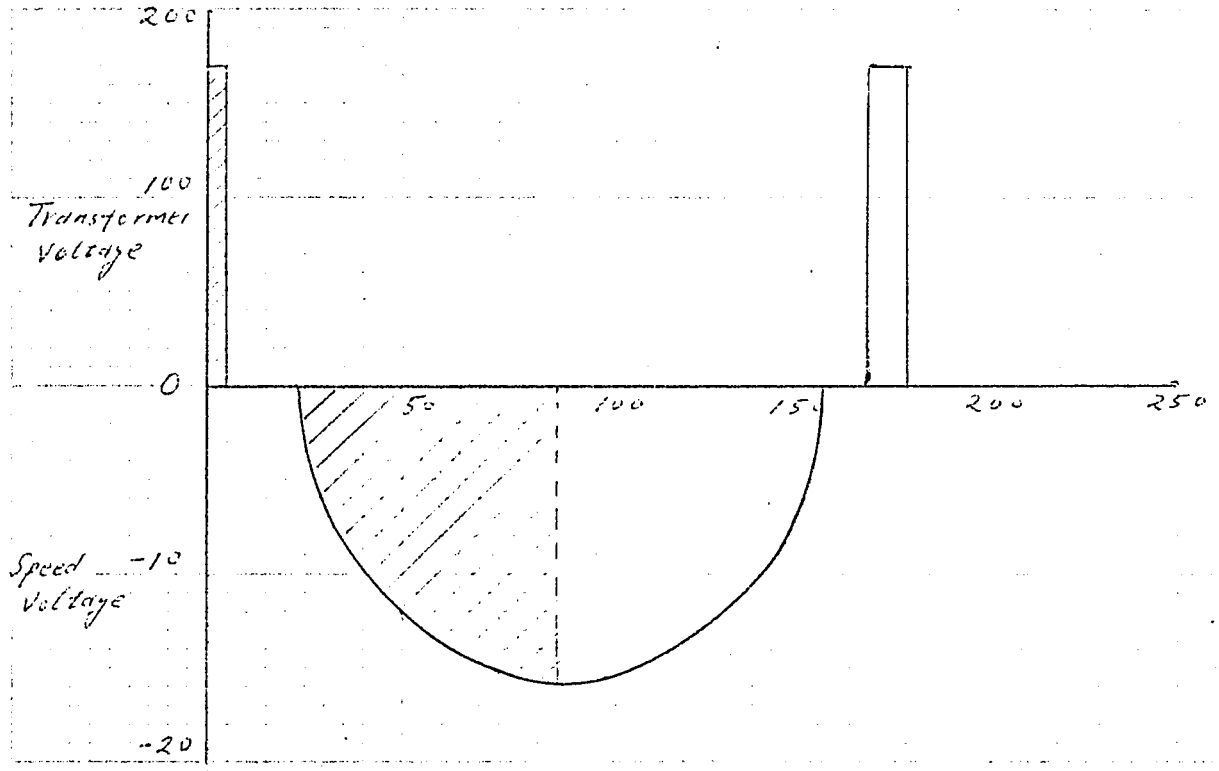

GRAPH 4

OPEN - CIRCUIT VOLTAGE CHARACTERISTICS

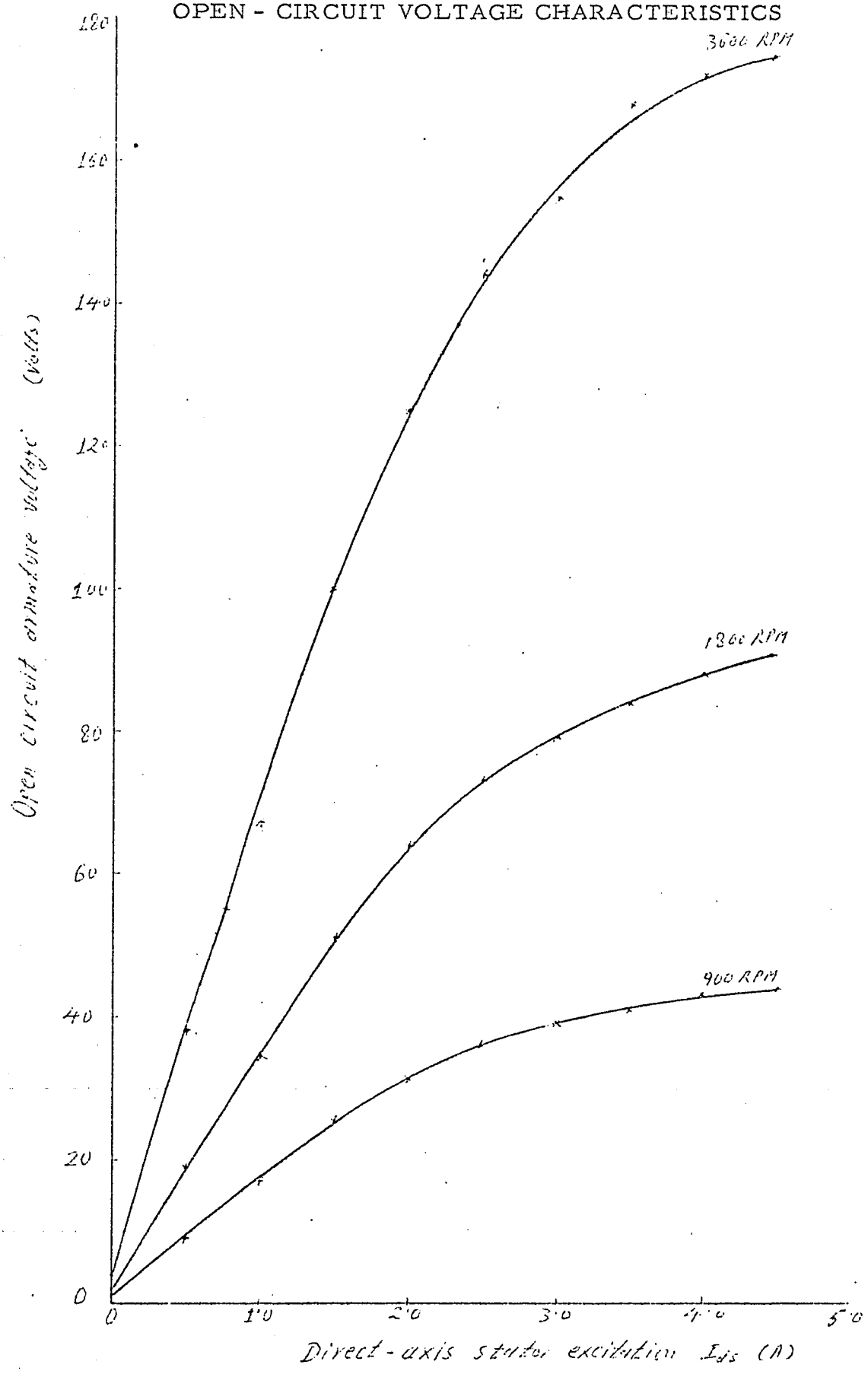

GRAPH 5

CALCULATION OF REDUCTION IN d-AXIS FLUX DUE TO ARMATURE M. M. F.

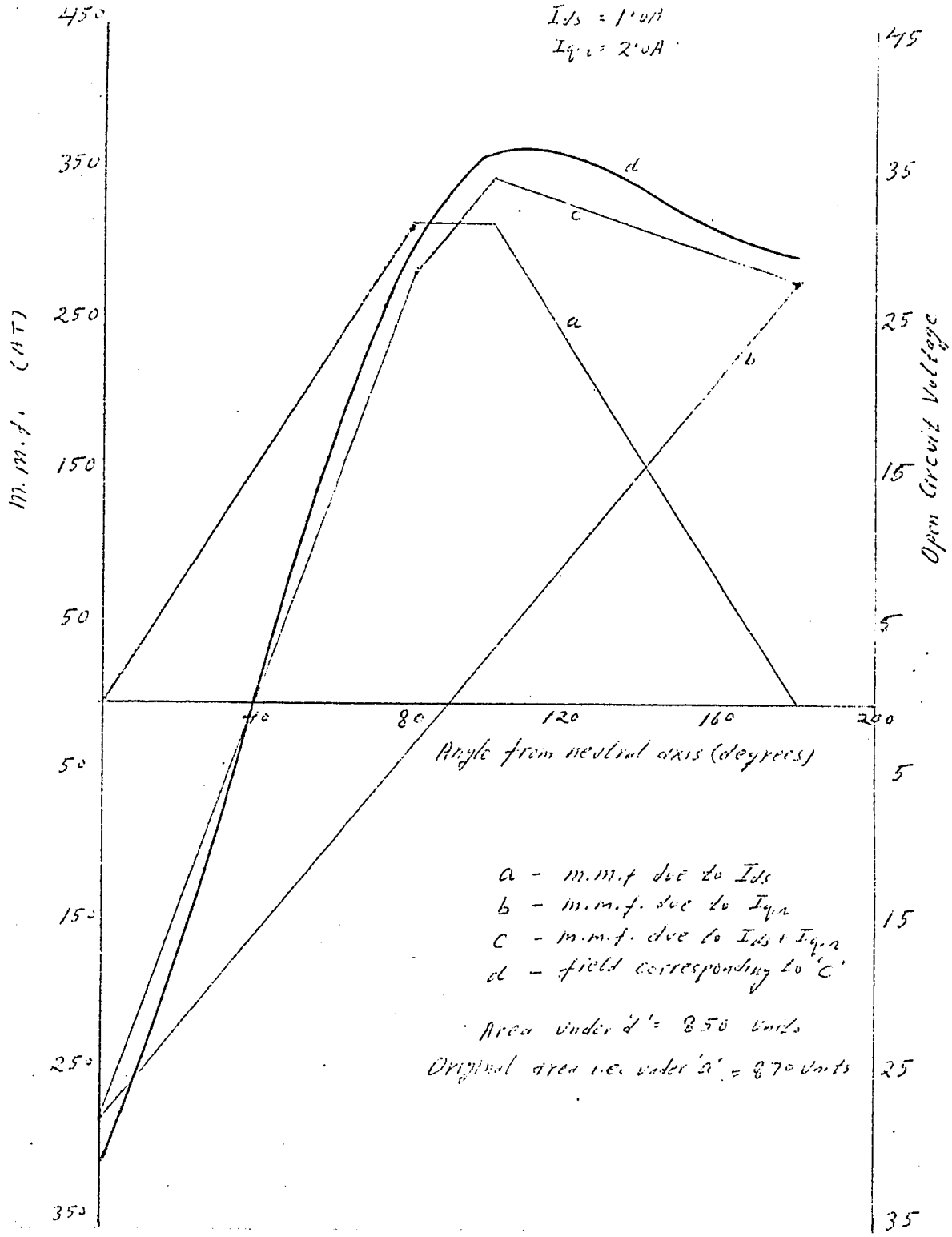

GRAPH 6

CALCULATION OF REDUCTION IN d-AXIS FLUX DUE TO ARMATURE M. M. F.

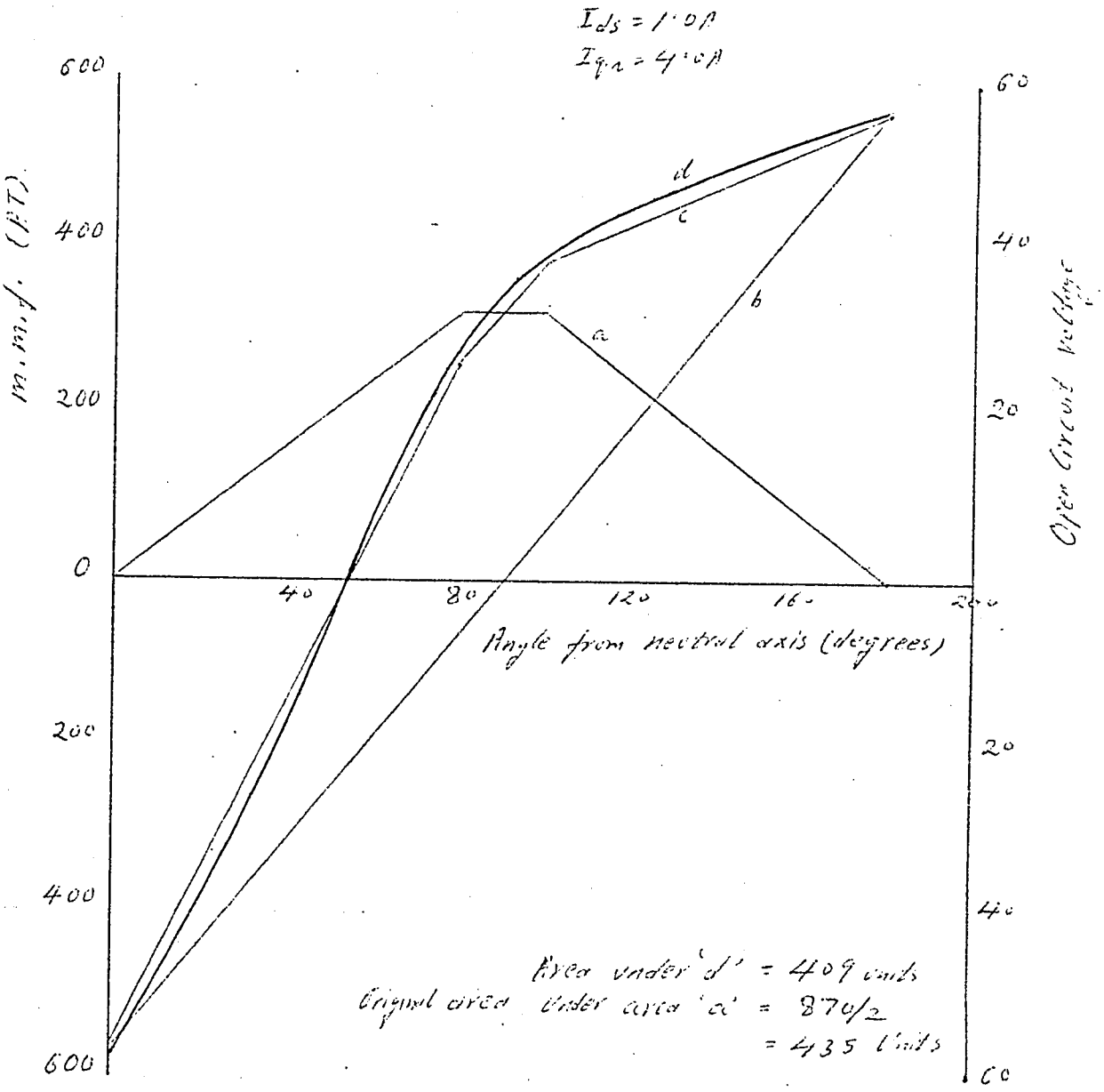

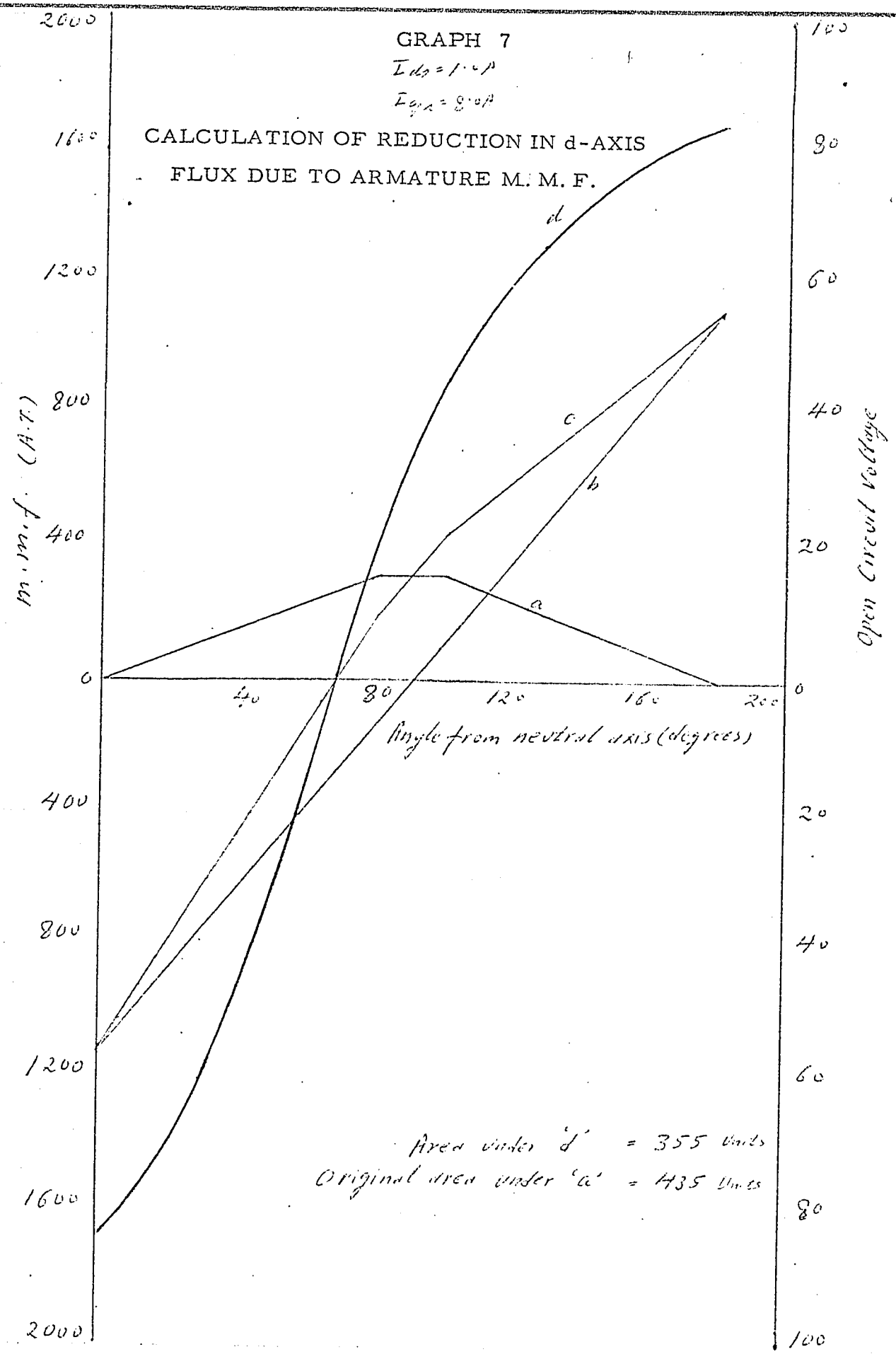
GRAPH 7
$I_{da} = 1{\cdot}0A$
$I_{qa} = 8{\cdot}0A$
CALCULATION OF REDUCTION IN d-AXIS
FLUX DUE TO ARMATURE M. M. F.
d
c
b
a
2000
1600
1200
800
400
0
400
800
1200
1600
2000
m.m.f. (A.T.)
40
80
120
160
200
Angle from neutral axis (degrees)
100
80
60
40
20
0
20
40
60
80
100
Open Circuit Voltage
Area under 'd' = 355 Units
Original area under 'a' = 435 Units

GRAPH 8

MOTOR SPEED CHARACTERISTIC

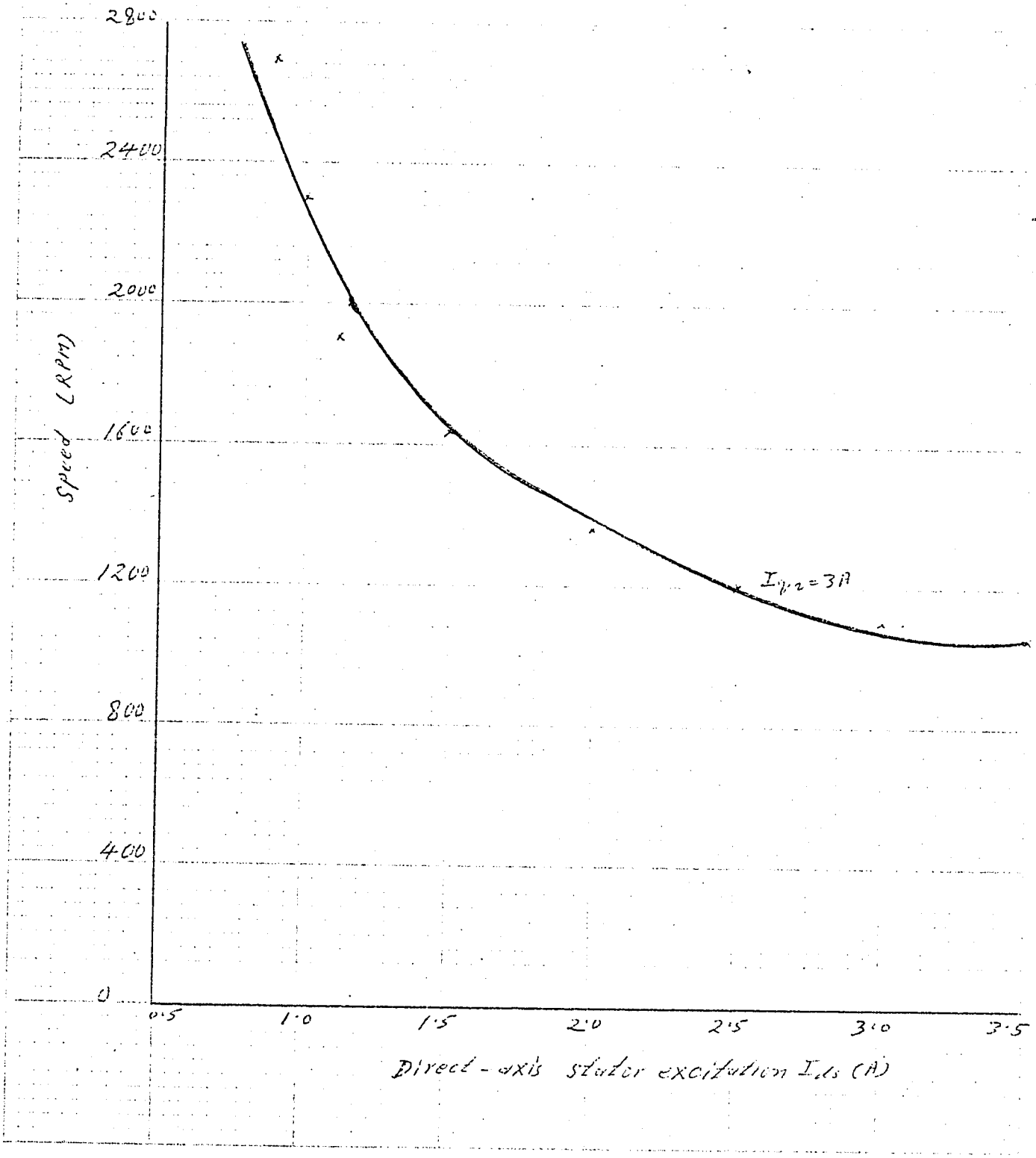

MOTOR SPEED (Lunit/sec)
-60
-50
-40
-30
-20
-10
10
20
30
40
50
Raising Speed
Lowering Speed
0.92

GRAPH 9

STEP RESPONSE ~~OF EQUIVALENT MODEL~~

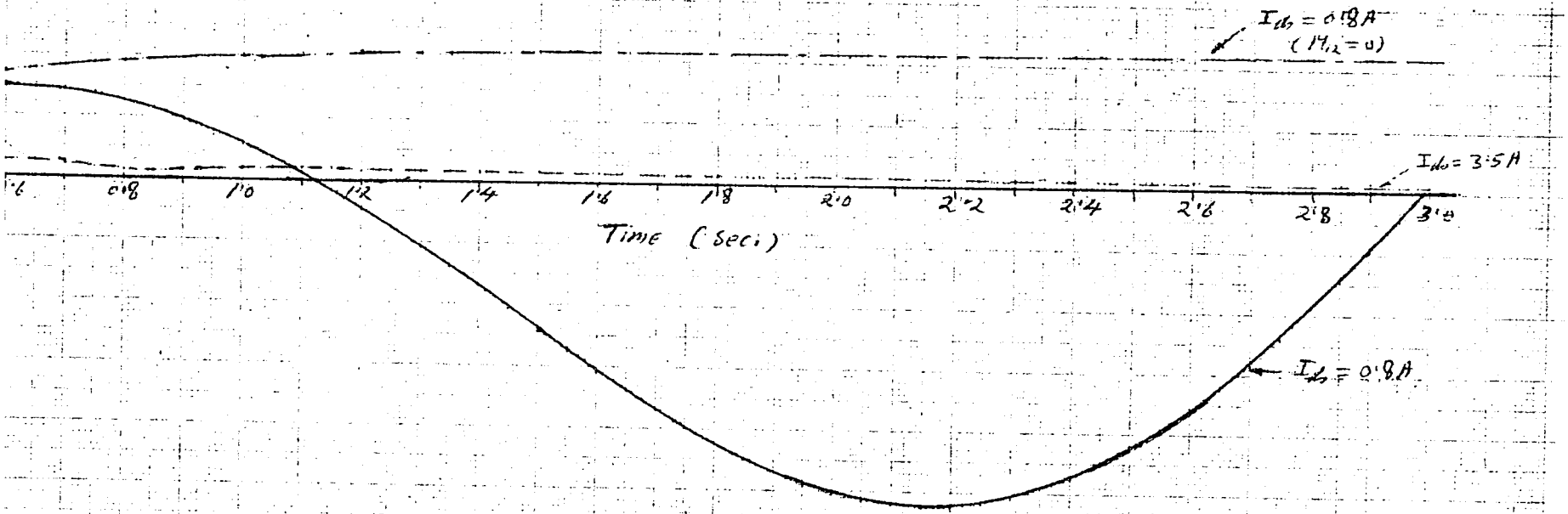

GRAPH 10

DETERMINATION OF MAGNETIC NEUTRAL AXIS

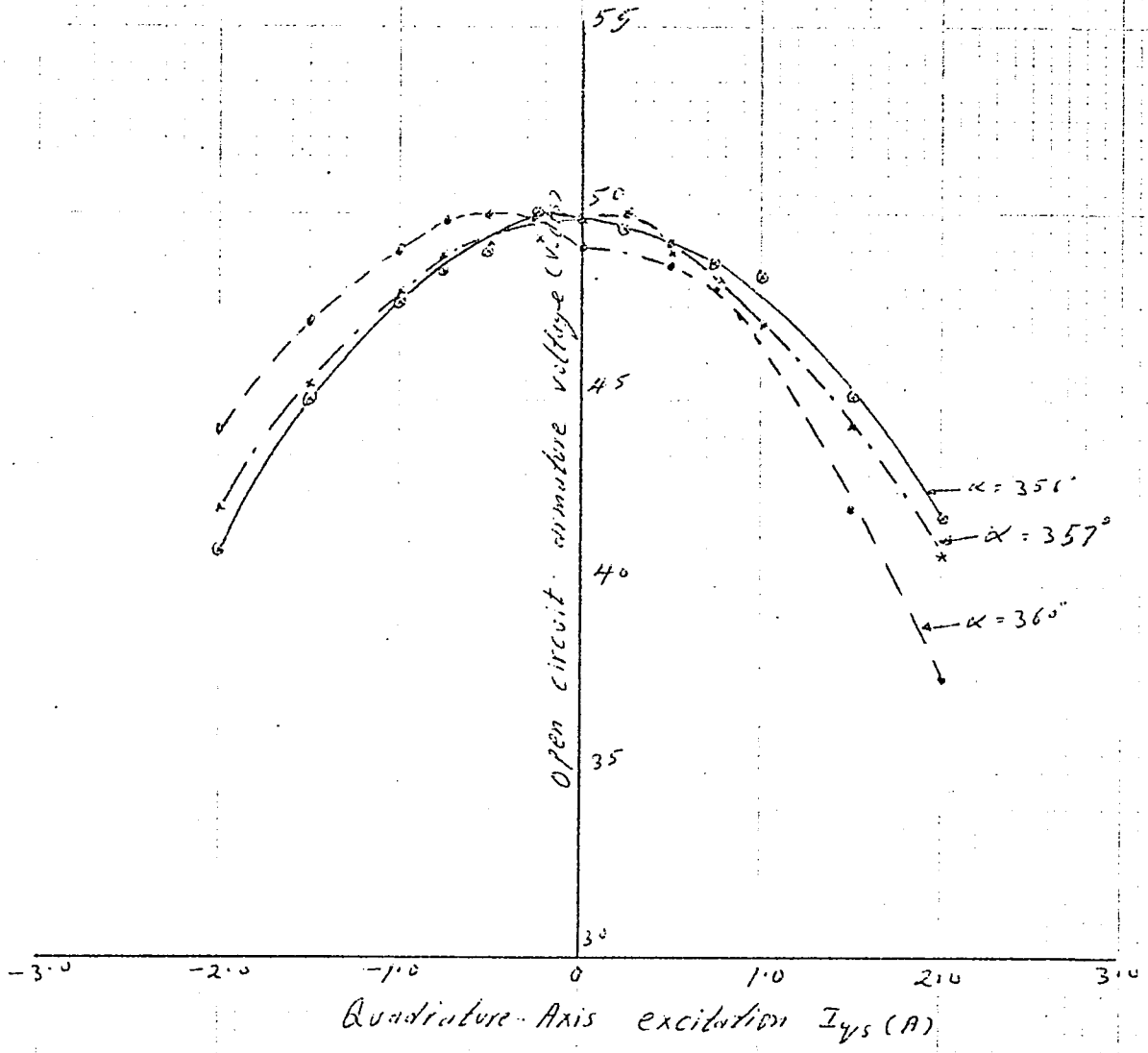

GRAPH 11

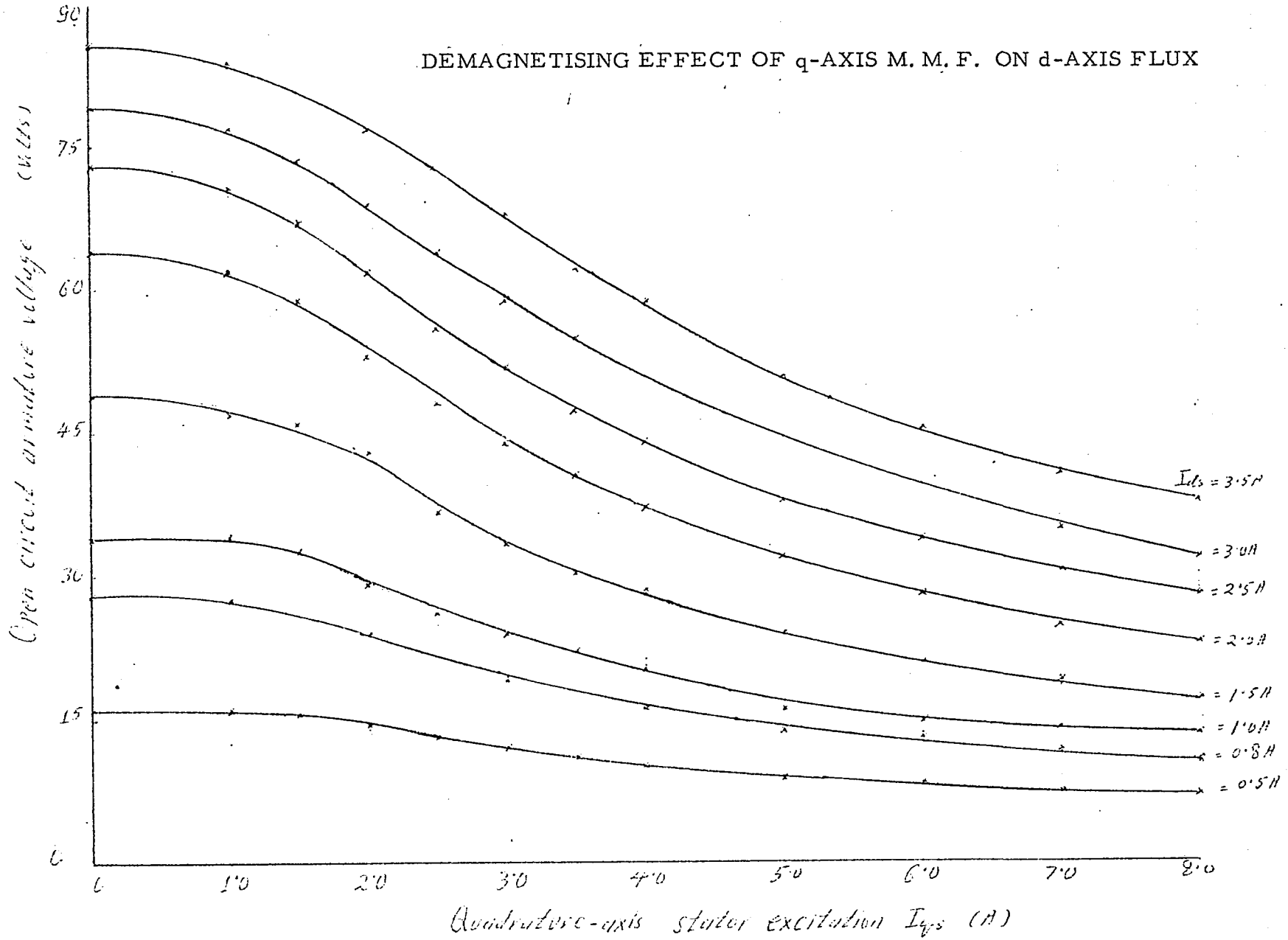
DEMAGNETISING EFFECT OF q-AXIS M. M. F. ON d-AXIS FLUX
Open circuit armature voltage (VOLTS)
90
75
60
45
30
15
0
0
1·0
2·0
3·0
4·0
5·0
6·0
7·0
8·0
Quadrature-axis stator excitation I_{qs} (A)
I_{ds} = 3·5A
= 3·0A
= 2·5A
= 2·0A
= 1·5A
= 1·0A
= 0·8A
= 0·5A

GRAPH 12

EFFECT OF q-AXIS EXCITATION ON MOTOR SPEED

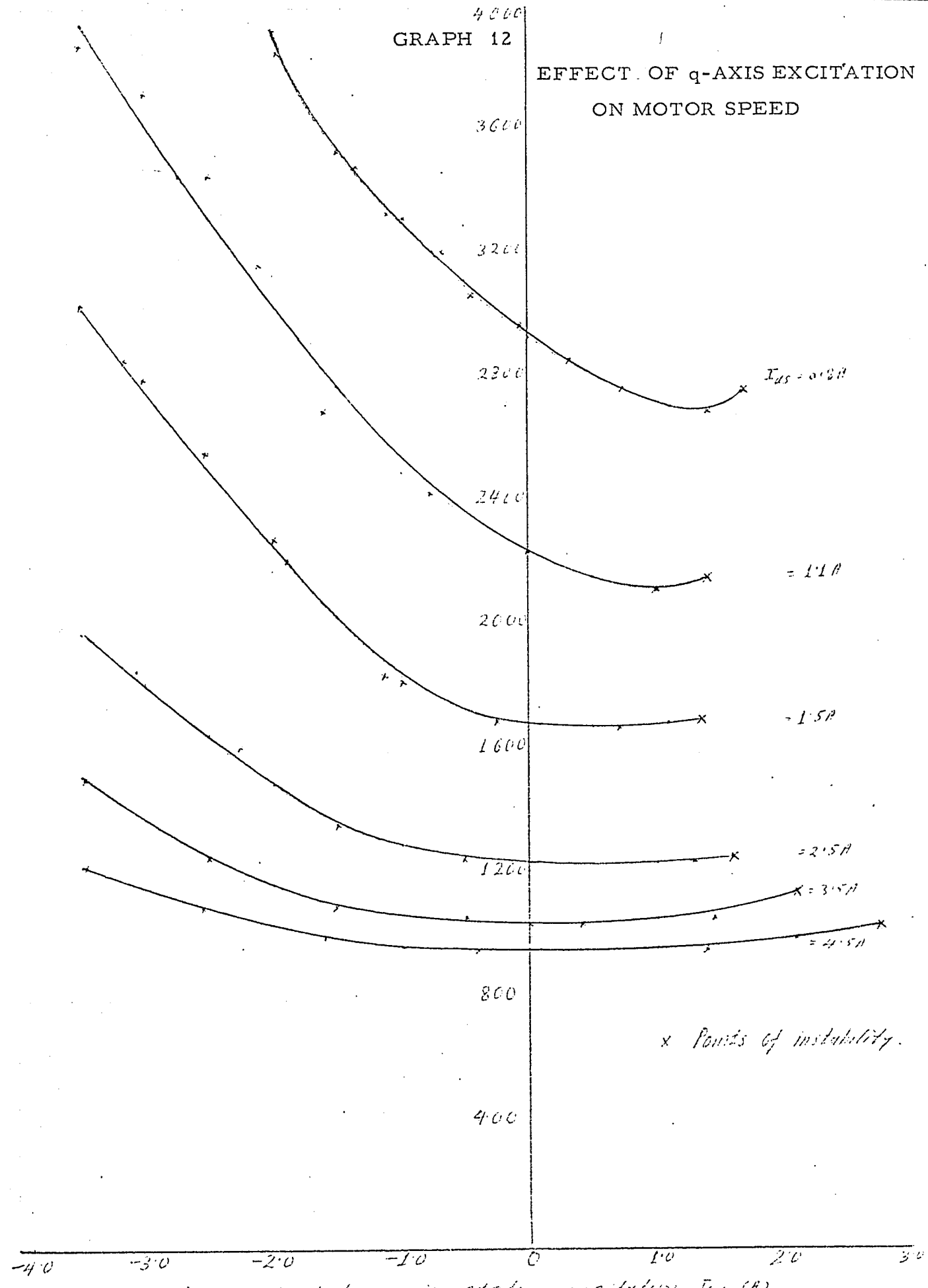

GRAPH 13

VARIATION OF ARMATURE CIRCUIT RESISTANCE WITH ARMATURE CURRENT

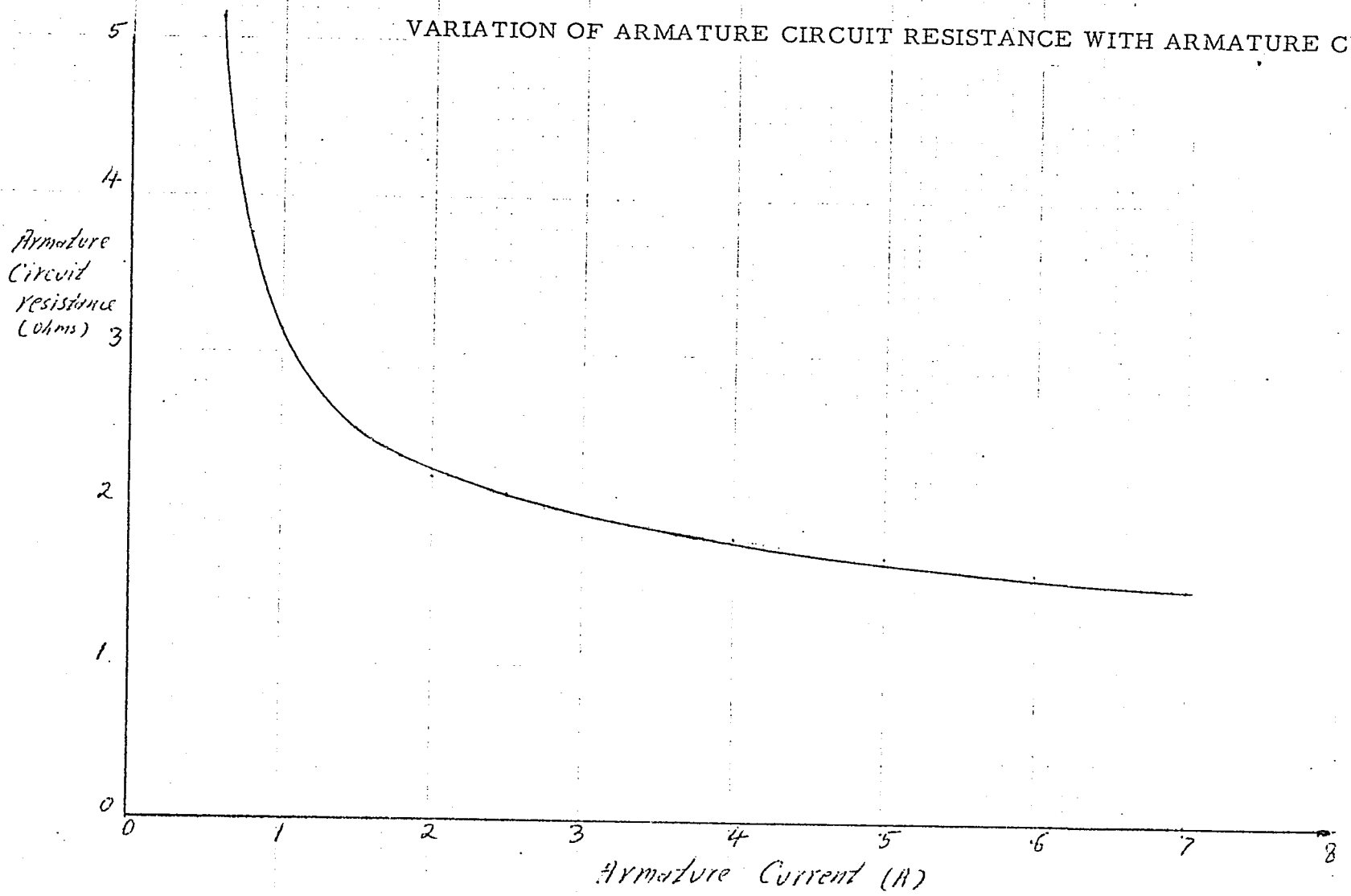

GRAPH 14

COMPUTED VARIATION OF AMPLITUDE OF OSCILLATIONS WITH ARMATURE CIRCUIT RESISTANCE

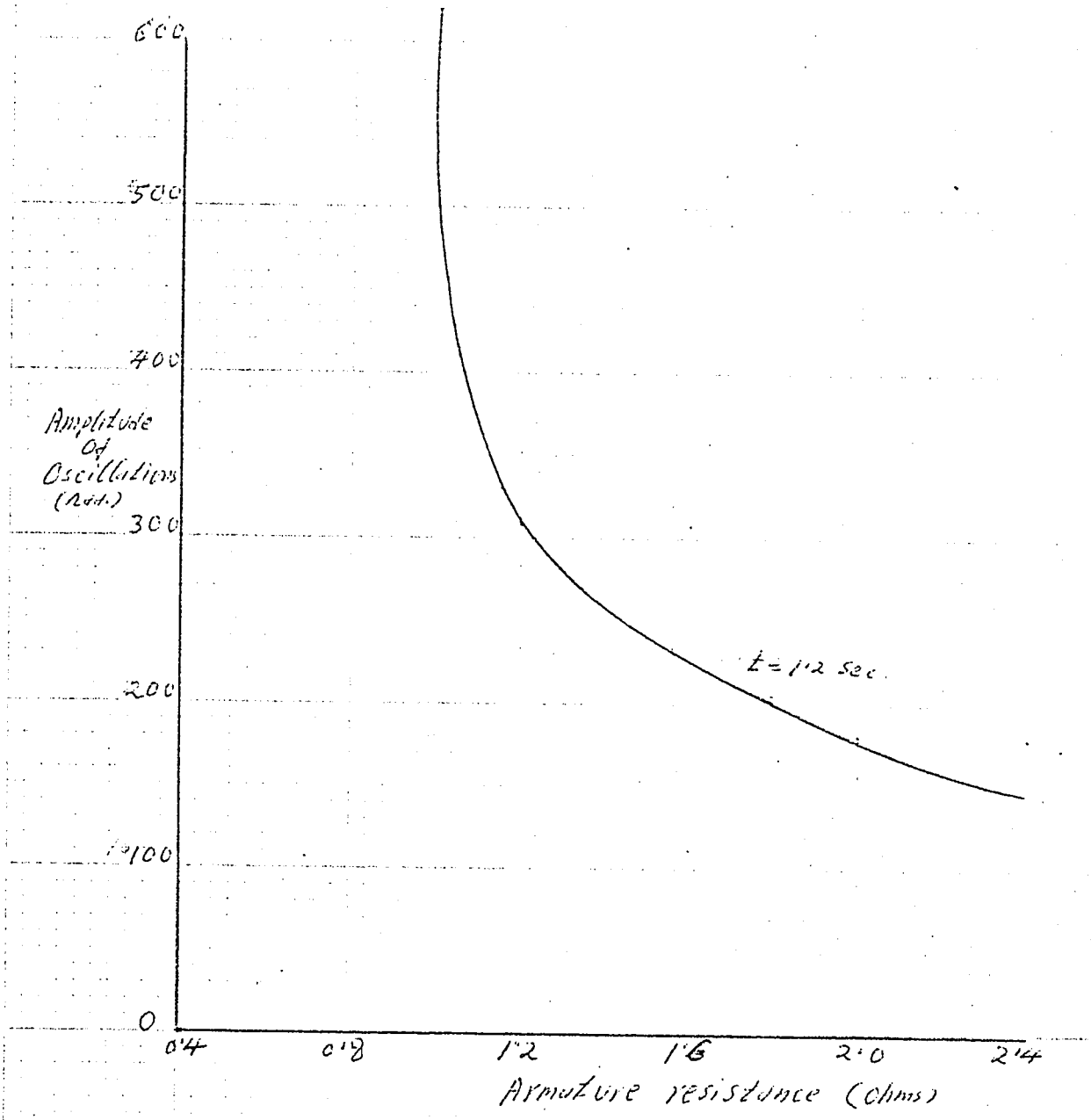

TEST 1

COMPARISON OF THE FIELD FORMS PRODUCED BY qr-AXIS M. M. F. AND qs-AXIS M. M. F.

CHART 1 (a)

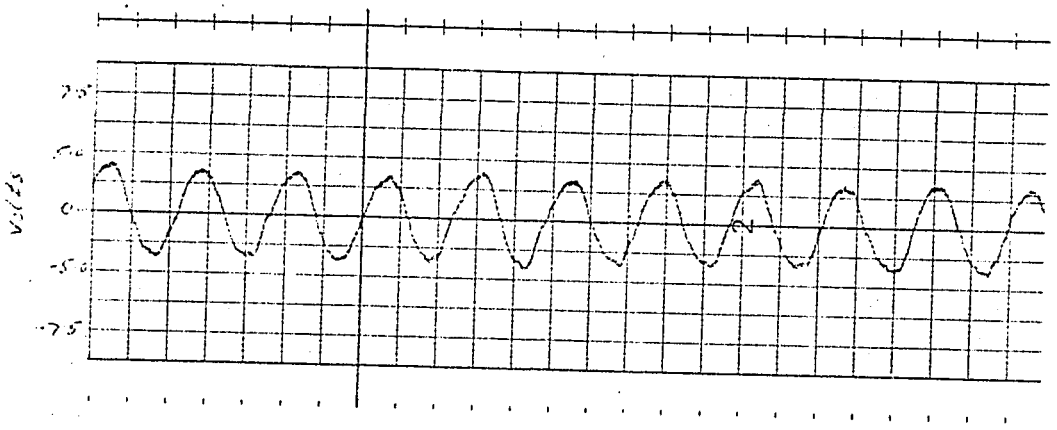

I_{qr} = 1A

Paper Speed 125 mm/sec.

CHART 1 (b)

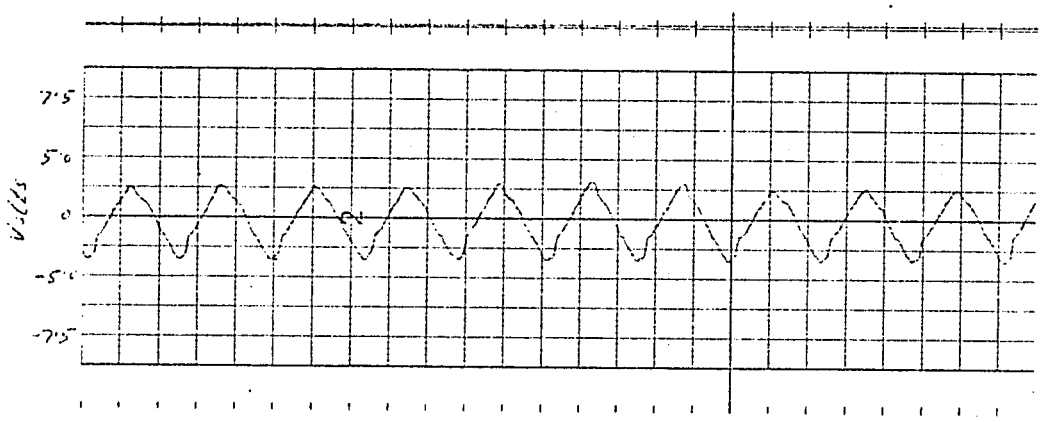

I_{qs} = 0.43A

Paper Speed 125 mm/sec.

TEST 1

COMPARISON OF THE FIELD FORMS PRODUCED BY qr-AXIS M. M. F. AND qs-AXIS M. M. F.

CHART 2 (a)

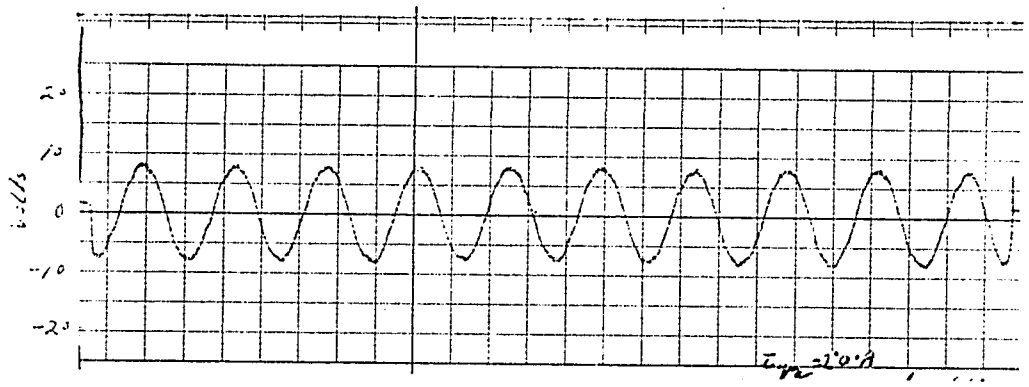

I_{qr} = 2.0A

Paper Speed 125 mm/sec.

CHART 2 (b)

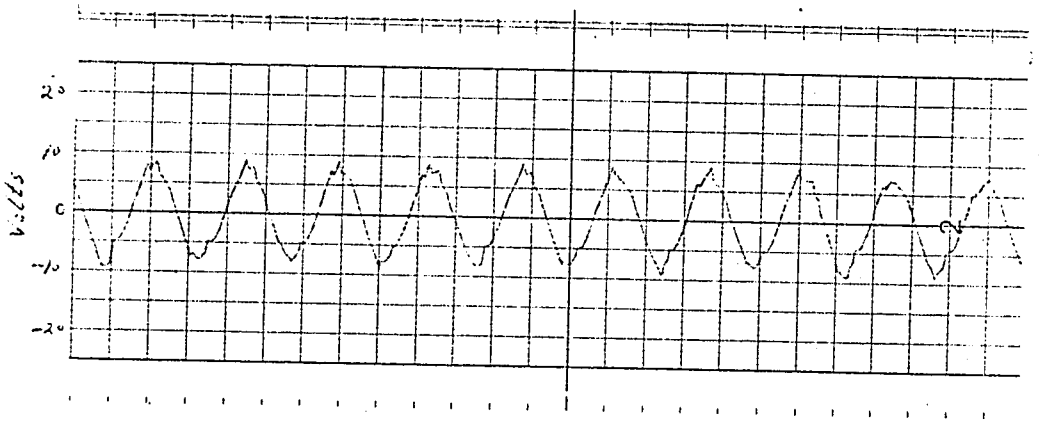

I_{qs} = 0.86A

Paper Speed 125 mm/sec.

TEST 1

COMPARISON OF THE FIELD FORMS PRODUCED BY qr-AXIS M. M. F. AND qs-AXIS M. M. F.

CHART 3 (a)

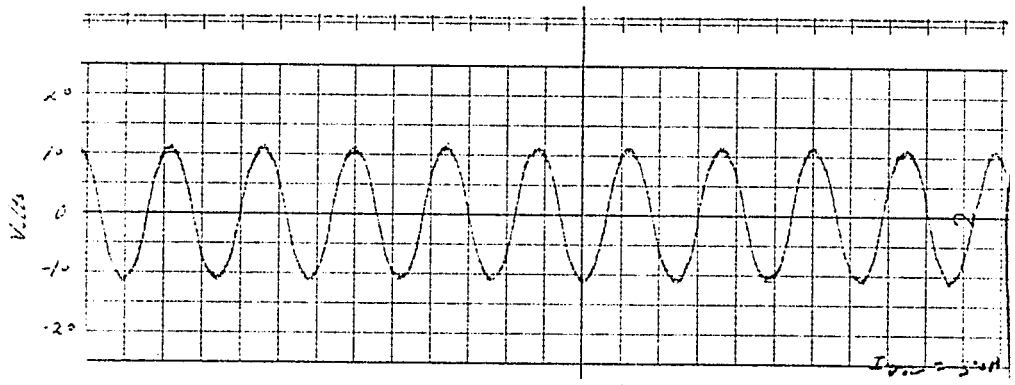

I_{qr} = 3.0A

Paper Speed 125 mm/sec.

CHART 3 (b)

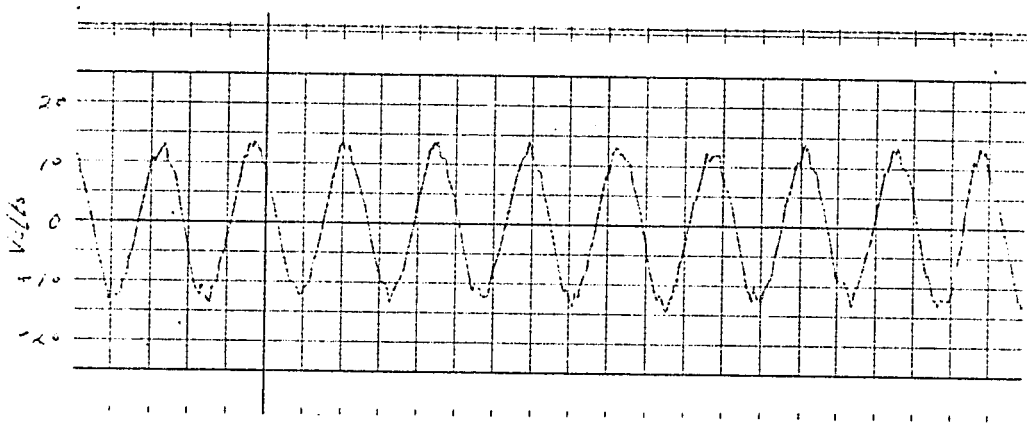

I_{qs} = 1.29A

Paper Speed 125 mm/sec.

TEST 3

DEMAGNETISING EFFECT OF q-AXIS M. M. F. ON THE d-AXIS FLUX

CHART 4

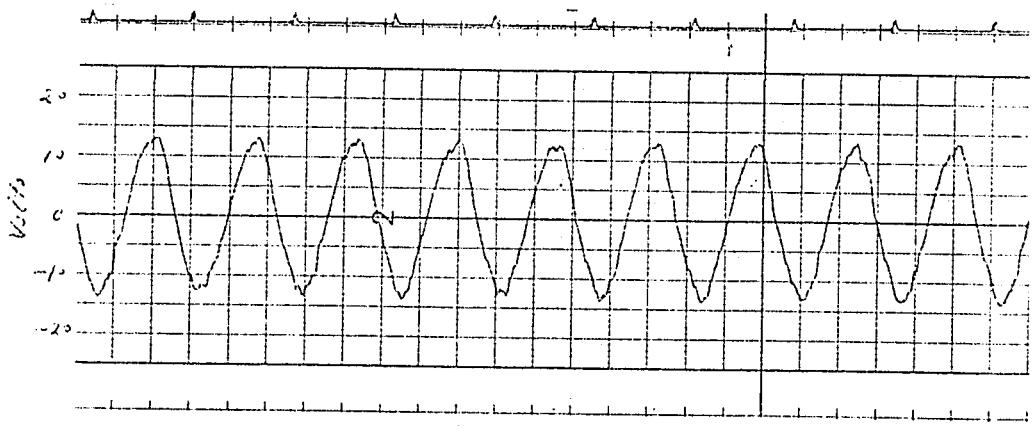

I_{ds} = 1.5A , I_{qr} = 0A

Paper Speed 125 mm/sec.

CHART 5

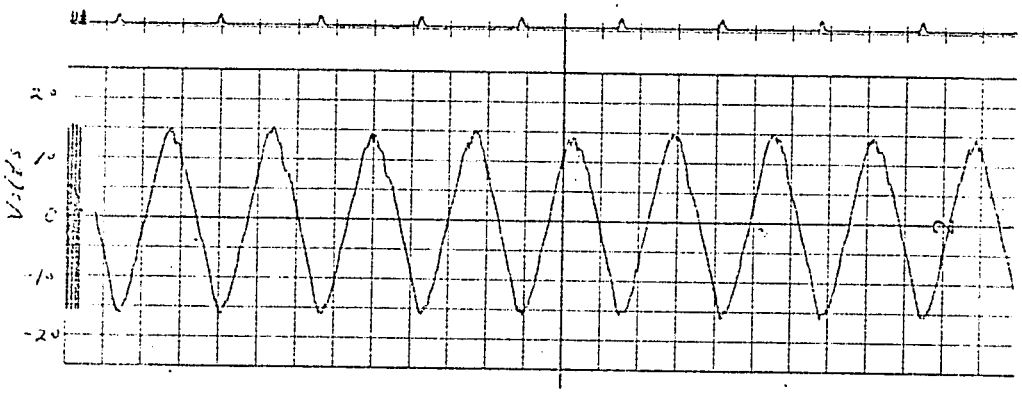

I_{ds} = 1.5A , I_{qr} = 2A

Paper Speed 125 mm/sec.

TEST 3

DEMAGNETISING EFFECT OF q-AXIS M. M. F. ON THE d-AXIS FLUX

CHART 6

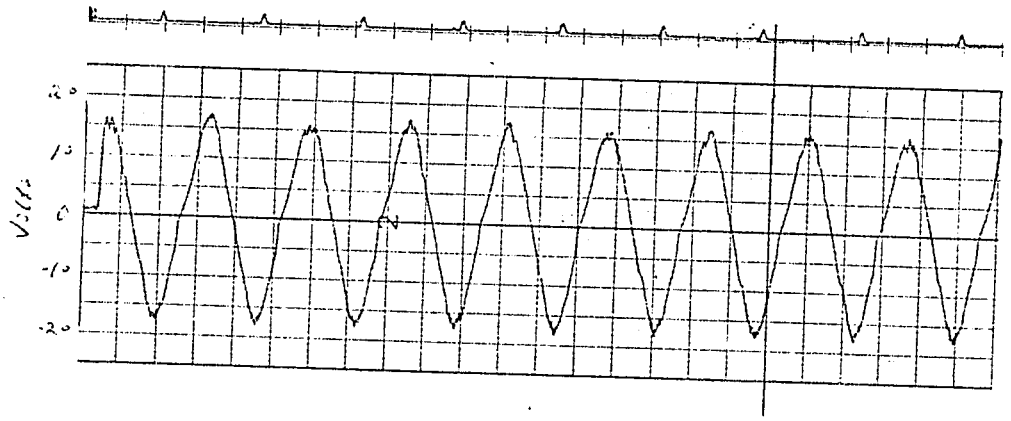

I_{ds} = 1.5A , I_{qr} = 3A

Paper Speed 125 mm/sec.

CHART 7

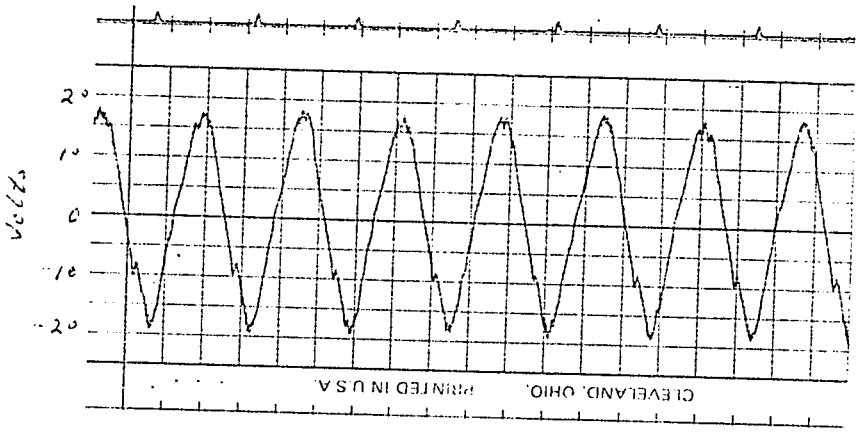

I_{ds} = 1.5A , I_{qr} = 4A

Paper Speed 125 mm/sec.

TEST 3

DEMAGNETISING EFFECT OF q-AXIS M. M. F. ON THE d-AXIS FLUX

CHART 8

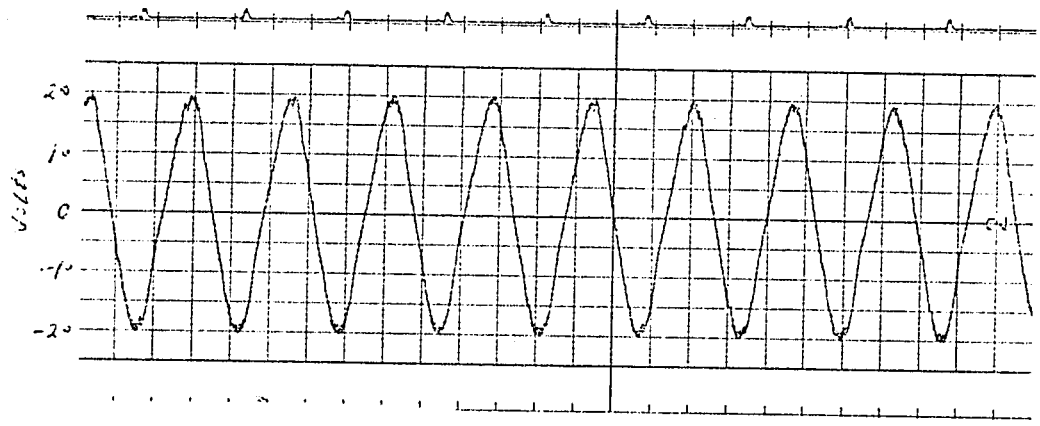

I_{ds} = 1.5A , I_{qr} = 5A

Paper Speed 125 mm/sec.

CHART 9

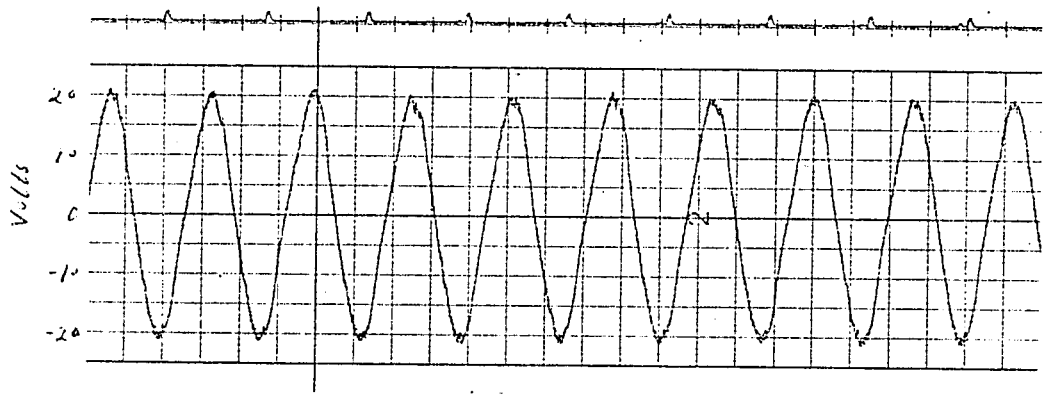

I_{ds} = 1.5A , I_{qr} = 6A

Paper Speed 125 mm/sec.

TEST 3

DEMAGNETISING EFFECT OF q-AXIS M. M. F. ON THE d-AXIS FLUX

CHART 10

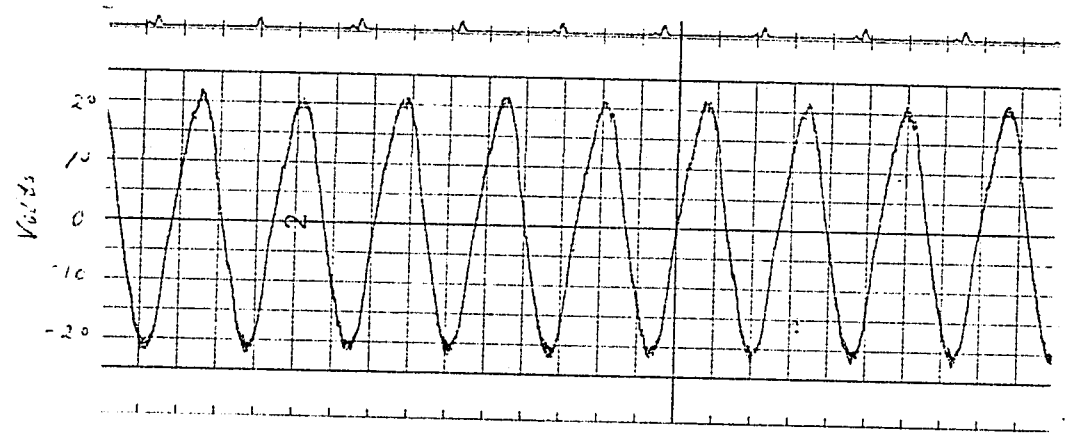

I_{ds} = 1.5A , I_{qr} = 7A

Paper Speed 125 mm/sec.

CHART 11

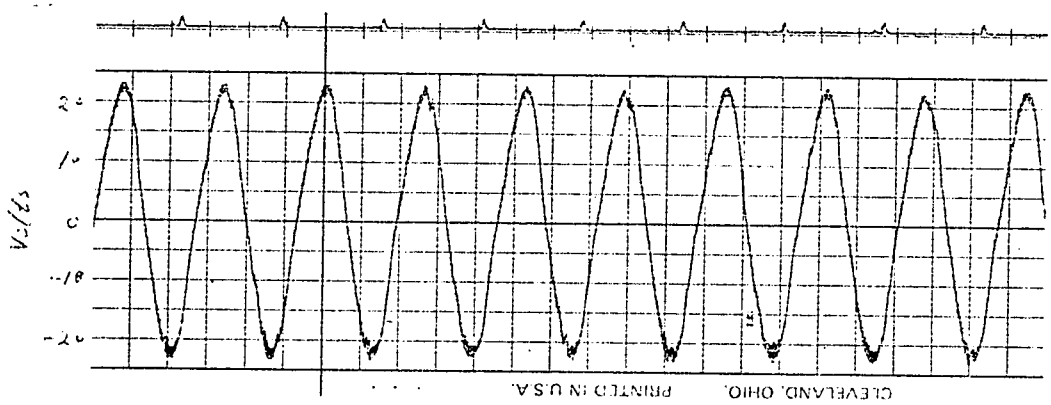

I_{ds} = 1.5A , I_{qr} = 8A

Paper Speed 125 mm/sec.

CHART 12

SPEED AND ARMATURE CURRENT DURING OSCILLATIONS

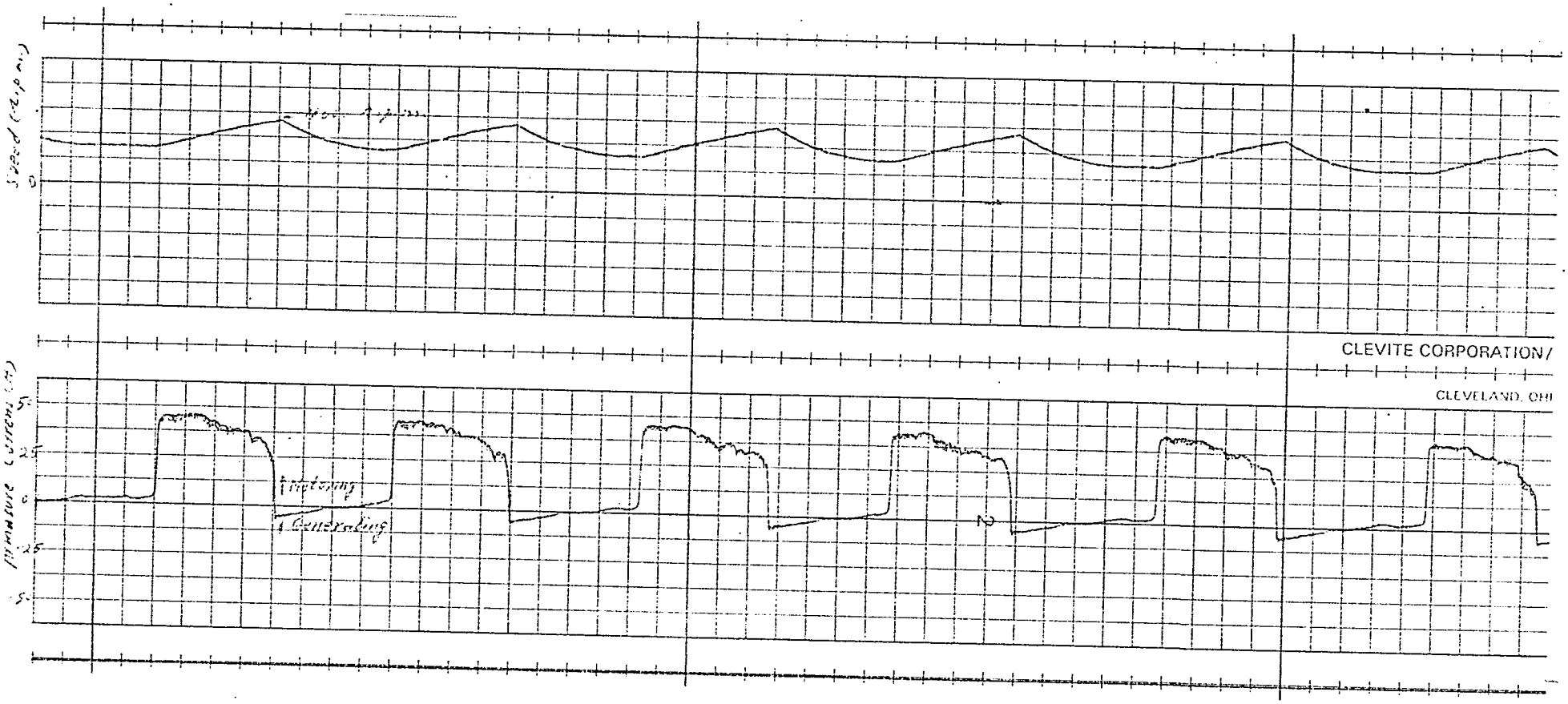

I_{ds} = 1.5A , V_{qr} = 50 volts , I_{qr} = 3.0A (before oscillations)

Paper Speed 125 mm/sec.